의학박사 학위논문

Activity-dependent modulation of intrinsic excitability in the cerebellar Purkinje cells

소뇌 퍼킨지 세포 내재적 흥분성의 활동-의존적 조절

2019 년 02 월

서울대학교 대학원

의과학과 생리학전공

심 현 근

Ph.D Dissertation of Biomedical Science

소뇌 퍼킨지 세포 내재적 흥분성의 활동-의존적 조절

Activity-dependent modulation of intrinsic excitability in the cerebellar Purkinje cells

February 2019

The Department of Biomedical Science,

Seoul National University

College of Medicine

Hyun Geun Shim

소뇌 퍼킨지 세포 내재적 흥분성의 활동-의존적 조절

지도 교수 김 상 정

이 논문을 의학박사 학위논문으로 제출함

2018년 10월

서울대학교 대학원
의과학과 생리학전공

심 현 근

심현근의 의학박사 학위논문을 인준함

2018년 12월

위 원 장 _____ (인)

부위원장 _____ (인)

위 원 _____ (인)

위 원 _____ (인)

위 원 _____ (인)

Activity-dependent modulation of intrinsic excitability in the cerebellar Purkinje cells

A Dissertation Submitted to the Faculty of the
Department of Biomedical Science
at
Seoul National University

by

Hyun Geun Shim

in Partial Fultillment of the
Requirements for the Degree of
Doctor of Philosophy

Advisor: Sang Jeong Kim
October 2018

Approved by Thesis Committee:

December 2018

Chair _____(Seal)
Vice Chair _____(Seal)
Examiner _____(Seal)
Examiner _____(Seal)
Examiner _____(Seal)

Preface

This Ph.D dissertation of biomedical science written by Hyun Geun Shim contains four chapters. Each chapters are modified from previously published papers in peer-reviewed journal. Chapter 1 is adopted from ***Experimental Neurobiology*** (Shim, H.G., Lee, Y.S., & Kim, S.J. (2018) The Emerging Concept of Intrinsic Plasticity: Activity-dependent Modulation of Intrinsic Excitability in Cerebellar Purkinje Cells and Motor Learning. Experimental Neurobiology, 27(3), 139-154). Chapter 2 is published in the ***Journal of Neurophysiology*** (Shim, H. G., Jang, S.S., Jang, D.C., Jin,Y., Chang,W., Park, J.M., & Kim, S.J. (2016) $mGlu_1$ receptor mediates homeostatic control of intrinsic excitability through I_h in cerebellar Purkinje cells. Journal of neurophysiology, 115(5), 2446-2455). Chapter 3 is adopted from ***Journal of Neuroscience*** (Shim, H.G., Jang, D.C., Lee, J., Chung, G., Lee, S., Kim, Y.G., Jeon, D.E. and Kim, S.J. (2017) Long-term depression of intrinsic excitability accompanied by the synaptic depression in the cerebellar Purkinje cells: Journal of Neuroscience, pp.3464-16; selected in featured article).

Abstract

Activity-dependent modulation of intrinsic excitability in the cerebellar Purkinje cells

Hyun Geun Shim
Department of Biomedical Science (Physiology major)
The Graduate School
Seoul National University College of Medicine

Learning rule has been thought to be implemented by activity-dependent modifications of synaptic function and neuronal excitability which contributing to maximization the information flow in the neural network. Since the sensory information is conveyed by forms of action potential (AP) firing, the plasticity of the intrinsic excitability (intrinsic plasticity) has been highlighted the computational feature of the brain. Given the cerebellar Purkinje cells (PCs) is the sole output neurons in the cerebellar cortex, coordination of the synaptic plasticity at the parallel fiber (PF) to PC synapses including long-term depression (LTD) and long-term potentiation (LTP) but also the intrinsic plasticity may play a essential role in information processing in the cerebellum. In this Dissertation, I have investigated several features of intrinsic plasticity in the cerebellar PCs in an activity-dependent manner and their cellular mechanism. Furthermore, the functional implications of the intrinsic plasticity in the cerebellum-dependent behavioral output are discussed. Firstly, I first cover the ion channels regulating the spiking activity of the cerebellar PCs and the cellular mechanisms of the plastic changes in excitability. Various ion channels indeed harmonize the cellular activity

and shaping the optimal ranges of the neuronal excitability. Among the ion channels expressed in the cerebellar PCs, hyperpolarization-activated cyclic nucleotide-gated (HCN) channels contribute to the non-Hebbian homeostatic intrinsic plasticity in the cerebellar PCs. Chronic activity-deprivation of PC activity caused the upregulation of agonist-independent activity of type 1 metabotropic glutamate receptor (mGluR1). The increased mGluR1 activity consequently enhanced the HCN channel current density through protein kinase A (PKA) pathway thereby downregulation of intrinsic excitability in PCs. In addition, the intrinsic excitability of PCs is found to be modulated by synaptic activity. Of interest, I investigated that the PF-PC LTD is accompanied by LTD of intrinsic excitability (LTD-IE). The LTD-IE indeed shared intracellular signal cascade for governing the synaptic LTD such as large amount of Ca^{2+} influx, mGluR1, protein kinase C (PKC) and Ca^{2+}-calmodulin-dependent protein kinase II (CaMKII) activation. Interestingly, the LTD-IE reduced PC spike output without changes in patterns of synaptic integration and spike generation, suggesting that the intrinsic plasticity alters the quantity of information rather than the quality of information processing. In consistent, the LTD-IE was shown in the floccular PCs when the PF-PC LTD occurs. Notably, not only the synaptic LTD but also LTD-IE was found to be formed at the conditioned dendritic branch. Thus, synaptic plasticity could significantly affect to the neuronal net output through the synergistic coordination of synaptic and intrinsic plasticity in the dendrosomatic axis of the cerebellar PCs. In conclusion, the activity-dependent modulation of intrinsic excitability may contribute to dynamic tuning of the cerebellar PC output for appropriate signal transduction into the downstream neurons of the cerebellar PCs.

Keyword : Synaptic plasticity, PF-PC LTD, intrinsic plasticity, cerebellar motor learning
Student Number : 2012-23669

Table of Contents

Chapter 3. Long-Term Depression of Intrinsic Excitability Accompanied by Synaptic Depression in Cerebellar Purkinje Cells

Chapter 4. Synergies between synaptic depression and intrinsic plasticity of the cerebellar Purkinje cells determining the Purkinje cell output

List of Figures and Table

Chapter 1

Chapter 2

Chapter 3

Chapter 4

Tables

General Introduction

The brain is one of the most complex system in the nature. It contains over a billion of neurons which form up to a hundred thousand of synaptic connection. The remarkable feature of this universe is that the system is endowed with a high degree of plastic changes in an activity-dependent manner rather than hardwired. Hence, the organisms are able to appropriately adjust environment around them and survive. Since Donald O. Hebb proposed Hebb's rule that neurons that fire together wire together, (Daoudal and Debanne, 2003; Debanne et al., 2018; Shim et al., 2018) activity-dependent synaptic plasticity has been considered as the cellular and molecular mechanism of learning and memory (Hebb, 1949). When neurons give repetitive and significant stimuli, alterations of synaptic transmitter release properties at the presynaptic neurons and receptor expression at the postsynaptic neurons occur. These changes in synaptic activity is appeared within few seconds, called short-term plasticity (Chang et al., 2012). The short-term plasticity has been implicated in dynamic and rapid regulation of synaptic activity (Atluri and Regehr, 1996; Mahon and Charpier, 2012; Turecek et al., 2016; Zhang and Linden, 2003). For instance, strong depolarization induces transient reduction of excitation and/or inhibition inputs, known as depolarization-induced suppression of excitation (DSE) and depolarization-induced suppression of inhibition (DSI), respectively (Kreitzer and Regehr, 2001; Satoh et al., 2013; Wang et al., 2012). When the neuronal activity occurs repeatedly, the weight of synaptic transmission occasionally prolonged over hours, referred as long-term plasticity (Atluri and Regehr, 1996; Mahon and Charpier, 2012; Shim et al., 2018; 2017). Bliss and Lomo (1973) firstly described this cellular phenomenon, especially long-term potentiation (LTP), long-lasting augmentation of the postsynaptic response in the hippocampus. Until recently, short-term and long-term plasticity has long been investigated in order to elucidate how the brain learns and stores information.

Persistent and experience-dependent alterations in synaptic function such as LTP

and long-term depression (LTD) have been largely regarded as memory storage in the modern neuroscience field (Mittmann and Häusser, 2007). However, other side of the memory engram has been postulated because the information processed within synapses is ultimately conveyed though the intrinsic excitability, neuronal ability to generate action potential (Kim and Linden, 2007; Zhang and Linden, 2003). There is accumulating evidence supporting the idea that information storage may require not only the synaptic plasticity but also the activity-dependent modulation of neuronal intrinsic excitability (intrinsic plasticity) (Gao et al., 2012). The intrinsic plasticity is not confined to the single synapse but accompanies non-synaptic and global changes (Belmeguenai et al., 2010; Shim et al., 2017). Therefore, the incongruity between synaptic and intrinsic plasticity may give rise to a controversy that the global changes of neuronal excitability would presumably distort the experience-dependent synaptic plasticity. Notably, synapse-specific and non-specific modifications synergistically contribute to the information processing and memory storage in the defined circuitry (Belmeguenai et al., 2010; Mittmann and Häusser, 2007; Rancz and Häusser, 2010; Shim et al., 2017). The intrinsic plasticity shapes the net output of neurons by integrating the synaptic inputs and consecutively translating them into the action potential (AP) firing. Therefore, synergies between synaptic and intrinsic plasticity would play a role in maximizing information processing such as encoding, transfer and storage.

The cerebellar Purkinje cells (PCs) is the inhibitory principal neurons in the cerebellar cortex, integrating excitatory and inhibitory inputs from widely spread dendrite branches. Abundant branches of dendritic tree in the cerebellar PCs receive two major excitatory synaptic inputs from parallel fiber (PF), the axon fiber of the granule cells, and climbing fiber (CF), the axon fiber of the inferior olivary (IO) neurons in the brainstem. Various sensory information from the pre-cerebellar region and spinal cord project into the cerebellum through the mossy fiber (MF) which forms synapses with the cerebellar granule cells. The cerebellar PCs integrate the sensory information from the PF and then provide inhibitory

instructive signals to the neurons in the vestibular nuclei (VN) and/or the deep cerebellar nuclei (DCN) in order to generate motor output. In addition to PF inputs, CF inputs into the cerebellar PCs encodes the feedback error signal corresponding to performances (Guo et al., 2014; Ke et al., 2009; Kimpo et al., 2014; Streng et al., 2017). In order to control goal-directed movement, this sensory feedback of error signals dynamically regulates the cerebellar output (Bloedel and Bracha, 1995; Yamazaki and Nagao, 2012). Indeed, the CF inputs onto the cerebellar PCs are regarded as the instructive signals in the cerebellar plasticity as the PF-PC synaptic plasticity is guided by timing rules between PF and CF activation (Safo and Regehr, 2008; Suvrathan et al., 2016). The synaptic plasticity between PF-PC synapses guided by instructive CF activation has long been regarded as the cellular basis of cerebellum-dependent motor learning (Suvrathan et al., 2016) in fact, is the heterosynaptic plasticity guided depending on the timing rules between PF and CF activation. The performance error signals are conveyed by CF to re-compute the motor signal from PCs, enabling finely tuned motor coordination through determining the cerebellar cortical activity. Many implications in cerebellar motor learning have suggested that the bidirectional plasticity of PF-PC synapses may be selectively engaged in specific behavioral paradigms (Boyden et al., 2006; Jörntell and Hansel, 2006). In spite of abundant studies of the PF-PC synaptic plasticity associated with cerebellum dependent behaviors, it has been less elucidated how the net output of the cerebellar PCs is regulated in an activity-dependent manner. Since the cerebellar PCs are the sole output of the cerebellar cortex, the plasticity of the intrinsic excitability in the neurons might play a pivotal role in the modulation of cerebellar motor behavior and learning. In this dissertation, I highlight the cellular and molecular mechanisms of activity-dependent intrinsic plasticity in the cerebellar PCs. Furthermore, I discuss the physiological significances of the PC intrinsic plasticity on the cerebellar dependent motor learning circuitry.

Chapter 1

Summary of the previous literatures and further implication for physiological significance of the intrinsic plasticity in the cerebellar Purkinje cells

Summary

What is memory? How does the brain process the sensory information and modify an organism's behavior? Many neuroscientists have focused on the activity- and experience-dependent modifications of synaptic functions in order to solve these fundamental questions in neuroscience. Recently, the plasticity of intrinsic excitability (called intrinsic plasticity) has emerged as an important element for information processing and storage in the brain. As the cerebellar Purkinje cells are the sole output neurons in the cerebellar cortex and the information is conveyed from a neuron to its relay neurons by forms of action potential firing, the modulation of the intrinsic firing activity may play a critical role in the cerebellar learning. Many voltage-gated and/or Ca^{2+}-activated ion channels are involved in shaping the spiking output as well as integrating synaptic inputs to finely tune the cerebellar output. Recent studies suggested that the modulation of the intrinsic excitability and its plasticity in the cerebellar Purkinje cells might function as an integrator for information processing and memory formation. Moreover, the intrinsic plasticity might also determine the strength of connectivity to the sub-cortical areas such as deep cerebellar nuclei and vestibular nuclei to trigger the consolidation of the cerebellar-dependent memory by transferring the information.

1.1 Ion channels and spiking activity of the cerebellar Purkinje cells

The intrinsic excitability is influenced by the conductance of voltage-gated ion channels generating ionic current carried by Na^+ and K^+ ions (I_{NA} and I_K, respectively), which affects the passive and active membrane properties (Hodgkin and Huxley, 1945; 1952a; 1952b; Hodgkin et al., 1952). The ion channels are expressed in somatic and dendritic (or both) regions and modulate the temporal summation of the synaptic inputs and ability to generate AP firing in axon hillock (Clark et al., 2005; Stuart and Häusser, 1994). A balance of ion channel conductance and expressional composition determines the characteristics of spiking activity as well as the neuronal excitability. The cerebellar PCs show a distinct spiking activity which fires spontaneously at high frequency. Many studies illustrated that the changes in ion channel conductance alter the neuronal spiking activity and behavioral outcomes (fig. 1).

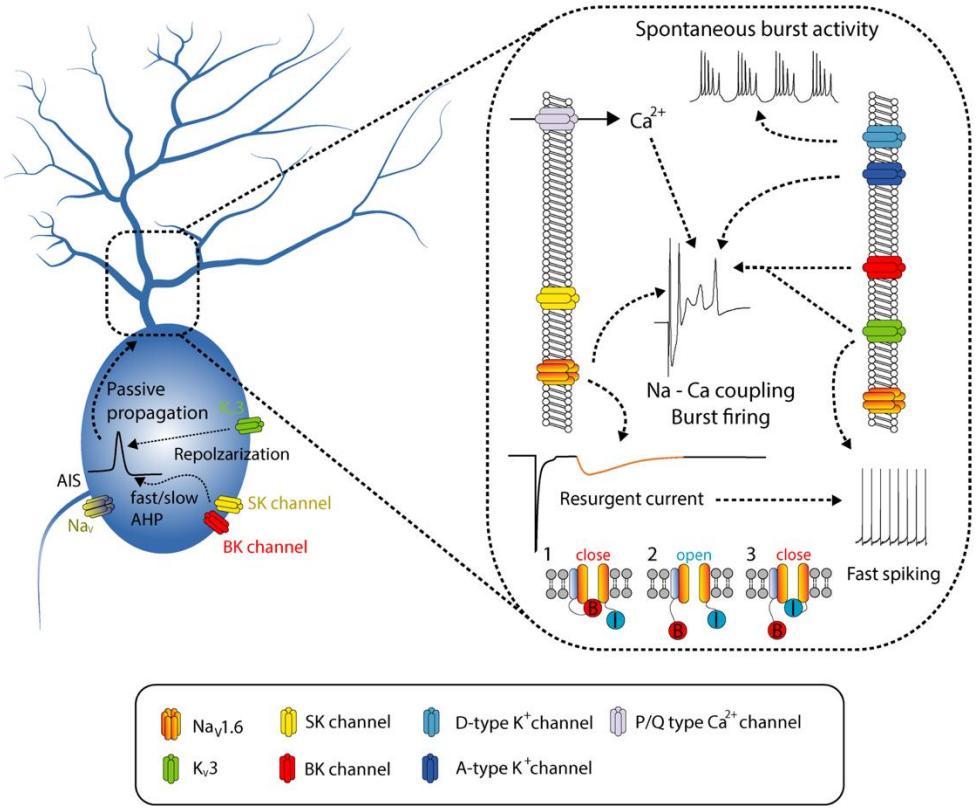

Figure 1. Schematic illustration for ion channels shaping intrinsic excitability of the cerebellar PCs. Among various ion channels, this review focused on the resurgent Na^+ channel ($Na_V1.6$), subthreshold-activated K^+ channels ($K_V1.1$, 1.2 and 1.6; $K_V1.4$ and K_V4, D-type and A-type K+ channel, respectively), suprathreshold-activated K^+ channels (K_V3 subfamily) and Ca^{2+}-activated K^+ channels (SK and BK channel). Action potential is initiated at the action potential initial segment (AIS) near the axon hillock and then passively propagated into the dendritic area. Somatic SK and BK channels determine the AP spike waveform such as the amplitude of afterhyperpolarization (AHP) and K_V3 subfamily regulates repolarization of AP. Because the cerebellar PCs, in particular, are fast-spiking neurons, mechanisms of rapid recovery from Na_V inactivation is required to stably maintain PC spiking behavior. $Na_V1.6$ activity enables to rapidly fire the AP spikes via shortening refractory period. Various ion channels synergistically and dynamically modulate the dendrosomatic activity of the cerebellar PCs.

1.1.1 Voltage-gated Na^+ channels

Voltage-gated Na^+ channels (Na_V) are involved in determining active properties of neurons including voltage threshold for generating AP at the axon hillock and amplitude of AP spike (Hodgkin and Huxley, 1952a; 1952b; Hodgkin et al., 1952). In the cerebellar PCs, various subtypes of voltage-gated Na^+ channels are expressed, for instance, $Na_V1.1$, $Na_V1.2$ and $Na_V1.6$ have been described in rodent PCs (Brysch et al., 1991; Callaway and Ross, 1997; de Ruiter et al., 2006; Schaller and Caldwell, 2003; Vega-Saenz de Miera et al., 1997). Observation of $[Na^+]_i$ changes and electrophysiological recordings via outside-out patch clamp configuration have revealed that Na^+ spikes are generated within the somatic area of PC and then passively spread into the dendrites (Callaway and Ross, 1997). Despite some subtypes of Na_V and changes in $[Na^+]_i$ in the PC dendrites were observed, backpropagation of AP into the dendrite from soma is absent, suggesting that the $[Na^+]_i$ influx and subtypes of Na^+ channels expressed in dendrites are not sufficient to generate AP in PC dendrites. In addition, electrophysiological recordings of I_{Na} in the cerebellar PCs have revealed a fast inactivating and/or a persistent conductance of Na^+ (Kay et al., 1998; Schaller and Caldwell, 2003).

Among subtypes of Na_V, $Na_V1.6$ shows a distinct feature, which contributes to transient and resurgent components, but not to persistent components (Table 1). $Na_V1.6$ was remarkably observed in the dendritic area in the cerebellar PCs (Caldwell et al., 2000). The resurgent I_{Na} facilitates reopen Na_V when the membrane potential is repolarized to approximately -40 mV following the long period of depolarization exceeds +30 mV enough to produce maximal inactivation of Na_V (Afshari et al., 2004; Khaliq et al., 2003; Raman and Bean, 1997; 2001; Raman et al., 1997). This distinctive current flow contributes to ensuring the fast-spiking activity of the cerebellar PCs via the rapid open-channel block and unblock mechanism because the PCs, in particular, spontaneously fire AP spikes at high frequency. Resurgent current, carried by $Na_V1.6$, has been found to be a mechanism by which the refractory period between AP firing is shortened by rapid

recovery from inactivation of I_{Na} (Khaliq et al., 2003; Raman and Bean, 2001). Transgenic mice which resurgent Na^+ current is disrupted showed an abnormality in the spiking activity of PCs and manifestation of cerebellar ataxia and failure of motor coordination (Khaliq et al., 2003; Valkova et al., 2017). Recent studies have shown that Na_V channel auxiliary subunit FGF14'b' isoform is involved in controlling the resurgent current and excitability of PCs (Yan et al., 2014). In parallel with previous observations, ablation of this auxiliary subunit manifests the abnormality of the firing activity in PCs and motor behavior (Bosch et al., 2015; Yan et al., 2014). Interestingly, inactivation of $Na_V1.6$ affects not only the motor performance but also associative classical conditioning and spatial memory formation. Purkinje cell-specific deletion of Scn8a, encoding $Na_V1.6$, impaired the performance in the delayed eyeblink conditioning and the Morris water maze (Woodruff-Pak et al., 2006).

1.1.2 Voltage-gated K^+ channels and Ca^{2+}-activated K^+ channels

K^+ channels are another major players in determining the excitability of the neurons. As molecular techniques have been advanced, various subtypes of K^+ channels and their gating properties have been characterized (Coetzee et al., 1999). Like Na^+ channels, many K^+ channels have shown quite distinct and divergent gating properties depending on the types of auxiliary proteins. K^+ channels are classified into several types, including voltage-gated channels (K_V), Ca^{2+}-activated K^+ channels (K_{Ca}), inwardly rectifying channels (inward rectifier) and Na^+-activated K^+ channels. In this summary, I focused on the roles of several K_V subfamilies (Table 2) and Ca^{2+}-activated K^+ channels (Table 2) in intrinsic firing properties of the cerebellar PCs.

Considering the Hodgkin-Huxley model, ionic flow carried by Na^+ and K^+ determines the active and passive properties of neurons. Of interest, K^+ conductance controls the resting membrane potential, membrane resistance, neuronal excitability, duration of AP and delay time to fire AP spike.

Electrophysiological observations and immunohistochemistry data have shown that various types of K^+ channels are expressed in cerebellar PC soma and dendrites (Etzion and Grossman, 1998; 2001; Gähwiler and Llano, 1989; Gruol et al., 1989; 1991; Martina et al., 2003; McKay and Turner, 2004; Raman and Bean, 1999). (Gähwiler and Llano, 1989) observed that outward I_K is found to be elicited by membrane depolarization above -30 mV from excised somatic membrane. This suprathreshold-activated I_K shows sensitivity for general K^+ current inhibitors, tetraethylammonium (TEA) and 4-aminopyrimidine (4-AP), indicating that the I_K is governed by K_V3 subfamily of K^+ channel (Raman and Bean, 1999; Southan and Robertson, 2000). This class of K^+ channels (especially $K_V3.3$ and 3.4) repolarizes the Na^+ spike discharge to maintain repetitive AP firing in both soma and dendritic area (Lien and Jonas, 2003; McKay and Turner, 2004; Rudy and McBain, 2001; Sekirnjak et al., 1997). Therefore, dysfunction of this subfamily results in the impairment of repetitive AP spike discharge with a high frequency and an abnormal behavior (Matsukawa et al., 2003). In addition, the pharmacological inhibition with 1- 10 mM of 4-AP or 2-5 mM TEA affects the dendritic Ca^{2+} spike discharge, indicating that the dendritic K_V3 channels contribute to shaping membrane excitability of PC dendrites as well as soma (Midtgaard et al., 1993). In spite of lacking backpropagation of Na^+ spikes into PC dendrites, membrane depolarization passively propagates into proximal and distal dendrites thereby generating regenerative Na^+ spikes and plateau potential which promotes bursting Na^+ spikes (de Ruiter et al., 2006; Llinás and Sugimori, 1980). In addition, strong depolarization induced by CF activation leads to Ca^{2+} influx into the dendrite, resulting in the $Na^+ - Ca^{2+}$ complex spike responses. The mixed $Na^+ - Ca^{2+}$ spike discharge activates dendritic $K_V3.1/3.3$ channels, enabling PC spiking activity to be stably maintained with high frequency though preventing Na^+ channel inactivation. When $[Ca^{2+}]_i$ is increased by CF activation, large conductance Ca^{2+}-activated K^+ (BK) channels are also activated. Interestingly, co-activation of K_V3 and BK channels promotes coupling between Na^+ and Ca^{2+} spike discharge via reducing

Na^+ channel inactivation, resulting in burst output of the cerebellar PCs (McKay and Turner, 2004).

Differently from K_V3 family, some other types of K^+ channels show distinct gating properties, for instance, K_V1 and 4 subtypes are activated at subthreshold voltage whereas K_V3 family shows high voltage-activating and fast deactivating voltage dependency (Coetzee et al., 1999). Storm (Storm, 1988) categorized the subthreshold-activated K^+ channels into 2 types depending on their sensitivity for 4-AP concentration and on the gating properties, A-type and D-type K_V channels, governed by $K_V1.4$, $K_V4.X$ and $K_V1.1$, 1.2, 1.6, respectively. D-type K^+ channels, sensitive to dendrotoxin (DTX) and low concentration of 4-AP, are well known for determining spike output timing, latency and threshold for AP firing onset and firing frequency (Cudmore et al., 2010; Dodson and Forsythe, 2004; Harvey, 2001; Hyun et al., 2013; Ovsepian et al., 2013; Storm, 1988). In the cerebellar PCs, large depolarization can induce $Na^+ - Ca^{2+}$ coupling in dendritic area leading to slowly depolarized potential (SDP), facilitating Na^+ burst spike generation. Pharmacological inhibition of the D-type currents shortens the SDP and reduces latency to Ca^{2+} spikes (Etzion and Grossman, 2001), suggesting that the D-type channels are involved in the regulation of dendritic excitability. Application of DTX in cerebellar slices also increases spontaneous rhythmic activity through the enhancement of rebound firing, indicating that D-type I_K plays a modulatory role in defining spiking pattern in PCs (Haghdoust et al., 2007). In addition, $K_V1.2$-containing K^+ channels have been shown to inhibit the spontaneous and non-specific Ca^{2+} activity in the PC dendrites to encode motor timing signals. Furthermore, these ion channels contribute to the synaptic integration of PF inputs (Khavandgar et al., 2005). Taken together, low-threshold activated and non-inactivating D-type K^+ channels take a part in the integration and generation of finely tuned signals in PCs, thereby signal tuning within physiological appropriate ranges.

Previous studies have shown that A-type K^+ channel and D-type K^+ channels

play similar physiological roles. For example, the A-type I_K contributes to spike acceleration and determines the firing patterns in the cerebellar PCs (Hounsgaard and Midtgaard, 1988; Sacco and Tempia, 2002). Strikingly, this subfamily of K^+ channels is absent in PC somata or dissociated PC, suggesting an exclusive dendritic expression (and axon fiber). In PC dendrites, K_V3 family is also expressed and regulates dendritic active properties. Given the distinct gating properties of A-type K^+ channels from K_V3 family, this subfamily of K^+ channels is implicated in regulating the subthreshold variations of the membrane potential and processing the synaptic inputs (Hoffman et al., 1997; Johnston et al., 2000) .

Instead of dendritic Na^+ channels, cerebellar PC dendrites express Ca^{2+} channels with high density. Therefore, strong depolarization causes synchronization of the passively conducted Na^+ spike and Ca^{2+} spike in dendrites to shape the appropriate spiking activity of PCs. The influx of dendritic Ca^{2+} can activate an ionic flow carried by K^+, Ca^{2+}-activated K^+ channels. These types of channels are classified into two; small conductance and large conductance Ca^{2+}-activated K^+ channel (SK and BK channel, respectively) (Table 3). Both SK and BK channels are also implicated in controlling the spiking activity in PCs (Ryu et al., 2017). When the dendritic membrane is depolarized by synaptic inputs, local $[Ca^{2+}]_i$ is elevated through P/Q type Ca^{2+} channels, leading to the activation of the SK channels (Womack et al., 2004). The SK channels are expressed in PC somata as well as in dendrites. Interestingly, dendrosomatic electrical coupling is governed by SK2 channels in PC soma and dendrite (Womack and Khodakhah, 2003). In addition, somatic and dendritic SK channels show distinct roles in regulating PC activity. SK channels in soma set the maximal level of PC firing frequency, and on the other hand, dendritic SK channels determine the extent of dendritic regions contributing to the firing rates of PCs. The other types of Ca^{2+}-activated K^+ channel, BK channels are also involved in the spiking activity in PCs. As I described above, co-activity of K_V3 and BK channels modulates dendritic Na^+ – Ca^{2+} coupling burst elicited by CF inputs through suppression of Na^+ channel inactivation (McKay and

Turner, 2004). Both SK and BK channels are activated by Ca^{2+} entering through P/Q type Ca^{2+} channels and regulate PC firing patterns. However, these channels differently contribute to firing behavior in PCs. SK channels have an impact on the setting intrinsic firing frequency (Womack and Khodakhah, 2003) whereas BK channels are involved in the regulation of AP waveform and presumably climbing fiber responses (Edgerton and Reinhart, 2003; McKay and Turner, 2004). Recent studies have shown that CF-evoked pause of spontaneous firing and generation of burst firing in PCs require BK channels coupled to Ca^{2+} channels (Irie and Trussell, 2017; Jin et al., 2017). Because SK and BK channels in PCs play a critical role in the regulation of firing behavior, dysfunction of these channels has been implicated in cerebellar disease such as ataxia. Mutations in P/Q type Ca^{2+} channels resulted in the decrease in the precision of PC pacemaking activity and perfusion of 1-ethyl-2-benzimidazolinone (EBIO), K_{Ca} activator improves the regularity of spontaneous firing and motor performance (Walter et al., 2006). In addition, dysregulation of SK and/or BK channels has been reported in various genetic ataxia animal models (Dell'Orco et al., 2015; Egorova et al., 2016; Sausbier et al., 2004; Walter et al., 2006), suggesting that modulation of SK and BK channels may be therapeutic targets for cerebella disease and motor dysfunction.

$Na_V1.6$ (Resurgent Na^+ channel)	
Expression	Dendrite, Node of ranvier
Gating properties	• Sensitivity for tetrodotoxin • Evoked by a step repolarization to -30 mV • Maximum current at Vm = -30 – -40 mV • $V_{1/2\ activation}$ = -40 mV, rising time = 5 – 6 ms • $V_{1/2\ inactivation}$ = -62 mV (low Na+), -53 mV (high Na+), τ_{decay} = 20 – 30 ms
Impact on excitability	• Reopening Na_V when the membrane potential is repolarized to approximately -40 mV • Shortens the refractory period between action potentials, high-frequency firing appears to be facilitated
Ablation	• Reduced spontaneous firing rates • Increased spike adaptation • Cerebellar ataxia & Dysfunction of motor coordination • Impairment of water maze and delayed eyeblink conditioning

Table 1. Active properties of resurgent Na+ channels in the cerebellar PCs and their physiological and pathological roles

$K_V1.4$ & K_V4 (A-type K^+ channel)	
Expression	Dendrite
Gating properties	• Sensitivity for high concentration of 4-AP about 1-10 mM (insensitive for DTX) • Fast-activating and inactivating channel • Activated at subthreshold voltage around -60 mV • $V_{1/2\ activation}$ = -24.9 mV; $V_{1/2\ inactivation}$ = -69.2 mV • $\tau_{deactivation}$ at -70 mV : 3- 4 ms
Impact on excitability	• Acceleration of AP spike • Firing frequency firing pattern (rhythmic Na-Ca spike burst) • Subthreshold variation of membrane properties
Impact on plasticity and learning	• Eyeblink conditioning derives dendritic excitability underlying downregulation of A-type K+ channel
$K_V1.1$, $K_V1.2$, $K_V1.6$ (D-type K^+ channel)	
Expression	Dendrite
Gating properties	• Sensitivity for low concentration of 4-AP about 0.2 - 1 mM and DTX (2.8 - 25 nM) • Low-threshold and non-inactivating channel • activated at -40 – -50 mV • $V_{1/2\ activation}$ = -20 – -30 mV ($K_V1.2$: -5 – 5 mV) • $\tau_{deactivation}$ = 14 – 23 ms
Impact on excitability	• Spike frequency and adaption, dendritic excitability • Amplitude and duration of rebound depolarization • Spontaneous bursts
$K_V3.3$ & $K_V3.4$	
Expression	Soma and Dendrite
Gating properties	• Sensitivity for TEA • Rapid activating at suprathreshold and rapidly inactivating channel • Peak amplitude at 30 mV from -70 mV • $V_{1/2\ activation}$ = -23.0 mV, τ_{decay} = 0.66 ms
Impact on excitability	• Repolarize the membrane potential and maintain repetitive firing • Dendritic burst firing through Ca^{2+}- Na^+ coupling
Impact on plasticity and learning	• Deletion of $K_V3.1/3.3$ causes ataxic behavior

Table 2. Active properties of voltage-gated K+ channels in the cerebellar PCs and their physiological and pathological roles

SK channel (SK2 subfamily)	
Expression	Soma and Dendrite
Gating properties	• Voltage-independent and Ca^{2+}dependent channel • Activated by Ca^{2+} influx through P/Q type Ca^{2+} channel • Sensitivity for apamin (63 pM)
Impact on excitability	• Regulation of firing frequency • Shaping fast afterhyperpolarization (AHP) amplitude • Climbing fiber-induced spike pause duration • Activity-dependent modulation of climbing fiber-evoked EPSP amplitude and dendritic local Ca^{2+} transient
Impact on plasticity and learning	• Activity-dependent downregulation of SK channel by eyeblink conditioning • Inhibition of SK channel prevents LTP-IE induction
BK channel	
Expression	Soma and Dendrite
Gating properties	• Voltage- and Ca^{2+}-dependent • $V_{1/2\ activation}$ = 50 mV at 4μM [Ca^{2+}] to -30 mV at 100μM [Ca^{2+}]
Impact on excitability	• Generation of burst firing through cooperating with K_V3 channels in dendrite • Climbing fiber-evoked spike pause and burst firing coupled to Ca^{2+} channel • Shaping medium or slow component of AHP
Impact on plasticity and learning	• Dysfunction of SK and BK channels is related to cerebellar ataxia

Table 3. Active properties of Ca^{2+}-activated K^+ channels in the cerebellar PCs and their physiological and pathological roles.

1.2 Activity-dependent plasticity of intrinsic. excitability through ion channel modulation

1.2.1 Activity- and experience-dependent intrinsic plasticity and ion channels

Many theories have implicated that the potentiation or depression of the synaptic transmission at the PF-PC synapses and non-synaptic intrinsic plasticity are required for cerebellar-dependent learning and memory. Intriguingly, the intrinsic plasticity requires an activity-dependent modulation of ion channels (figure 2) (Belmeguenai et al., 2010; Hyun et al., 2013; 2015; Ohtsuki et al., 2012; Shim et al., 2017; 2016). The ion channels in the cerebellar PCs are regulated by various factors such as an activation of metabotropic receptor or synaptic plasticity-related intracellular signaling (Belmeguenai et al., 2010; Shim et al., 2016; 2017; Smith and Otis, 2003). When the chronic changes in network activity occur, the neuronal activity is homeostatically regulated in order to maintain the stability of network activity (Cudmore and Turrigiano, 2004; Nataraj et al., 2010; Rutherford et al., 1997; Turrigiano et al., 1994). Prolonged application of tetrodotoxin (TTX) to organotypic cultures of cerebellar slices exhibits downregulation of the intrinsic excitability (Shim et al., 2016). This homeostatic intrinsic plasticity is derived from an augmentation of hyperpolarization-activated cyclic nucleotide-gated (HCN) channel current (I_h) in the cerebellar PCs. Interestingly, the activity-dependent upregulation of I_h in PCs requires an agonist-independent activity of metabotropic glutamate receptor 1 (mGluR1) and its G_S-coupled downstream of PKA signaling. Ablation of HCN channels in PCs exclusively disrupts the integration of inhibitory synaptic inputs and bi-stability of PC firing behavior (Nolan et al., 2003). Furthermore, HCN channels regulate a balance between excitation and inhibition through the integration of glutamatergic and GABAergic transmission and firing stability, thereby promoting memory formation at the late stages of cerebellar learning (Rinaldi et al., 2013).

Recently, plasticity of the intrinsic excitability of the cerebellar PCs has been found to be accompanied by the synaptic plasticity (Belmeguenai et al., 2010; Shim et al., 2017; Yang and Santamaria, 2016). In fact, PF-PC synaptic LTP derives the long-term potentiation of intrinsic excitability (LTP-IE). LTP-IE requires the downregulation of SK2 channels in dendritic area. The SK channel-dependent intrinsic plasticity may play a role in shaping the cerebellar PC output to adjust the impact of synaptic inputs within optimal ranges. The LTP-IE dampens the impact of PF inputs on the firing behavior of PCs, enabling effects of non-potentiated, weaker synaptic inputs on cellular output signal to minimize (Belmeguenai et al., 2010). Interestingly, although local dendritic Ca^{2+} signaling is enhanced after formation of LTP-IE, prior induction of intrinsic plasticity prevents subsequent induction of synaptic LTP in PCs. Therefore, the role of intrinsic excitability in signal processing in the PCs is quite distinct from other types of neurons such as hippocampal pyramidal neurons or cortical neurons because enhanced Ca^{2+} signaling has been regarded as enlargements of synaptic inputs and increases in possibility of subsequent plasticity induction (Ramakers and Storm, 2002; Watanabe et al., 2002). Considering that one important role of SK channels is setting the firing frequency in physiological limits, SK channel-mediated LTP-IE may ensure that excitatory drive stays within the physiological limits and prevent non-specific subsequent synaptic plasticity induction thereby stabilizing and maximizing the information processing after learning.

In addition to the intrinsic plasticity followed by induction of LTP, the activity-dependent downregulation of PF-PC synaptic function accompanies the intrinsic plasticity. Yang et al. (Yang and Santamaria, 2016) described that the potentiation of excitability in PCs is found following an induction of PF-PC LTD through downregulation of HCN channel conductance. Many observations have shown that the associative eyeblink conditioning training exerts modification of synaptic strength (PF-PC LTD) as well as intrinsic properties of the cerebellar PCs (potentiation of excitability) (Fiala et al., 1996; Hauge et al., 1998). Those

described that the activity-dependent plasticity of intrinsic excitability may be homeostatically regulated which is similar to hippocampal intrinsic plasticity (Brager and Johnston, 2007; Fan et al., 2005). Alternatively, Shim et al. (Shim et al., 2017) demonstrated that the intrinsic excitability is found to be decreased following induction of synaptic LTD. This result is parallel with the previous observation in which population spiking activity is attenuated by synaptic LTD induction (Lev-Ram et al., 2003). Those contradictory results may be derived from different experimental conditions: Yang et al. (Yang and Santamaria, 2016) delivered PF stimuli with somatic depolarization instead of CF activation whereas Shim et al. (Shim et al., 2017) synaptically induced synaptic plasticity by delivering simultaneous and conjunctive stimulation of PF and CF within specific time-window. Behavioral training could induce neural plasticity through divergent pathways. Thus, the intrinsic plasticity following synaptic depression may be presumably modulated in various aspects including potentiation or depression of firing rates, responsiveness of synaptic inputs or patterns of spiking activity to achieve maximizing the information storage in the cerebellar circuits.

Several observations have shown that associative eyeblink conditioning accompanies the experience- and use-dependent plasticity in the cerebellar cortex (Halverson et al., 2015; Jirenhed et al., 2017; Johansson et al., 2014; Schreurs et al., 1998; 1997). The experience-dependent plasticity of dendritic membrane excitability can be maintained 1 month after conditioning. Recently, it was shown that the delayed eyeblink conditioning increases intrinsic excitability and changes in AP waveforms, presumably derived from SK channel down-regulation (Titley et al., 2018). There are several evidence supporting that the memory trace in PCs is not just an increase or a decrease in firing rates. In fact, PC activity reflects adaptively timed activity pattern with intrinsic cellular mechanisms rather than a temporal pattern of excitatory or inhibitory synaptic inputs (Halverson et al., 2015; Jirenhed et al., 2017; Johansson et al., 2014). Taken together, experience-dependent modulation of PC intrinsic excitability is another form of memory engram for the

cerebellar-dependent motor learning.

1.2.2 Possible mechanisms for LTD-IE

Since Ito hypothesized that synaptic LTD between PF-PC synapses is the principal elements for the cerebellar-dependent motor learning (Ito, 1982), much of investigation has been extensively focused on the cellular mechanism of the modification of synaptic function to account memory storage in the cerebellum and motor control. Unlikely to synaptic plasticity or LTP-IE, the underlying mechanism for LTD-IE has less been elucidated. Previous reports described that the intrinsic plasticity and synaptic plasticity indeed share intracellular signaling including protein phosphatase and/or protein kinases (figure 2). Several signaling molecules are required to induce PF-PC LTD such as protein kinase C (PKC) and CaMKII. In the hippocampus, HCN channel activity is mediated by PKC signaling during mGluR-dependent plasticity induction, which results in intrinsic plasticity. However, mGluR-PKC signaling suppresses I_h, insisting that the LTD-IE in the cerebellar PCs may not be reflected by this signaling cascade. CaMKII is also known for a crucial element of synaptic and intrinsic plasticity. In the VN neurons, the activity-dependent plasticity of excitability requires bidirectional modulation of BK channels mediated by the balance between PKC and CaMKII activity (McElvain et al., 2010; Nelson et al., 2005; Smith et al., 2002; van Welie and Lac, 2011). The cerebellar PF-PC synaptic LTD recruits CaMKII signaling which increases open probability of BK channels, thus this type of K_{Ca} may be one possible candidate for the activity-dependent intrinsic plasticity in the cerebellar PCs. Since the cellular and molecular basis for LTD-IE of the cerebellar PCs remain unclear, the detailed mechanisms for the intrinsic plasticity should be further investigated.

Intrinsic plasticity plays a complementary role in integrating synaptic inputs and generating cellular output signal (Brager and Johnston, 2007; Fan et al., 2005; Grasselli et al., 2016; Mahon and Charpier, 2012; Nataraj et al., 2010; Shim et al.,

2017). Synaptic-driven potentiation or depression of excitability show the same polarity with the corresponding direction of synaptic plasticity (Belmeguenai et al., 2010; Shim et al., 2017), indicating that the modifications in synaptic strength are synergistically reflected into the final net output of PCs following plasticity. When the synaptic weight is strengthened, the PC output signal is more potentiated, not compensated by intrinsic properties. In addition, cerebellar PC intrinsic plasticity occurs in the branch-dependent manner (Ohtsuki et al., 2012), indicating that synaptic inputs from specific-branches are potentiated by increased membrane excitability limited in conditioned dendritic branches. Otherwise, the plastic changes in synaptic transmission might be contaminated by global changes of excitability and less reflected into the neuronal firing output signal.

1.2.3 Upside down: to what extent does bidirectional intrinsic plasticity in the cerebellar dependent-motor learning do?

What is the physiological consequence of the bidirectional modulation of intrinsic excitability following plasticity induction or behavioral training? Vestibulo-ocular reflex (VOR) and optokinetic response (OKR) is a representative behavioral paradigm of cerebellar-dependent motor learning. The VOR gain, the ratio of vestibular stimuli to adaptive eye-movement, can be increased or decreased depending on the learning paradigm. Boyden and Raymond (Boyden et al., 2006) reported that the VOR gain-up and -down learning are selectively engaged by the aspects of synaptic plasticity. There was a supporting evidence of this view in which injection of mGluR1 antagonist into the cerebellar flocculus, the core area for VOR learning in the cerebellum, suppresses gain-up learning whereas gain-down learning is not affected by either agonist and antagonist of mGluR1 (Titley et al., 2010). In addition, an ultrastructural observation shows a reduction of surface AMPA receptor following the adaptive eye-movement learning, suggesting that the cerebellar LTD would occur during the motor learning (Wang et al., 2014). Most recently, it was revealed that the adaptive eye-movement training is associated with

modifications of synaptic transmission at the PF-PC synapses (Inoshita and Hirano, 2018), indicating the prominent roles of bidirectional synaptic plasticity at PF-PC synapses in the motor learning.

In contrast to Ito's cerebellar LTD theory, many studies have shown that the PF-PC LTD may not be a sufficient cellular mechanism underlying motor learnings in spite of abundant studies describing the critical roles of PF-PC LTD in VOR learning (Ito, 2013; Jörntell and Hansel, 2006; Ke et al., 2009; Schonewille et al., 2010; 2011; Wulff et al., 2009). (Miles and Lisberger, 1981b; 1981a) proposed an alternative mechanism for motor learning, which suggests principal roles of VN neurons in the motor memory storage. There is, however, accumulating evidence showing that motor memory storage requires neuronal plasticity at multiple sites including neurons in the cerebellar cortex and VN (Boyden et al., 2004; Gao et al., 2012). Recently, a computational model for motor memory storage provided insights into the mechanism by which motor memory traces are seemingly transferred from cortical neurons (PC) to sub-cortical region (VN) (Clopath et al., 2014; Yamazaki and Nagao, 2012)Cumulative experimental data has shown that encoding the adaptive motor memory in the cerebellar cortex occurs within a few hours and the critical time window for memory transfer is approximately 2.5 – 4 hours after training (Kassardjian et al., 2005; Okamoto et al., 2011a). Interestingly, (Ito, 2013) recently suggested that an early adaption is dependent on the cerebellar cortical activity and the late phase of adaptation is accompanied by plasticity in the VN neurons. In parallel, the changes in the population spiking activity in VN neurons are manifested a day after training whereas there is no significant alteration of VN activity within an hour after training (Shutoh et al., 2006). Until recently, this prediction for memory consolidation mechanism has not been investigated in a cellular and circuit level. Recent papers suggested that the intrinsic plasticity of the PCs might be the mechanism of the memory transfer from cerebellar cortex to sub-cortical areas (Ryu et al., 2017; Shim et al., 2017). Collectively, computational implications and experimental observations have both

agreed to Ito's recent suggestion in which PF-PC synaptic plasticity may take part in the memory acquisition and plasticity in MF-VN synapses may be involved in long-term memory storage beyond two long-lasting conflicts for VOR memory: Marr-Albus-Ito's cerebellar LTD hypothesis vs. Miles and Lisberger' MF-VN synaptic plasticity theory.

(Belmeguenai et al., 2010) and (Shim et al., 2017) insisted that the intrinsic plasticity is modulated by synaptic activity pattern-dependent manner and this bidirectionality may function as an amplifier of the synaptic modification, enabling to transduce the finely tuned signal into the relay neurons such as neurons in DCN or VN. Given that the neural plasticity in the neurons in the cerebellar cortex and VN shows bidirectionality, the intrinsic plasticity would be also selectively engaged by certain forms of learning paradigm and the synergies with synaptic modulation may complete the scenario for the memory storage in the motor circuitry including cerebellum and VN.

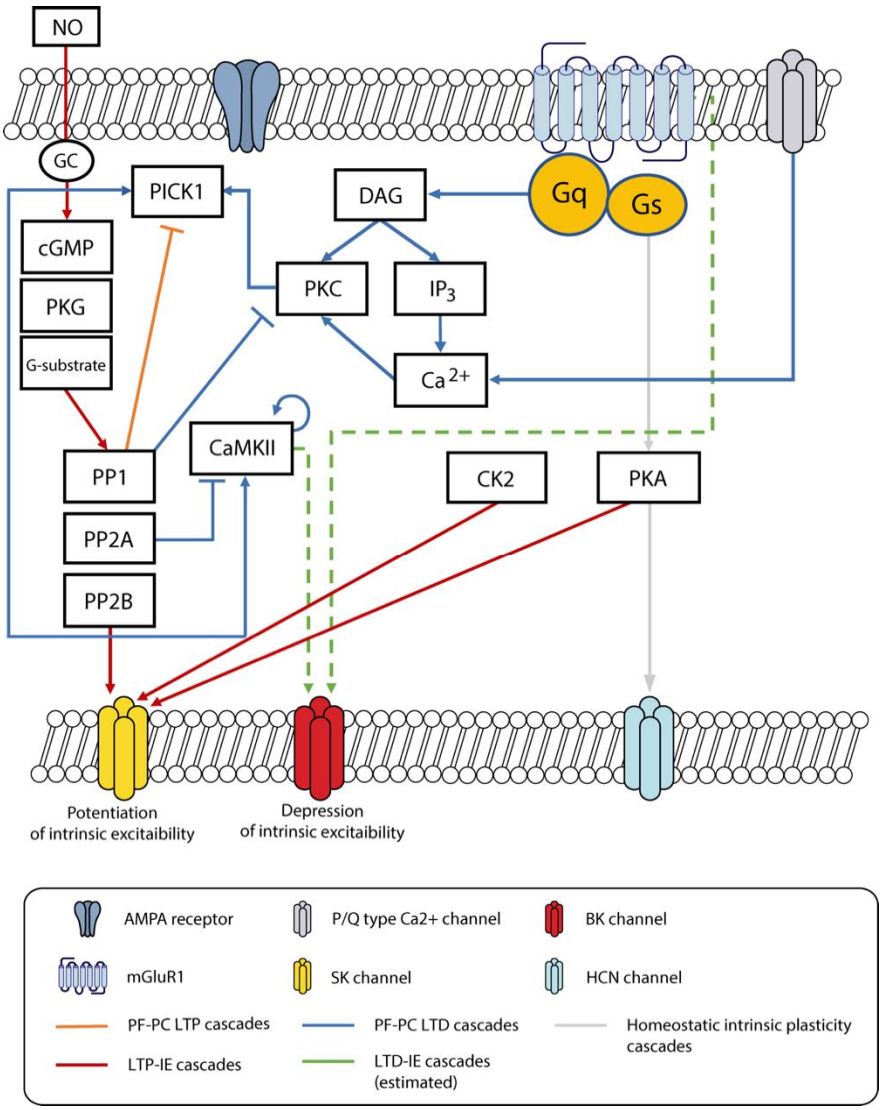

Figure 2. Schematic illustration for molecular signal cascade for synaptic and intrinsic plasticity in the cerebellar PCs. Intrinsic plasticity indeed shares intracellular signal cascade for synaptic plasticity, in which LTP-IE requires activation of phosphatases such as PP1 and PP2B whereas LTD-IE is dependent on PKC activation. In contrast to abundant studies describing the cellular mechanisms and behavioral outcomes of LTP-IE, detailed mechanisms of LTD-IE and its behavioral impact are still elusive although synaptic LTD has long been considered as cellular basis for cerebellar motor learning. In this review, BK channels are proposed for one plausible ion channels involved in LTD-IE. CaMKII activation is found to be involved in upregulation of BK channel activity (green dot line) in the VN neurons.

1.3 The further implication of intrinsic plasticity in the. memory circuits

There are many unanswered questions to be solved in terms of the intrinsic plasticity and behavior. In the classical view of the intrinsic plasticity, changes in excitability have been considered to play pivotal roles in promoting subsequent induction of synaptic plasticity through the up- or downregulation of dendritic ion channels. Thus, the intrinsic plasticity of neurons has been thought as simply a supportive mechanism for activity-dependent modification of synaptic function although the information is conveyed by the AP spikes between neurons. However, some of the suggestions have described that activity-dependent modifications of ion channels can also undergo experience-dependent long-term plasticity beyond changes in synaptic weight (Crestani et al., 2018; Gao et al., 2012; Kim and Linden, 2007; Lisman et al., 2018; Park et al., 2016; Zhang and Linden, 2003; Zhou et al., 2009). Furthermore, cumulative evidence has shown that memory trace should move from one brain region to another brain region to consolidate the long-term memory (Frankland and Bontempi, 2005; Nagao et al., 2013; Okamoto et al., 2011a; Preston and Eichenbaum, 2013; Restivo et al., 2009; Squire and Wixted, 2011; Wang et al., 2014)Intrinsic plasticity may be one plausible mechanism of memory transfer via modulating the strength of connectivity between memory circuits.

Since the majority of researches have been performed to elucidate the mechanisms of cerebellar memory formation by using *in-vitro* cell lines or brain slices, the memory circuits should be assumed by using mathematical models that are made from biochemical observations, physiological recordings and behavioral assessments. Nevertheless, there has been an incongruity between theoretical models and actual experimental data which has to be reconciled. Recently, technical advances have enabled neuroscientists to overcome the experimental

limitations and expand the research scope from modifications in individual neurons to macroscopic alteration involved in shaping the memory *in vivo*. Observations of neuronal ensemble activity from freely moving animals provide insights into how the information is processed within given local circuits. In learning period, neurons that show ensemble activity may encode the similar information and these neurons will be wired to fire together so that the connectivity between them will be strengthened. Indeed, engram cells who store memory show higher excitability than others, indicating that forming stable ensemble may reflect the induction of intrinsic plasticity in the neurons (Lisman et al., 2018). Collectively, experience-dependent modulation of neuronal excitability determines the net out signals in neurons and generates synchronized population activity to project the information into another brain area.

In the neural circuitry for the cerebellar-dependent motor learning, it is unclear how the information is transferred to the sub-cortical area including DCN and VN neurons from cerebellar PCs is unclear. In the hippocampus, electrophysiological recording and optogenetic manipulation of neural circuits have revealed that the specific frequency of an oscillatory neural activity, called sharp wave ripple (SWR), involves in memory transfer from the hippocampus to cortex (BuzsÁk, 1998; Carr et al., 2011; Poo et al., 2016; Tang and Jadhav, 2018). During learning, an interplay between synaptic and intrinsic plasticity increases the number of SWR replay events and thereby consolidating the long-term memory. Although the oscillatory activity of the cerebellum has been reported, detailed mechanisms and its physiological roles in formation of memory engram in the motor learning circuits have yet to be investigated. During VOR learning, spike discharge in the cerebellar PCs shows a sinusoidal pattern in response to vestibular head movement (Fukushima et al., 1993; 1996; Mizukoshi et al., 1983). Interestingly, the phase of the oscillatory pattern of PC firing activity is altered after the training session, indicating that the response timing to sensory stimuli may be endowed with plastic changes. Therefore, the intrinsic plasticity of PCs may modify the patterns to

integrate the synaptic inputs and to generate the spike discharge in response to sensory information.

Since memory is stored throughout the brain region, synergistic modulation of circuit dynamics might play critical roles. Various cutting-edge technologies enable to monitor the activity of large neuronal population and to manipulate the strength of neural circuits and corresponding behavioral outcomes. For example, recent studies using wide-field and high resolution in-vivo two-photon Ca^{2+} imaging approaches from behaving animals revealed the groundbreaking finding of the how the cerebellar granule cells process the sensory information (Giovannucci et al., 2017; Wagner et al., 2017). These results from *in vivo* experiments lead us to re-evaluate the previously established hypothesis of the intrinsic excitability based on the results largely obtained from *in vitro* experiments. Many studies suggest that the PC modulates the membrane potential of the VN neurons by providing a tonic inhibition or strong hyperpolarization to induce rebound burst firing of neurons in DCN or VN. Although plasticity in both cerebellar cortex and VN play roles in the VOR memory storage, the neural plasticity occurs at the distinct time window (Kassardjian et al., 2005; Okamoto et al., 2011a; Shutoh et al., 2006; Yamazaki et al., 2015). These observations have suggested the serial relationship of neural plasticity between the cerebellar cortex and VN, it is, however, still elusive how the memory is transferred from cerebellar cortex to sub-cortical area. Cell type- and engram cell-specific tagging and manipulation with a high temporal and spatial resolution may help elucidating the role of PC output modulation during VOR training and memory transfer period. The modular structure of the cerebellar cortex has been considered as an unit for an information processing, thus ensemble activity of the cerebellar PCs may provide strong instructive signals to VN neurons (Gao et al., 2016). Investigation from freely moving awake animals may give us the insight into the circuit mechanisms for sensory information processing and memory storage in the cerebellar motor learning circuits.

Chapter 2

Type 1 metabotropic glutamate receptor mediates homeostatic control of intrinsic excitability through hyperpolarization-activated current in cerebellar Purkinje cells

Introduction

Central nervous system is highly endowed with plasticity in an activity-dependent fashion. Long-lasting alteration of the neural activity causes plastic changes in neuronal activity in the given circuits to keep the optimal ranges of network activity, this change is called as homeostatic plasticity. Of interest, the homeostatic intrinsic plasticity maintains the stability of neuronal network activity against environmental or pathological destabilization, which includes the modulation of post-synaptic neurotransmitter receptors and the differential expression of ion channel genes (Desai et al., 1999; Naudé et al., 2013). It therefore serves as a basis for the neural network to achieve an optimal activity range. Intrinsic cellular excitability, in particular, determines the total output of a neuron by integrating synaptic inputs and consecutively translating them into the firing of an action potential (AP). Thus, homeostatic intrinsic excitability plays a pivotal role in maintaining the network balance and maximizing information storage by tuning the average firing rate through the modulation of multiple neurotransmitter receptors and voltage-dependent channels (Stemmler and Koch, 1999). Homeostatic intrinsic plasticity is a fascinating model on the plastic changes in neural circuits in both physiological and pathological conditions (Beraneck and Idoux, 2012; Lambo and Turrigiano, 2013; O'Leary et al., 2014). However, much of the detailed cellular and molecular basis for these regulatory mechanisms are largely unknown.

Type 1 metabotropic glutamate receptor (mGluR1) is involved in short-term and long-term plasticity of the neurons. Interestingly, the mGluR1 has been found to be required either Hebbian or homeostatic synaptic plasticity using similar intracellular signaling cascades including calcium influx as well as induction of the immediate early gene Homer1a, Arc and eukaryotic elongation factor2 (eEF2) (Hu et al., 2010; Shepherd et al., 2006; Sutton et al., 2007). In addition, mGluR-dependent synaptic plasticity also can lead to change the intrinsic excitability

(Brager and Johnston, 2007). Moreover, mGluR was found to be involved in homeostatic intrinsic plasticity among 873 novel chronic activity-regulated transcripts (Lee et al., 2015). Given the note that there are mutual intracellular signalings for hebbian and homeostatic scaling, homeostatic regulation of intrinsic excitability could share a signal cascade with intrinsic plasticity following the Hebbian rule. Therefore, I investigated whether mGluR1s contribute to homeostatic intrinsic plasticity. To test this, I prepared organotypic slice cultures of rat cerebellum to mimic the physiological neuronal connection in the cerebellar cortex and electrophysiological properties were observed by whole-cell patch clamp technique. The intrinsic excitability of the cerebellar PCs was decreased through the upregulation of hyperpolarization-activated current (I_h) after 2-days of chronic activity deprivation by applying 1 μM of tetrodotoxin (TTX), Na^+ channel blocker. Interestingly, homeostatic suppression of the PC excitability was prevented by co-application of mGluR1 inverse agonist, suggesting that agonist-independent constitutive activity of the mGluR1 may be required for homeostatic regulation of intrinsic excitability. The homeostatic upregulation of I_h was also abolished by co-application of mGluR1 inverse agonist with activity-deprivation. These observations indicate that homeostatic intrinsic excitability in cerebellar PCs is mediated by the agonist-independent activity of the mGluR1 through activity-dependent regulation of I_h.

Material and Method

1. Animals

All animals and experimental procedure described in this dissertation were approved by the Institution's Animal Care and Use Committee of Seoul National University College of Medicine and were in accordance with the ethical standards of the institutional research committee.

2. Slice preparation

Brain slices were obtained from postnatal days 10 male Sprague Dawley rats. After brain dissection, 250 μm cerebellar sagittal slices were made with a vibrating tissue slicer (Microm HM 650V) in ice-cold standard artificial cerebrospinal fluid solution (aCSF): (in mM) 124 NaCl, 2.5 KCl, 1 NaH_2PO_4, 1.3 $MgCl_2$, 2.5 $CaCl_2$, 26.2 $NaHCO_3$ and 20 D-glucose, bubbled with 95% O_2, 5% CO_2, pH 7.4). Sagittal planes of cerebellar slices were transferred onto membrane of culture insert (pore size 0.4 μm) in 6-well-plastic plates. Culture medium (1 ml), composed of 50% basal medium with Earle's salts, 25% HBSS, 25% Heat-inactivated horse serum, 1% L-glutaMaxTM-1 and 5 mg/ml glucose, was added into each well below the culture inserts. Cultured slices were incubated at 35°C in an atmosphere of humidified 5% CO_2, and half of medium was replaced every 2-3 days.

3. Western blot analysis

For western blot, cultured slices were homogenized with homogenizing buffer (1% Triton X100, 0.1% SDS, 50 mM Tris-HCl, 0.3 M sucrose, 5 mM EDTA with protease inhibitor cocktail and pH 7.5) on ice. Lysates were boiled for 2 min at 60°C and loaded by 4-12% gradient SDS-PAGE gel. Separated proteins were transferred to PVDF membrane. The membrane blocked with 5% skim milk in TBS-T (24.7 mM Tris, 137 mM NaCl, 2.7 mM KCl and 1% Tween 20, pH 7.4) for 1 h and incubated with Anti-$mGlu_1$ receptor α (anti-mouse, 1:2000, BD Bioscience), Anti-β-actin (anti-mouse, 1:3000, Sigma) for additional 1 h. After washing with TBS-T, the membrane was incubated overnight at 4°C with

horseradish-peroxidase-conjugated appropriate goat IgG (1:2000, Stressgen). The immunoblots were developed with enhanced chemiluminescence (ECL) solution (Invitrogen). For quantifying the band, Quantity One (Bio-Rad) was used.

4. Electrophysiology

Whole-cell patch clamp configurations were made from 10-12 days *in vitro* (DIV) slices. Slices were put onto a submerged recording chamber on the stage of Olympus microscope (BX50WI, Japan) and perfused with aCSF at 32°C, and kept in place with a nylon-strung platinum anchor. All recordings were performed using multiclamp 700B patch-clamp amplifier (Axon Instruments) with a sampling frequency of 20 kHz and signals were filtered at 2 kHz. For current clamp experiments, standard aCSF was used as extracellular solution described above; for voltage clamp experiments to isolate $I_{h,}$ slices were incubated with extracellular solution composed of (in mM) 115 NaCl, 1.2 NaH_2PO_4, 5 KCl, 2 $CaCl_2$, 1 $MgCl_2$, 25 $NaHCO_3$, 20 glucose, 1 $BaCl_2$, 5 tetraethyl ammonium (TEA), 1 4-aminopyrimidine (4-AP), 1 $NiCl_2$, 0.1 $CdCl_2$, 0.01 NBQX, 0.1 Picrotoxin and 0.0005 TTX, bubbled with 90% O_2, 5% CO_2, pH 7.4 (Nolan et al. 2003). Both excitatory and inhibitory synaptic inputs were all blocked by 10 μM 2,3-dihydroxy-6-nitro-7-sulfamoyl-benzo[f]quinoxaline-2,3-dione (NBQX) and 100 μM picrotoxin, respectively. Patch pipettes (3-4 MΩ) were borosilicate glass and filled with internal solution containing (in mM), 9 KCl, 10 KOH, 120 K-gluconate, 3.48 $MgCl_2$, 10 HEPES, 4 NaCl, 4 Na_2ATP, 0.4 Na_3GTP, and 17.5 sucrose, pH adjusted to 7.25. Electrophysiological recordings were started 5 min after obtaining the whole-cell configuration to let the internal solution diffuse enough into the cytosol.

5. Data acquisition and analysis

All data were acquired by Clampex software (Molecular Devices) and analyzed by IgorPro 8.1 (Wavemetrics). Otherwise I note, a cell was clamped at -70 mV

with current injection and neurons with the injection current below -500 pA were discarded from this analysis. To evaluate the PC excitability, a series of current steps of 1s duration ranging from +100 pA to +500 pA in 100 pA increments with a step interval of 4.5 s was applied to the cell from the membrane potential of -70 mV. Input resistance (R_{in}) was measured by injecting brief current (-200 pA or +100 pA; 100 ms) and was determined from the negative peak voltage deflection during current injection. Voltage threshold ($V_{threshold}$) of AP was defined as the voltage where the dV/dt first exceeds 30-60 mV/ms. Membrane capacitance (C_m) was calculated by $C_m = \tau/R$, at which the time constant (τ) and series resistance (R_S) were calculated fitting a single exponentials to the voltage responses of the test pulse (-5 mV). Resting membrane potential (V_m) was measured when injected current was absent in current clamp mode with 1 μM TTX to prevent spontaneous AP firing. The AP waveform, including AP amplitude, half-width, 10-90% rise time and first spike latency was analyzed from the first evoked AP of the firing train when +400 pA of the depolarizing current was injected. AP amplitude was determined as difference between peak amplitude and the voltage threshold of the AP. Half-width and 10-90% rise time were the time duration at the half-maximal voltage, elevation time from 10% to 90% of the maximal AP voltage, respectively. The first spike latency was defined as the delay from beginning point of depolarizing current injection to the voltage threshold where the upstroke phase of the first spike was initiated. Fast afterhyperpolarization (fAHP) and medium afterhyperpolarization (mAHP) were measured by calculating the difference between voltage threshold and hyperpolarized negative peak voltage after the first AP or depolarizing square current injection, respectively.

The amount of voltage sag determined as difference between the maximum and steady state voltage during the hyperpolarizing current injection from -100 pA to -600 pA with increment of -100 pA for 1 s with a step interval of 5 s. This sag amplitude was converted to sag percent, representing percentage change between two states. $[(V_{Max} - V_{Steady\ state})/V_{Max}] \times 100$. For I_h current isolation in voltage

clamp, membrane potential was held at – 45 mV and step voltage was applied from -50 mV to -120 mV with increments of -5 mV of 2.5 s.

Data are presented as mean ± SEM and statistical evaluations were performed using two sample *t*-test, two-way repetitive measured ANOVA with post *hoc* Tukey's test and Mann-Whitney U test by Origin 8.5 and SigmaPlot 12.0 software, and the normal distribution was verified.

Results

2.1 Chronic activity-deprivation reduces intrinsic excitability of the cerebellar Purkinje cells

To set up the chronic activity-deprivation model in the cerebellar cortex, I made organotypic cerebellar cultures rather than primary culture neurons to better preserve in vivo circuits. Cerebellar network activity was deprived by applying 1 μM of TTX for 2 days in order to investigate homeostatic intrinsic plasticity in cerebellar PCs (fig. 3A). Cultured slices were used at least a week after preparation. To measure the PC excitability, square-wised brief current step was injected into the PC soma from the membrane potential of about -70 mV under the presence of excitatory and inhibitory synaptic blockers (1 s, from +100 pA to +500 pA with an increment of 100 pA, step interval 4.5 s, see Materials and Methods). Depolarized-evoked AP firing rates of control and TTX-treated (deprived) PCs were compared. Activity-deprivation reduced the intrinsic excitability of the PCs over most ranges of the current injection (fig. 3B, firing frequency (Hz): control = 31.2 ± 1.7 at 400 pA injection, n = 24; deprived = 20.4 ± 1.9, n = 20; control vs. deprived: $p<0.001$, two way RM ANOVA). The active properties of the neurons were analyzed from the first spike of the evoked spike train when +400 pA current was injected (fig. 3C and D, Table 4). Deprived PCs showed higher current threshold ($I_{threshold}$) for evoking spikes whereas $V_{threshold}$ did not change (fig. 3C and D, $I_{threshold}$ (pA): control = 200.6 ± 10.7; deprived = 235 ± 8.2; control vs. deprived: $p<0.05$; $V_{threshold}$ (mV): control = -40.2 ± 1.0; deprived = -40.3 ± 1.0; control vs. deprived: $p = 0.95$). The passive membrane properties C_m and V_m were not altered by activity-deprivation [Table 4, C_m (pF): control = 242.6 ± 17.2; deprived = 259.1 ± 10.4; control vs. deprived: $p = 0.4$, V_m (mV): control = -52.9 ± 1.2; deprived = -50.6 ± 1.4; control vs. deprived: $p = 0.2$]. To measure input resistance, voltage response was measured when brief hyperpolarizing and subthreshold depolarizing current (-200 pA and +100 pA) were injected in the current clamp mode (fig. 3E). Input

resistance was significantly reduced in deprived neurons resulting in less response to a current inputs of voltage deflection (control = 85.8 ± 5.4 MΩ; deprived = 59.2 ± 4.5 MΩ; control vs. deprived: $p < 0.001$). The AP waveform including the AP amplitude (control = 55.3 ± 1.0 mV; deprived = 57.8 ± 1.0 mV), the half-width (control = 0.39 ± 0.01 ms; deprived = 0.39 ± 0.01 ms) and AP rise time (control = 0.25 ± 0.01 ms; deprived = 0.22 ± 0.01), first spike latency (control = 24.6 ± 1.7 ms; deprived = 28.8 ± 2.1 ms) and fAHP (control = 10.3 ± 0.8; deprived = 9.3 ± 1.0) was not changed in the activity-deprived condition (Table 4). mAHP was increased in the deprived neuron (Table 4, control = 9.8 ± 0.7; deprived = 12.7 ± 0.9; control vs. deprived: $p<0.05$, statistical evaluation of all active and passive properties were done by two sample t-test).

2.2 Homeostatic intrinsic plasticity of the cerebellar Purkinje cells is mediated activity-dependent modulation of I_h

Among the parameters of the AP waveform (Table 4), the input resistance was found to be reduced after prolonged inhibition of the network activity (fig. 3E). This result led me to hypothesize that hyperpolarization-activated cyclic nucleotide gated (HCN) channel is involved in homeostatic regulation of PC excitability based on the previous observations reporting that the I_h modulates the cellular excitability via regulating input resistance (Brager and Johnston, 2007). To answer this, sag potential and rebound depolarization were measured by hyperpolarizing step current injection (from -100 pA to -600 pA with an increment of -100 pA for 1 s with a step interval of 5 s) in the current clamp mode (fig. 3F – H). Considering the differences of peak voltage corresponding to the hyperpolarizing currents between neurons, the sag potential was normalized by the maximal negative voltage then recalculated as a percentage (fig. 3G). In deprived neurons, all I_h components were elevated (voltage sag (mV): control = 6.7 ± 0.6 at -400 pA injection, n = 12; deprived = 10.2 ± 0.8 at -400 pA injection, n = 14; control vs. deprived: $p<0.05$, two-way RM ANOAVA ; sag % (%): control = 24.0 ± 1.8;

deprived = 40.3 ± 2.2 at -400 pA injection; $p<0.001$, two sample t-test; rebound depolarization: control = 4.0 ± 0.3; deprived = 7.3 ± 0.6 at -400 pA injection; $p<0.001$, two sample t-test). Furthermore, I measured I_h from the control and deprived neurons in voltage clamp mode. To isolate and compare I_h, hyperpolarizing voltage steps ranging from -45 mV to -120 mV for 1 s with increment of -5 mV were injected in the presence of Na^+, K^+ and Ca^{2+} channel inhibitors (see the Material and method). The hyperpolarization-induced current was recalculated into current density. In parallel with sag potential, I_h density was augmented in deprived neurons compared to the control (fig. 3I, control I_h density = -1.0 ± 0.1 pA/pF at Vm = -100 mV, n = 15; deprived I_h density = -1.5 ± 0.1 pA/pF, n = 14; control vs. deprived: $p<0.05$, Two-way RM ANOVA). The tail current was normalized to the maximal amplitude, and then, the resulting data were fitted with a Boltzmann function (fig. 3J). The half-maximal voltage ($V_{50\%}$) was not shifted (control = 84.9 ± 0.5 mV; deprived = -85.9 ± 0.8 mV), suggesting that voltage-dependency was not affected by activity-deprivation.

To test whether the downregulation of intrinsic excitability was mediated by elevation of I_h, the firing rates from the control and deprived neurons were compared before and after applying 4-Ethylphenylamino-1,2-dimethyl-6-methylaminopyrimidinium chloride (ZD 7288), a selective inhibitor of HCN channels (fig. 3L and M). When the HCN channels was blocked, firing rates were robustly increased in both groups. However, there were no significant differences of firing rates after application of ZD7288 between control and deprived neurons (fig. 3L, control: pre firing frequency (Hz) = 26.7 ± 4.3, ZD 7288 = 45.4 ± 3.5; deprived: before firing frequency (Hz) = 11.7 ± 2.5, after = 46.7 ± 2.1). In addition, the input resistance was also increased following application of the ZD 7288; the difference between the control and deprived neurons was also indisputably abolished by ZD 7288 (fig. 3M, control: pre ZD 7288 input resistance (MΩ) = 89.3 ± 6.7, post ZD 7288 = 224.2 ± 23.5, n = 6; deprived: pre ZD 7288 input resistance = 60.6 ± 6.0, post ZD 7288 = 178.2 ± 9.7, n = 5; pre ZD 7288 $p<0.05$, post ZD

7288 p = 0.12, two sample t-test). Therefore, I conclude that the activity-dependent modulation of I_h underlies the homeostatic intrinsic plasticity in the cerebellar PCs.

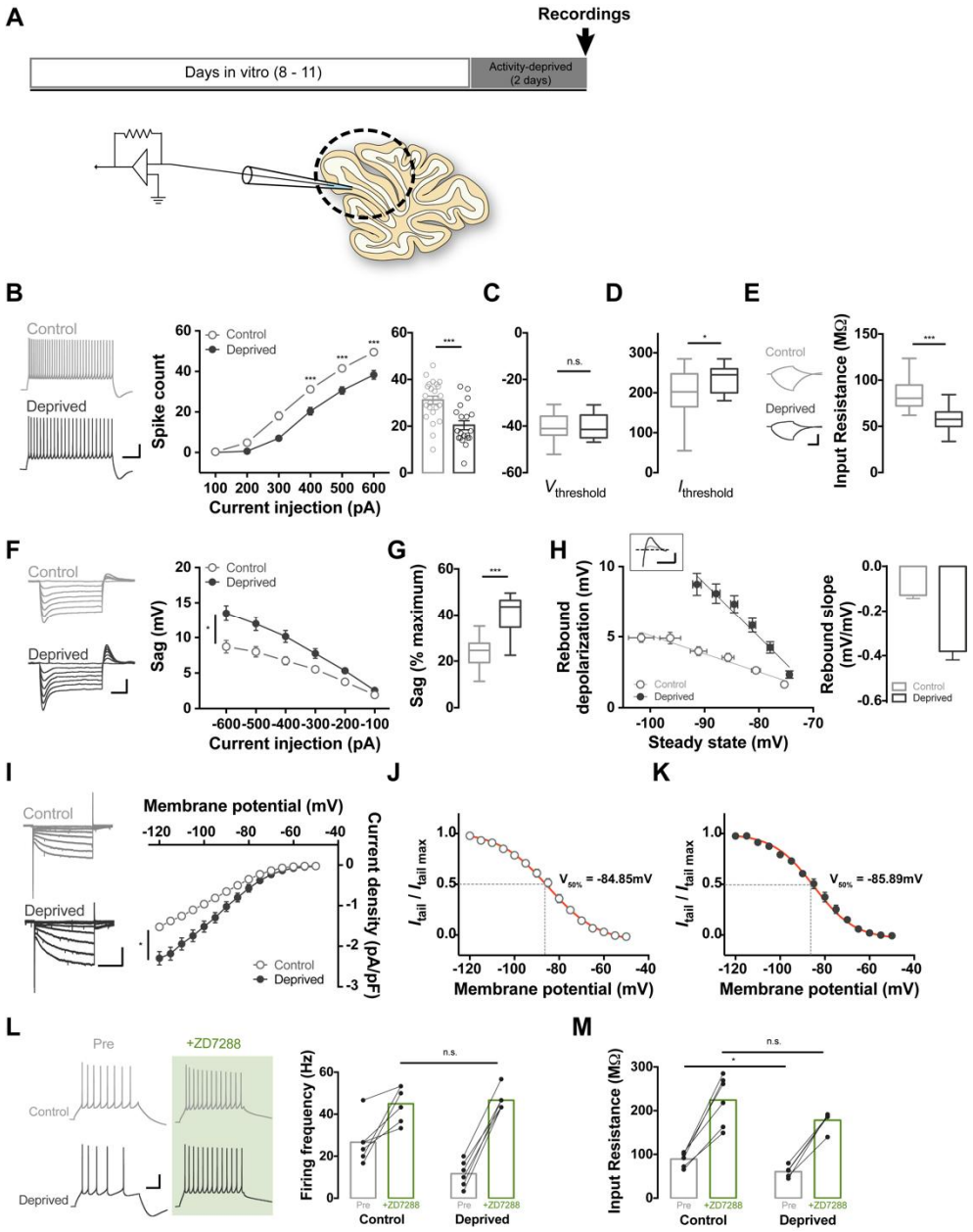

Figure 3. Chronic activity-deprivation reduces intrinsic excitability of the cerebellar Purkinje cells through upregulation of I_h. (A) Experimental scheme. Network activity totally deprived by treatment of 1 μM tetrodotoxin (TTX) for 2 days in organotypic cerebellar slice culture. Electrophysiological recording was performed at anterior lobule (lobule III–V). (B) Representative traces (left), plots (middle) and bar graphs at + 400 pA injection (right) showing that chronic activity-deprivation decreased intrinsic excitability of PCs. (C - D) Bar graph showing that chronic activity deprivation increased current threshold ($I_{threshold}$), but voltage threshold ($V_{threshold}$). (E) Representative traces (left) and summarizing graph (right) showing the input resistance was decreased after chronic activity deprivation. Grey, control; black, deprived. (F) Representative traces (left) and plots (right) showing that voltage sag was significantly increased in deprived neurons (black) vs. control (grey). (G) Bar graph of normalized sag voltage by maximal potential showing the increased voltage sag in

deprived neurons. (H) Representative traces (inset), plot (bottom), and bar graph (right) showing relationship between rebound depolarization and steady-state voltage and calculated rebound slope from control and deprived. (I) Representative traces (left) and plots (right) showing that I_h density was increased in deprived neurons vs. control. (J - K) Tail current was normalized by maximal tail current amplitude and fitted by Boltzmann function from control (J) and deprived neurons (K). (L) Representative traces (left) and summarizing plot (right) showing that decrease in the intrinsic excitability of the deprived (gray) neurons was restored to control (green) in ZD 7288. (M) Bar graph showing the decrease in input resistance in deprived neurons was abolished by ZD 7288. Asterisks in B marked by post hoc Tukey's test, pairwise comparison followed by Two-way RM ANOVA, D, E, G, L and M marked by t-test and F and I marked by Two-way RM ANOVA; *P < 0.05, ***P < 0.001; n.s., no significance.

Parameter	Control	Deprived
$V_{threshold}$ (mV)	-40.2 ± 1.0	-40.3 ± 1.0
$I_{threshold}$ (pA)	200.6 ± 10.7	235.0 ± 8.2
AP amplitude (mV)	55.3 ± 1.0	57.8 ± 1.0
Harf-width (ms)	0.4 ± 0.01	0.4 ± 0.01
Rist time (ms)	0.25 ± 0.05	0.22 ± 0.01
First-spike latency (ms)	24.6 ± 1.6	28.8 ± 2.1
fAHP (mV)	10.3 ± 0.8	9.3 ± 1.0
mAHP (mV) *	9.8 ± 0.7	12.7 ± 0.9
R_{in} (MΩ) ***	85.8 ± 5.4	59.2 ± 4.5
V_m (mV)	-52.9 ± 1.2	-50.6 ± 1.4
C_m (pF)	241.6 ± 17.2	259.2 ± 10.4

Table. 4. Parameters of AP properties and waveform. Among active membrane properties, $I_{threshold}$, was increased under deprived condition whereas $V_{threshold}$ were not changed (see also figure 1). AP waveform including AP amplitude, half-width, 10-90% rise time and first spike latency, was monitored. The parameters were not affected by activity-deprivation. mAHP was increased in deprived neurons, whereas fAHP was not altered. Among the passive membrane properties (C_m, V_m and R_{in}), the only R_{in} was changed by activity-deprivation. For comparison of the active and passive membrane properties, changes were described here to those shown in figure 1C and D; *$p<0.05$, ***$p<0.001$.

2.3 Homeostatic intrinsic plasticity of the cerebellar Purkinje cells requires agonist-independent action of mGluR1

The activation of mGluR1 induces plasticity of the intrinsic excitability by initiating a signal cascade resulting in the regulation of ion channels such as I_h, Ca^{2+} channels, and K^+ channels (Brager and Johnston, 2007; Kammermeier et al., 2000). In addition, I observed that the homeostatic intrinsic plasticity requires upregulation of I_h following activity-deprivation. Interestingly, agonist-independent (constitutive) activity of mGluR has been found to be required for interplay between the Hebbian and homeostatic synaptic plasticity (Hu et al., 2010). It is, however, unclear whether homeostatic intrinsic plasticity also underlies agonist-independent activation of mGluR1 for a homeostatic perspective. Given the note that amount of mGluR1 is regulated in an activity-dependent manner (Ehlers, 2003), I hypothesized that the constitutive activity of the mGluR1 is required for homeostatic control of intrinsic excitability in the cerebellar PCs. To answer this, the amount of mGluR1 in the cerebellar cortex was compared with control and deprived slices. In parallel with the previous observation, mGluR1 expression level was increased after 2-days of inactivation of network activity in the cerebellar slices (fig 4A, control vs. deprived: $p < 0.05$, Mann-Whitey U test). This result suggests that mGluR1 may contribute to homeostatic intrinsic plasticity because the facilitated agonist-independent activity of GPCRs corresponds with increased protein level (Smit et al., 1996). To further examine the mGluR hypothesis, I treated inverse agonist of mGluR1, (3aS,6aS)-Hexahydro-5-methylene-6a-(2-naphthalenylmethyl)-1H-cyclopenta[c]furan-1-one (BAY 36-7620) (10 μM), or neutral antagonist, 7-(Hydroxyimino)cyclopropa[b]chromen-1a-carboxylate ethyl ester (CPCCOEt) (100 μM) for 2 days to control and TTX-treated slices (fig. 4B). The inverse-agonist, BAY 36-7620, binds within the transmembrane domain of mGluR1 and stabilizes the receptor in the inactive form (Nakashima et al., 2013). On the other hand, CPCCOEt is classified as a neutral, non-competitive antagonist which inhibits agonist binding in the N-terminus and suppression of agonist-

induced signaling (Ango et al., 2001; Litschig et al., 1999). When the neutral antagonist was treated with activity-deprivation for 2 days, downregulation of excitability was shown like as the preceding data presented in fig. 3B [fig. 4C and D, control + CPCCOEt: firing frequency (Hz) = 31.4 ± 2.2 at 400 pA injection, Δfiring frequency (% of change from control presented in fig. 3B) = -0.62 ± 7.03%, n = 11; deprived + CPCCOEt: firing frequency = 23.0 ± 3.1, Δfiring frequency = -26.20 ± 9.95%, n = 10; control vs. control + CPCCOEt: $p = 0.69$; deprived vs. deprived + CPCCOEt: $p = 0.58$, Two way RM ANOVA (firing frequency); deprived vs. control + CPCCOEt: $p = 0.004$; deprived vs. deprived + CPCCOEt: $p > 0.71$, One way ANOVA post-*hoc* tukey test (Δfiring frequency)]. Interestingly, application of the BAY 36-7620 prevented homeostatic intrinsic plasticity [fig. 4F and G; control + BAY 36-7620: firing frequency = 34.3 ± 2.9 at 400 pA injection, Δfiring frequency = 10.26 ± 10.21%, n = 11; deprived + BAY 36-7620: firing frequency = 33.9 ± 1.8, Δfiring frequency = 8.60 ± 5.60%, n = 13; control vs. control + BAY 36-7620: $p = 0.31$; deprived vs. deprived + BAY 36-7620: $p < 0.05$, Two way RM ANOVA (firing frequency); deprived vs. control + BAY 36-7620: $p < 0.001$; deprived vs. deprived + BAY 36-7620: $p < 0.001$, One way ANOVA post-*hoc* tukey test (Δfiring frequency)]. The changes in the input resistance were in parallel with the aspects of excitability change following co-treatment of TTX and mGluR1 inhibitors for 2 days. Inverse agonist of mGluR1 prevented homeostatic downregulation of the input resistance whereas CPCCOEt showed no significant effects (fig. 4E and H, control + CPCCOEt = 90.6 ± 5.8 MΩ; deprived + CPCCOEt = 74.9 ± 2.8 MΩ; $p = 0.03$; BAY 36-7620: control + BAY 36-7620 = 86.1 ± 6.1 MΩ; deprived + BAY 36-7620 = 83.8 ± 5.7 MΩ; $p > 0.79$, two sample t-test). In line with excitability changes, co-treatment of BAY 26-7620 prevented homeostatic upregulation of I_h whereas CPCCOEt was ineffective to the channel modulation (fig. 4 I and J). As the data presented in fig 3, the inhibitors showed no significant effect to gating properties of HCN channels (fig. 4K – M). Taken together, these observations suggest that the homeostatic intrinsic plasticity of PCs

requires the agonist-independent action of the mGluR1.

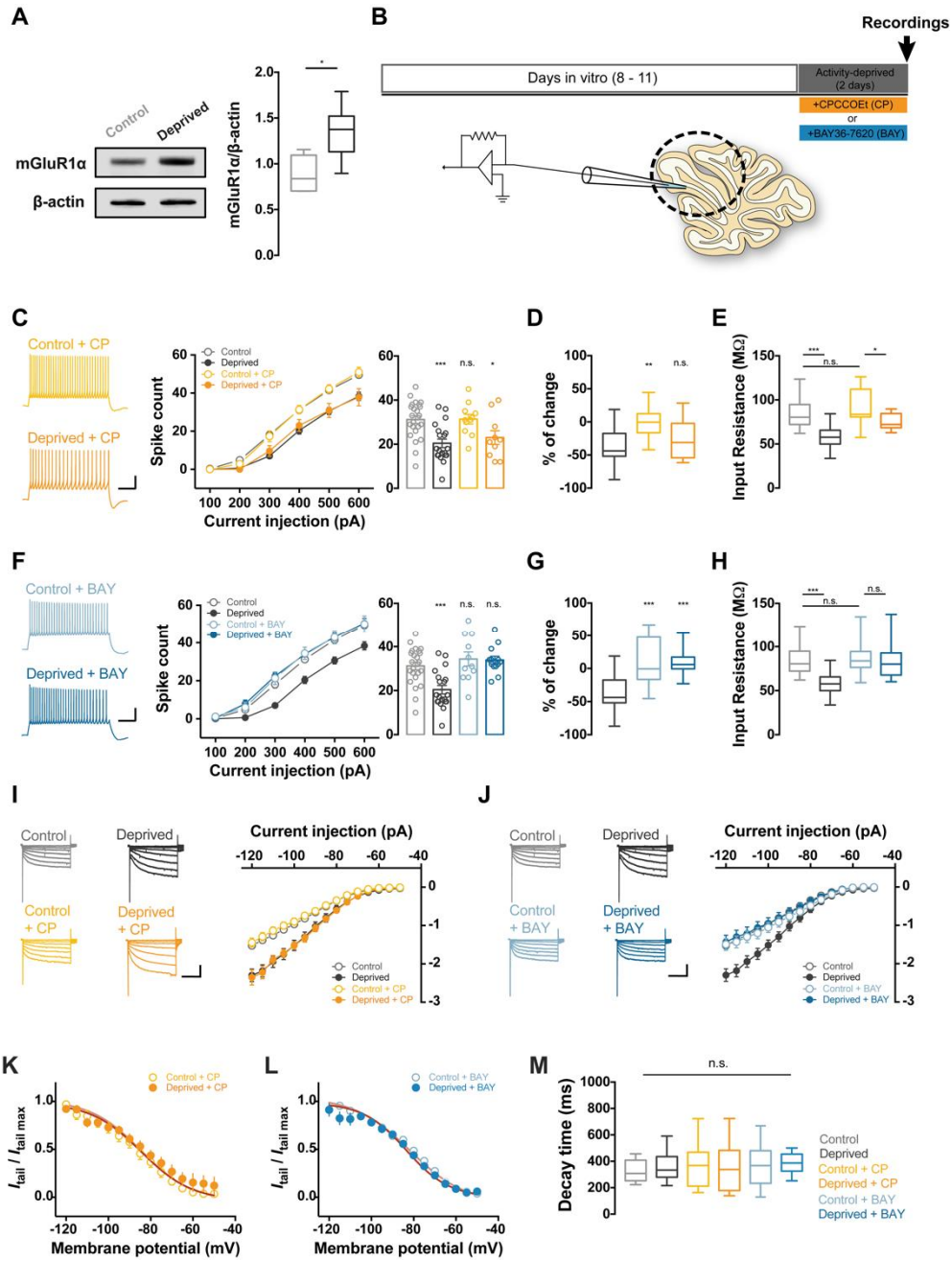

Figure 4. Homeostatic intrinsic plasticity of cerebellar PCs was required to agonist-independent activity of mGluR1. (A) immunoblotting of mGluR1α from control and deprived neuron (left) and summarizing bar graphs (right) showing that chronic activity deprivation increased the protein level of mGluR1. (B) Experimental scheme mGluR1 inhibitors, CPCCOEt (CP) or BAY 36–7620 (BAY) were treated for 2 days in presence or absence of TTX. (C) Representative traces (left), summarizing bar graphs (middle; at +400 pA injection), and plots (right) showing that there were no effects of antagonizing mGluR1 by CP on homeostatic intrinsic plasticity (grey open: control; black closed: deprived, described in fig. 3; yellow open: CP only; orange closed: CP + deprived). (G) Box and

whisker plots showing the % value of changes compared to the value of excitability and input resistance (E) in control neurons. (F) Representative traces (left), summarizing bar graphs (middle; at +400 pA injection), and plots (right) showing that inverse agonist inhibited homeostatic intrinsic plasticity (grey open: control; black closed: deprived, described in fig. 3; light blue open: BAY only; dark blue closed: BAY + deprived). (G) Box and whisker plots showing the % value of changes compared to the value of excitability and input resistance (H) in control neurons. (I – J) Inverse agonist prevented homeostatic upregulation of I_h of PCs. (K – L) Tail current was normalized by maximal tail current amplitude and fitted by Boltzmann function from CPCCOEt-treated (K) and BAY-treated neurons (L). (M) Box and whisker plots showing the decay time of the h-current throughout the group. There were no significant differences between groups. All asterisks marked by t-test. *P < 0.05, **P < 0.01, ***P < 0.001; n.s., no significance.

2.4 Homeostatic intrinsic plasticity of the cerebellar Purkinje cells is mediated PKA activity

I asked if homeostatic upregulation of I_h was dependent on the agonist-independent activity of the mGluR1. The I_h density in the control and deprived neurons was measured after treatment with CPCCOEt or BAY 36-7620 (fig. 4I and J). The homeostatic regulation of I_h was restrained by treatment with the BAY 36-7620 (fig. 4J, control + BAY 36-7620 I_h density = -1.1 ± 0.1 pF, n = 13; deprived + BAY 36-7620 I_h density = -1.0 ± 0.2 pF, n = 13, at Vm = -100 mV; control + BAY 36-7620 vs. deprived + BAY 36-7620: $p = 0.6$; deprived vs. deprived + BAY 36-7620: $p < 0.001$, Two-way RM ANOVA). On the other hand, the neutral antagonist of mGluR1 did not prevent the homeostatic changes of I_h (fig. 4I, control + CPCCOEt I_h density = -0.9 ± 0.1 pF at Vm = -100 mV, n = 13; deprived + CPCCOEt I_h density = -1.5 ± 0.1 pF, n = 13; control + CPCCOEt vs. deprived + CPCCOEt: $p < 0.001$; deprived vs. deprived + CPCCOEt: $p = 0.5$, Two-way RM ANOVA). These findings suggest that the agonist-independent activity of the mGluR1 plays a pivotal role in homeostatic intrinsic plasticity through I_h.

Upstream regulators of I_h have been identified, including protein kinase A (PKA) (Narayanan et al., 2010), Ca^{2+}-calmodulin dependent protein kinase (CaMKII) (Fan et al., 2005) and auxiliary subunit TRIP8B (Santoro et al., 2004). Although the G_q-type of G protein is primarily involved in the excitatory responses of cerebellar PCs, coupling of the mGluR1 to G_S protein activates adenylyl cyclase, and thus, cAMP accumulates resulting in the activation of PKA (Aramori and Nakanishi, 1992; Sugiyama et al., 2008; Tateyama and Kubo, 2006). Therefore, I asked whether PKA activation is required for the homeostatic control of firing rates in cerebellar PCs. To answer this, a PKA inhibitor (500 nM), (5R,6S,8S)-Hexyl 6-hydroxy-5-methyl-13-oxo-6,7,8,13,14,15-hexahydro-5H-16-oxa-4b,8a,14-triaza-5,8-methanodibenzo[b,h]cycloocta[jkl]cyclopenta[e]-as-indacene-6-carboxylate (KT 5720), was applied to organotypic slices with TTX for 2 days. Interestingly, the application of KT 5720 prevented the homeostatic intrinsic plasticity (fig. 5A,

firing frequency (Hz): control + KT 5720 = 29 ± 3.6, n = 7; deprived + KT 5720 = 31.9 ± 3.6, n = 7 at + 400 pA injection; control + KT 5720 vs. deprived + KT 5720, $p = 0.9$; deprived vs. deprived + KT 5720, $p < 0.05$, Two-way RM ANOVA). In addition, KT 5720 also abolished the reduction of input resistance in the TTX-treated neurons (fig. 5B, control + KT 5720 = 90.6 ± 2.5 MΩ, n = 7; deprived + KT 5720 = 83.6 ± 4.8 MΩ, n = 7; control + KT 5720 vs. deprived + KT 5720, $p = 0.2$, deprived vs. deprived + KT 5720, $p < 0.005$, two sample t-test). This observation indicates that PKA activation mediates homeostatic intrinsic plasticity in cerebellar PCs.

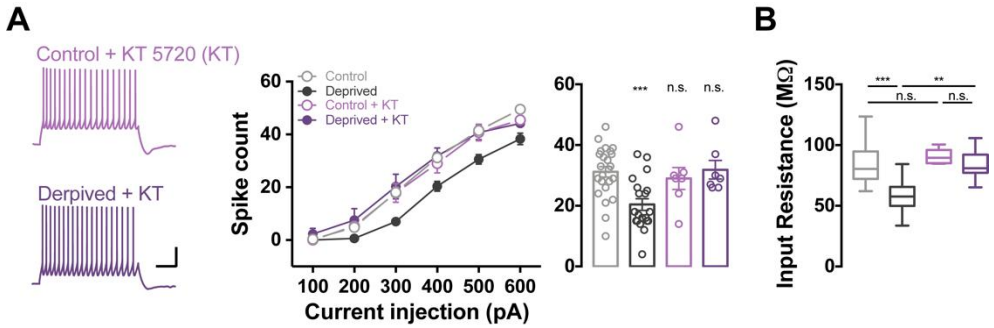

Figure 5. Homeostatic intrinsic plasticity was dependent on PKA pathway. (A) Representative traces (left) and bar graph (middle; at +400 pA injection) and plots (right) showing that treatment of PKA inhibitor KT 5720 (KT) prevented homeostatic intrinsic plasticity in cerebellar PCs. (B) Bar graph showing the reduced input resistance was recovered by KT (500 nM). open purple circle: KT only; closed purple circle: deprived + KT; open grey circle: control; closed black circle: deprived. Control and deprived values are as described in Fig. 3. Asterisks marked by t-test; *P < 0.05, *P < 0.05, ***P < 0.001; n.s., no significance.

Discussion

The present study described a novel mechanism by which homeostatic regulation of intrinsic excitability in the cerebellar PCs requires the agonist-independent activity of mGluR1 in response to the long-lasting changes in cerebellar network activity. Interestingly, homeostatic changes in PC excitability were prevented by the mGluR1 inverse agonist but not the neutral antagonist, indicating that the homeostatic control of intrinsic excitability might underlie agonist-independent action of the mGluR1 signaling (Ango et al., 2001; Hu et al., 2010). In addition, this work presented the evidence showing the downstream pathway for constitutive activity of mGluR1 involved in homeostatic control of PC activity. Application of KT 5720 under the activity-deprived condition exerted inhibition of homeostatic intrinsic plasticity in the cerebellar PCs. PKA activity has been found to be downstream of mGluR1 activation (Aramori and Nakanishi, 1992; Sugiyama et al., 2008; Tateyama and Kubo, 2006), therefore, agonist-independent action of mGluR1 presumably links to PKA signaling. Taken together, homeostatic control of intrinsic excitability in the cerebellar PCs may require the mGluR1-PKA-I_h pathway.

I presented here the reduction of the PC excitability following chronic activity-deprivation. At first glance, this result may show contradictory to the conventional concept of homeostatic regulation in which prolonged inactivation of the network activity induces boosting the neuronal excitability and/or excitatory synaptic drive (Desai et al., 1999; Galante et al., 2000). However, in the GABAergic neurons, it has been observed that synaptic strength (Chang et al., 2010) and firing rates (Sun, 2009) decrease in response to days-long inhibition of network activity. The data I presented here is in agreement with previous studies in that cerebellar PCs are GABAergic neurons. This reduced excitability observed in the cerebellar PCs after chronic activity blockade could induce disinhibition of the silenced cerebellar

cortex which efficiently increase the network excitability against chronic activity deprivation. There are no simple ways to maintain the stability of the neuronal network activity against activity perturbation because neural activity is rather dynamically modulated (Hengen et al., 2013; Keck et al., 2013). For this reason, 2 day-inhibition of network activity by TTX has been widely used to induce homeostatic plasticity, however, neural activity can change day-to-day. Furthermore, the time course to induce plasticity in *vivo* far differs from in *vitro*. This is the first observation of homeostatic control in the cerebellar PCs and physiological in *vivo* models have yet to be established. Based on this study, an in vivo model of homeostatic control of the cerebellar activity in the physiological or pathological circumstances is needed to be developed. Consequently, it could be possible to explore dynamically regulated neural activity in an activity-dependent manner.

In the present study, I suggest that the agonist-independent activity of the mGluR1 is required for the homeostatic intrinsic plasticity of cerebellar PCs. Interestingly, it has been observed that the receptor can be spontaneously activated even in the absence of the agonists (Ango et al., 2001; Roosterman, 2014; Scheer et al., 1996). A previous study has shown that the intracellular protein Homer regulates the agonist-independent constitutive activity of the mGluR1 by interacting with partner, such as the SHANK and MAGUK proteins (Tu et al., 1999). Neuronal excitation during synaptic plasticity or manifestation of convulsive seizures results in expression of the immediate early gene Homer1a (Brakeman et al., 1997), and the interaction between the mGluR1 and long-form Homer proteins, subsequently, is disrupted leading to the constitutive activity of the receptor (Ango et al., 2001). In the TTX model for the homeostatic plasticity, there is minute possibility that Homer 1a is involved in the activity deprivation-driven reduction of excitability because neuronal depolarization commonly induces Homer1a (Minami et al., 2003), but rather is due to the downregulation of the long-form Homers which induces the agonist-independent activation of mGluR1 in the

cerebellar PCs. Indeed, knock-down of Homer3 facilitates the mGluR1 activity by shifting equilibrium between its inactive and active conformation (Ango et al., 2001). The complex receptor-intracellular protein interactions in response to chronic changes in network activity is needed to be further investigated in the aspects of neural plasticity and/or pathological fashion.

The level of GPCR activity, a functional readout of the group1 mGluR, has been found to be determined by the balance between the inactive (R) and active (R*) form of the receptor (Chidiac et al., 1994). Conformational changes of the receptor from the R to R* are regarded as one of the underlying mechanisms of constitutive activity (Scheer et al., 1996). Alternatively, an increased density of GPCRs enhances the agonist-independent activity of the receptor through an increase in the absolute amount of R* (Smit et al., 1996). I observed that activity-deprivation elevates mGluR1α, and this may reflect strengthened GPCR signaling through an increased amount of the R* form of the receptor. In addition, when the PKA pathway as the downstream of the receptor (Aramori and Nakanishi, 1992; Sugiyama et al., 2008; Tateyama and Kubo, 2006) is inhibited under activity-deprived condition, homeostatic intrinsic plasticity is abolished, suggesting that chronic activity-deprivation condition activates PKA. Given that the mGluR1 activates adenylyl cyclase by the coupling of the receptor to the G_S protein leading to accumulate cAMP (Tateyama and Kubo, 2006), those results implicate that the chronic blockade of network activity activates mGluR1 signaling resulting in the downregulation of firing rates through the PKA pathway. When mGluR1 is activated, various cell responses can be induced through coupling to several types of G proteins. Coupling of mGluR1 to G_{q11} triggers accumulation of inositol 1,4,5-trisphosphate (InsP3) resulting in activation of the protein kinase C (PKC) pathway (Francesconi and Duvoisin, 2000; Tateyama and Kubo, 2006). Several previous studies reported that the PKC activation suppresses I_h (Brager and Johnston, 2007). This leads to an increase in intrinsic excitability which contradicts my observation. Although G_S- and G_{q11}-coupling can be simultaneously and independently

triggered by mGluR1 activation, PKA is a more plausible upstream regulator of the elevated I_h. For this reason, the cerebellar PC homeostatic intrinsic plasticity seems to require PKA signaling rather than PKC activity. In this study, I observed the upregulation of I_h in the deprived PCs without changes in gating properties of the channels, implying that the upregulation of current density may underlie the increased channel expressional level. Narayanan et al. (2010), on the other hand, have describe that Ca^{2+}-store depletion leads to increases in I_h conductance through the PKA signaling without protein synthesis. However, they observed the changes in HCN channel activity in response to acute effect of Ca^{2+}-depletion by CPA treatment. In addition, many implications have shown that the homeostatic plasticity is derived from transcription and/or translation (Desai et al., 1999; Shepherd et al., 2006; Sutton et al., 2007; Hu et al., 2010; Chang et al., 2010; Naudé et al., 2013; Lee et al., 2015). Therefore, homeostatic upregulation of I_h might result from not only transcriptional and/or translational alterations of the ion channels or auxiliary units but also the cAMP responsiveness to HCN channel activity.

Various ion channels determine the active and passive electrical properties of neuronal membranes, including membrane potential and AP threshold, and contribute to the synaptic integration and firing fidelity. Synaptic stimuli and/or somatic depolarization form plastic changes in neuronal excitability by changing the composition and conductance of ion channels (Belmeguenai et al., 2010; Hyun et al., 2013). From a homeostatic viewpoint, ion channels are dynamically regulated to achieve the network stability, and accordingly, AP firing rates are tuned within physiological ranges (Desai et al., 1999). Given the decreased input resistance in the deprived neurons, I focused on I_h among ion channels which contribute to neuronal excitability. However, the activity of many other ion channels need to be measured. A previous study showed that visual deprivation changes $I_{threshold}$ and input resistance which is in agreement with this work (Nataraj et al., 2010) (fig. 3 and Table 1). Hence TEA-sensitive delayed-rectifier type K^+

channel (K_V 2.1) are also possible candidate for homeostatic control of the PC excitability. Although Ca^{2+}-activated K^+ channels can be involved in homeostatic intrinsic plasticity, these are excluded because they have less of an effect on input resistance and $I_{threshold}$ (Belmeguenai et al., 2010).

HCN channels are widely expressed in several brain regions (Notomi and Shigemoto, 2004), and they contribute to the regulation of neural activity. Because I_h generates a tonic inward current at resting state, it is known as a pacemaker to initiate neuronal oscillation and rhythmic burst activity (Jahnsen and Llinás, 1984; Llinás and Jahnsen, 1982; McCormick and Pape, 1990). A previous study showed that the pharmacological blockade of I_h modifies membrane bi-stability, thereby inducing the spontaneous quiescence period (Williams et al., 2002). This indicates that I_h maintains the membrane potential which enables tonic AP activity even when the activity of PCs is disrupted by hyperpolarizing inputs. Given that I_h stabilizes the cellular membrane potential within an appropriate range by its unusual gating properties (Nolan et al., 2007), the activity-dependent regulation of I_h may play a role in homeostatic plasticity following a chronic activity-disturbance condition. Homeostatically elevated I_h reduces input resistance leading to a dampened membrane deflection to given current stimulation, and this will act as a cellular stabilizer to preserve the membrane potential. Furthermore, a potentiated rebound potential keeps the membrane potential close to the AP threshold and consequently leads to 'history-independent integration' (Nolan et al., 2003). Therefore, I suggest that the activity of cerebellar PCs is fine-tuned by the consequences of I_h modulation when the network activity is deprived.

Homeostatic plasticity has been regarded as a key mechanism of disease initiation (Friedman et al., 2014). Chronic activity-deprivation reduces the firing rates of cerebellar PCs, and it could be related to cerebellar disorders including Friedreich ataxia and spinocerebellar ataxias because lowered excitability is linked to the cellular phenomenon of disease (Hourez et al., 2011). Given that the constitutive activity of GPCRs is correlated to various human diseases, this work

provides insight into possible therapeutic targets though modulation of GPCR-mediated homeostatic intrinsic plasticity. In addition, I also provide insight into the cellular basis of homeostatic control of firing rates of cerebellar PCs, and these findings broaden the understanding of homeostatic intrinsic plasticity of the cerebellar cortex.

Chapter 3

Long-Term Depression of Intrinsic Excitability Accompanied by Synaptic Depression in Cerebellar Purkinje Cells

Introduction

A long-standing question in the neuroscience field is how the brain stores the information from the surroundings and subsequently modifies the weight of input and output signals to adjust behavior. To answer this question, activity-dependent changes in synaptic function such as long-term potentiation (LTP) and LTD have been intensively investigated as the cellular mechanisms of this phenomenon (Kandel et al., 2014). Activity- and experience-dependent alteration of neuronal intrinsic excitability (intrinsic plasticity) also have been implicated in the other side of engram for information processing and memory storage (Straka et al., 2005; Zhang and Linden, 2003). In fact, the non-synaptic intrinsic plasticity is found to be accompanied by synaptic plasticity in the various type of neurons (Belmeguenai et al., 2010; Brager and Johnston, 2007; Fan et al., 2005; Shim et al., 2017). This form of neural plasticity indeed complements the synaptic inputs and synergistically generates a total net output of the neurons.

The synaptic plasticity between PF and PC synaptic area, especially PF-PC LTD was held as a view of underlying mechanism for the cerebellum-dependent motor learning (Ito, 1982; Jörntell and Hansel, 2006). For decade, there are is accumulating evidence showing that the synaptic plasticity at the multiple site throughout the cerebellar circuitry beyond PF-PC LTD (Boyden et al., 2004; 2006; Gao et al., 2012). In addition, several implications have shown that memory trace of the cerebellar motor memory should be transferred into the sub-cortical area such as vestibular nucleus (VN) for shaping long-term memory storage (Kassardjian et al., 2005; Okamoto et al., 2011b). Interestingly, Ito who firstly proposed cerebellar LTD hypothesis suggested that the fast adaptation of the VOR learning is based on the LTD at PF-PC synapses and slow adaptation is derived from mossy fibre (MF) to the vestibular nucleus (VN) neuron synapses (Ito, 2013). Indeed, the cerebellar PCs integrate the input from the pre-cortical region and

generate an output signal, and thereby transfer the information to the post-cortical area. Thus, the activity of cerebellar PCs plays a central role in the acquisition of the cerebellar motor memory such as vestibulo-ocular reflex (VOR) learning, beyond the synaptic plasticity (Kassardjian et al., 2005; Okamoto et al., 2011b). Moreover, the spiking activity of PCs has a large impact on the cerebellar-motor memory consolidation (Galliano et al., 2013; Wulff et al., 2009), indicating the output of PCs may play a critical role in the memory processing within the motor circuitry. Therefore, observation of an activity-dependent modulation of the intrinsic excitability will provide insight into understanding the information processing and memory storage in cerebellar circuits beyond the synaptic plasticity in terms of the motor learning. In spite of the physiological significance of the intrinsic plasticity, characteristics of the intrinsic plasticity accompanied by PF-PC LTD remain unclear.

Here, I address the question how intrinsic plasticity is modulated following synaptic depression of PCs by using whole-cell patch clamp technique from the cerebellar slices from 4- 6 weeks old male C57BL/6 mice. I found that the conjunctive activation of PF and climbing fibre (CF), the well-known induction protocol for PF-PC synaptic LTD, induced long-term depression of intrinsic excitability (LTD-IE) as well. Both synaptic and intrinsic plasticity are the Ca^{2+}-dependent and share the PKC pathway. This learned pattern of the neuronal output, notably, functions as the amplifier of the depressed synaptic strength rather than modifying the strategy for input integration and output generation.

Material and Methods

1. Animals and Slice preparation

All animal use was in accordance with protocols approved by the Institution's Animal Care and Use Committee of Seoul National University College of Medicine. Cerebellar parasagittal slices were dissected into 250 μm by vibratome (Leica, VT1200) from anaesthetized 4- 6 weeks old male C57BL/6 mice in ice-cold standard artificial cerebrospinal fluid (aCSF) contained with the following (in mM): 125 NaCl, 2.5 KCl, 1 $MgCl_2$, 2 $CaCl_2$, 1.25 NaH_2PO_4, 26 $NaHCO_3$, 10 glucose bubbled with 95% O2 and 5% CO2. For recovery, slices were incubated at 32 ˚C for 30 minutes and further 1 hour at room temperature.

2. Electrophysiology

Slices were put onto a submerged recording chamber on the stage of Olympus microscope (BX50WI, Japan) and perfused with aCSF, and kept in place with a nylon-strung platinum anchor. All recordings were performed using EPC9 (HEKA Elektronik) and multiclamp 700B patch-clamp amplifier (Axon Instruments) with a sampling frequency of 20 kHz and signals were filtered at 2 kHz. To isolate excitatory synaptic inputs, inhibitory synaptic inputs were totally blocked by 100 μM picrotoxin. Patch pipettes (3-4 MΩ) were borosilicate glass and filled with internal solution. Composition of the internal solution is described in the Material and Method of Part 1. The membrane potential was held on -70 mV in voltage-clamp (VC) and current-clamp mode (CC). Recordings were discarded if the series resistance (R_s) varied by > 15% and the injection current for the holding potential exceeded 600 pA. PFs in the molecular layer and CF in the granule cell layer were stimulated by an ACSF-filled electrode. I used two different protocols to induce the PF-PC LTD in CC mode for 5 min: 1) 300 times of repetitive co-activation of PF and CF at 1 Hz (LTD-tetanus); 2) 30 times of pairing-stimulation consisted of 7 PF stimuli at 100 Hz followed by 1 CF stimulus delayed by 150 ms every 10 sec (LTD-burst). To evaluate the PCs excitability, a series of current steps of 500 ms duration ranging from +100 pA to +500 pA with increments of 100 pA with a step

interval of 4.5 s from a membrane potential of -70 mV was injected in CC mode.

3. Calcium imaging

Ca^{2+} measurements were performed with a confocal laser-scanning head (FV300 Olympus, Japan) attached to an upright microscope confocal microscope (BX51WI, Olympus, Japan), using a 40× water immersion objective (NA 0.8, LUMPlanFl/IR; Olympus, Japan), in parallel to the electrophysiological recording. To measure dendritic calcium transients, Oregon Green 488 BAPTA-1 (OGB-1, 0.2mM) was added to internal solution in patch pipette. PCs was dialysed for at least 30min after introducing intracellular solution prior to imaging. Alexa fluor 594 red fluorescence was added to saline in stimulation pipette. Confocal images were acquired with Fluoview (Olympus, Japan) software as XYT frame scans for a chosen region of interest, and analyzed with NIH ImageJ software. Baseline fluorescence frame was subtracted from max fluorescence frame and filtered using Gaussian blur 3D. Then I applied the same threshold to different intensity of stimulation data and measured the area using ImageJ *Analyze particles* algorithm.

4. Data acquisition and analysis

All data were acquired by Clampex software (Molecular Devices) and analyzed by IgorPro 8.1 (Wavemetrics). I evaluated the LTD by normalizing to the average of baseline PF-EPSC, and recording was excluded if the baseline current or the number of evoked spikes varied by > 20 %. Electrical properties of the neurons were monitored with following parameters: R_S was calculated by fitting a single exponentials to the voltage responses of the test pulse (-5 mV); Input resistance was determined from negative peak voltage deflection in response to brief hyperpolarizing current injection (-100 pA; 100 ms); Voltage threshold ($V_{threshold}$) of AP was defined as the voltage where the dV/dt first exceeds 30-60 mV/ms); AP amplitude was determined as difference between peak amplitude and the voltage threshold of the AP; Half-width were the time duration at the half-maximal voltage; Fast afterhyperpolarization (fAHP) and medium afterhyperpolarization (mAHP) were measured by calculating the difference between voltage threshold and

hyperpolarized negative peak voltage after the first AP or depolarizing square current injection, respectively. All analysis for electrical properties was performed by custom-made Matlab code.

Data were presented as mean ± SEM and statistical evaluations were performed using normality test, equal variant test, independent *t*-test, One-way repetitive measured (RM) ANOVA and Two-way RM ANOVA with post *hoc* tukey test by Origin 8.5 and SigmaPlot 12.0 software. Sample size was approved by power analysis using the G*power 3.1.9.2.

Results

3.1 LTD of intrinsic excitability of PC accompanied by PF-PC LTD

In order to investigate whether excitability changes in PCs are accompanied by synaptic LTD, the whole-cell path-clamp recording was performed from cerebellar slices of 4 to 6 weeks old mice under the presence of picrotoxin, $GABA_A$ receptor inhibitor. PF-PC LTD was induced by tetanising PF and CF simultaneously (1 Hz, 300 times, 5 min; Tetanus; fig. 6A). The amplitude of excitatory postsynaptic current (EPSC) was monitored before and after the tetanisation of PF and CF to confirm whether PF-PC LTD was formed. In the same recording, intrinsic excitability was also measured in current clamp mode by injecting square-wised brief current step from the membrane potential of about -70 mV (500 ms, from +100 pA to +500 pA with an increment of 100 pA, step interval 4.5 s, see Materials and Methods), and determined by counting the number of depolarisation-evoked spikes before and after the Tetanus protocol. As a control, co-activation of PF and CF was omitted during the induction period in the control neurons but the other condition and protocol were the same with LTD-induced neuron. Both the EPSC and the excitability were stable in the control group ($n = 9$, $n = 8$, respectably; fig. 6B – D). Simultaneous stimulation of PF and CF resulted in the EPSC reduction to 71.3 ± 6.0 % ($n = 7$; fig. 6B), which is the well-established PF-PC synaptic LTD phenomenon. Concurrently, downregulation of the intrinsic excitability was accompanied by the synaptic LTD in comparison with the baseline ($n = 7$, $F = 17.4$, $p < 0.001$, two-way RM ANOVA; fig. 6E – F) in all ranges of current injection. Intrinsic excitability was shown to be significantly reduced to 76.4 ± 4.7 % of baseline when 500 pA of current was injected after tetanization.

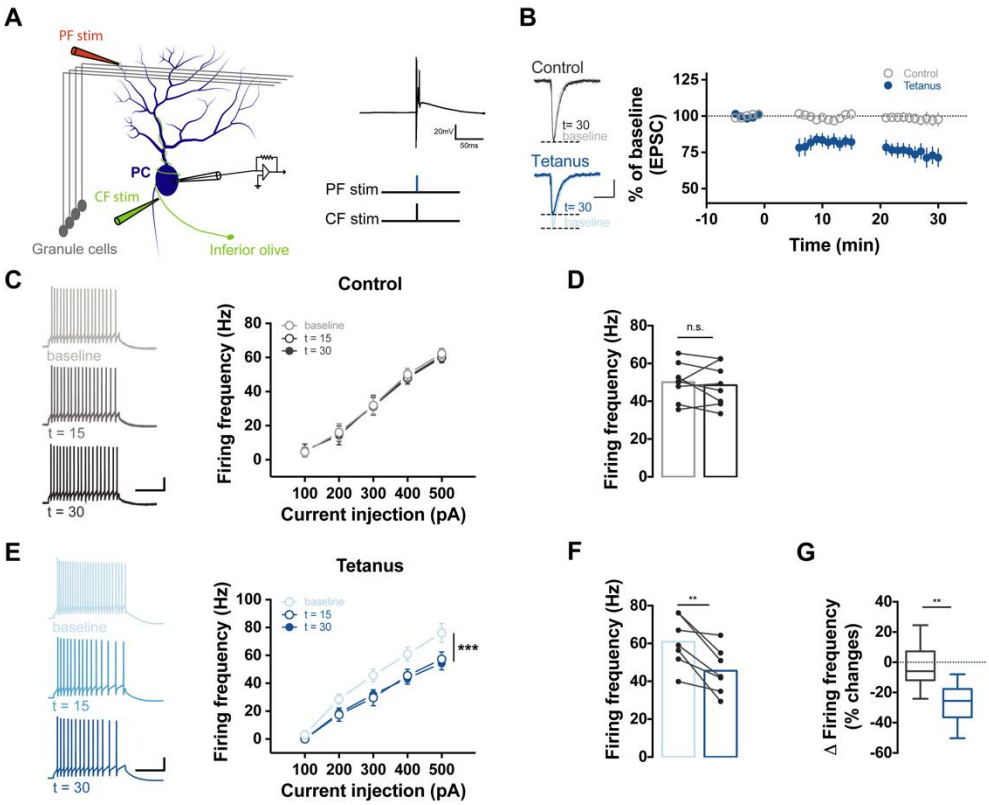

Figure 6. Synaptic LTD accompanied by LTD of intrinsic excitability. (A) PF–PC LTD induction protocol. PF and CF were simultaneously stimulated with 1 Hz for 5 min 300 times. Scale bars, 20 mV (vertical) and 50 ms (horizontal). (B) Normalized EPSC of both groups. LTD was successfully induced in 1 Hz LTD group and there were no changes of EPSCs in control group. Control, open, n = 9; LTD-Tetanus, filled, n = 7. Scale bars in raw traces, 100 pA (vertical) and 50 ms (horizontal). (C – D) Intrinsic excitability of control group. Somatic depolarizing current injection-evoked firing frequency was not changed during recording. Baseline, 15 min, n = 9; 30 min, n = 8; $F = 0.219$, $p = 0.806$. Scale bars in raw traces, 20 mV (vertical) and 200 ms (horizontal). (E – F) Intrinsic excitability of LTD-Tetanus group. Firing frequency was significantly reduced after LTD induction (n = 7, $F = 17.4$, $p < 0.001$). Scale bars in raw traces are the same as in C. (G) Box and whisker plots showing the % value of change in firing frequency in control (grey) and Tetanus group (blue). For statistics, two-way RM ANOVA was used for C and E. Post hoc Tukey's test was used for different time group comparison. Error bar indicates SEM. $^{**}p < 0.01$, $^{***}p < 0.001$.

A previous study revealed that the PF stimulation with 1 Hz failed to induce intrinsic plasticity *in vivo* because 1 Hz PF stimulation was not exceeding the background activity (Belmeguenai et al., 2010). To adequately reflect the activity pattern of the granule cells *in vivo*, I introduced the PF burst protocol (7 of 100 Hz PF burst followed by single CF stimulation with the stimulus interval of 150 ms, 30 times, sweep interval 10s, 5 min; Burst; figure 7A). With this protocol, synaptic LTD was also reliably elicited (n = 10; fig. 7B) but the synaptic plasticity was relatively slowly developed. Because of the different kinetics of decrease in EPSC, excitability was measured 20 min and 40 min after the induction. Consistent with the results from LTD-Tetanus protocol, the evoked spike count was considerably decreased following conjunctive activation of PF and CF ($n = 10$, $F = 21.1$, $p < 0.001$, two-way RM ANOVA; fig. 7E and F). A previous study described that cerebellar LTD required the precisely timed-pairing of PF and CF activation, in which inter-stimuli interval was from -50 ms to + 300 ms between PF and CF to induce the synaptic plasticity (Safo and Regehr, 2008). To test whether the time window of pairing is a pivotal element for LTD-IE induction, I delivered the non-conjunctive stimulating (Pseudo burst) protocol (fig. 7A). In an Pseudo burst protocol delivered condition, synaptic depression was not induced (n = 11; fig. 7B). Interestingly, intrinsic excitability was decreased 20 min after induction, however, the reduction was recovered 40 min after application of LTD-Pseudo ($t = 20$, $p = 0.002$; $t = 40$, $p = 0.092$; post-hoc tukey test after Two-way RM ANOVA; fig. 7C – D). Magnitude of the intrinsic plasticity was significantly obvious in Burst group comparing to Pseudo burst group (fig. 7G, Pseudo burst: Δfiring frequency = -6.11 ± 4.70%; Burst: Δfiring frequency = -22.57 ± 3.70%, $p = 0.014$, unpaired t-test). These results indicated that uncoupled-conjunction of the PF and CF was insufficient for the maintenance of the intrinsic plasticity.

		$V_{threshold}$ (mV)	AP amplitude (mV)	fAHP (mV)	mAHP (mV)	FWHM (ms)
Control	baseline	-47.8 ± 2.2	69.7 ± 6.1	14.3 ± 1.7	5.1 ± 1.2	0.34 ± 0.02
	t=15	-47.7 ± 1.9	67.1 ± 5.8	14.5 ± 1.6	4.2 ± 0.7	0.36 ± 0.02
	t=30	-48.1 ± 2.0	67.7 ± 6.2	14.5 ± 1.5	3.7 ± 0.6	0.36 ± 0.02
LTD-Tetanus	baseline	-49.3 ± 1.0	86.6 ± 4.2	13.5 ± 0.7	7.4 ± 0.6	0.33 ± 0.02
	t=15	-50.9 ± 1.4	85.0 ± 3.4	14.1 ± 0.5	4.8 ± 0.3 ***	0.33 ± 0.02
	t=30	-52.3 ± 1.8 *	85.8 ± 3.7	13.4 ± 0.6	4.0 ± 0.6 ***	0.33 ± 0.02
LTD-Pseudo	baseline	-48.8 ± 1.2	74.0 ± 2.2	12.4 ± 0.6	6.7 ± 0.6	0.31 ± 0.01
	t= 20	-49.2 ± 1.2	74.3 ± 1.9	12.6 ± 0.7	4.8 ± 0.6 ***	0.32 ± 0.00
	t = 40	-49.2 ± 1.3	73.6 ± 2.2	13.2 ± 0.7	4.0 ± 0.4 ***	0.32 ± 0.01
LTD-Burst	baseline	-47.7 ± 0.9	81.4 ± 3.9	13.1 ± 0.7	7.3 ± 0.6	0.28 ± 0.01
	t= 20	-48.7 ± 0.7	81.1 ± 4.0	14.0 ± 0.5	5.0 ± 0.4 ***	0.29 ± 0.00
	t = 40	-48.7 ± 1.0	79.7 ± 4.3	13.5 ± 0.5	4.5 ± 0.6 ***	0.30 ± 0.01

Table 5. Active properties of action potential before and after LTD induction.
Among active membrane properties, voltage threshold ($V_{threshold}$) was significantly changed in LTD-Tetanus group (30min, $p = 0.012$). Medium afterhyperpolarization (mAHP) was considerably decreased in all stimulated groups, including LTD-Tetanus, LTD-Pseudo and LTD-Burst (All groups, $p < 0.001$). Other parameters, such as AP amplitude, fast AHP (fAHP) and full-width-half-maximum (FWHM), were not altered

To further examine changes in the intrinsic properties, I analyzed the properties of action potential (AP) (Table 5). I found that the voltage threshold was shifted to approximately 3 mV of hyperpolarisation 30 min after the tetanisation [n = 7, -49.3 ± 1.0 (baseline) vs. -52.3 ± 1.8 (t = 30), p = 0.012, post-hoc tukey test after One-way RM ANOVA], but there were no changes in other groups. The reduction of medium after-hyperpolarisation (mAHP) was observed in all groups except control group. These reductions were most obvious and significant among the properties of AP [Tetanus; 7.4 ± 0.6 mV (baseline) vs. 3.8 ± 0.6 mV (t = 30), F = 28.803, p < 0.001, Burst; 7.3 ± 0.6 (baseline) vs. 4.5 ± 0.6 (t = 40), F = 24.3, p < 0.001, Pseudo burst; 6.7 ± 0.6 (baseline) vs. 4.0 ± 0.4 (t = 40), F = 28.4, p < 0.001, One-way RM ANOVA]. Robust reduction of input resistance was also observed in LTD-induced neurons (Tetanus; 85.7 ± 3.0%, p < 0.001, Burst; 92.2 ± 1.9%, p = 0.023, post-hoc tukey test after One-way RM ANOVA; Table 5). The change of input resistance in Pseudo burst group showed similar pattern to that of the excitability. It was slightly reduced 20 min after induction, but recovered in 40 min (t = 20, 94.6 ± 2.1 %, p = 0.027; t = 40, 95.7 ± 2.3 %, p = 0.082, post-hoc tukey test after One-way RM ANOVA). The changes of the other parameters were less prominent. Given the altered AP properties, LTD-IE was derived from altered intrinsic properties, not resulting from the decreased synaptic weight.

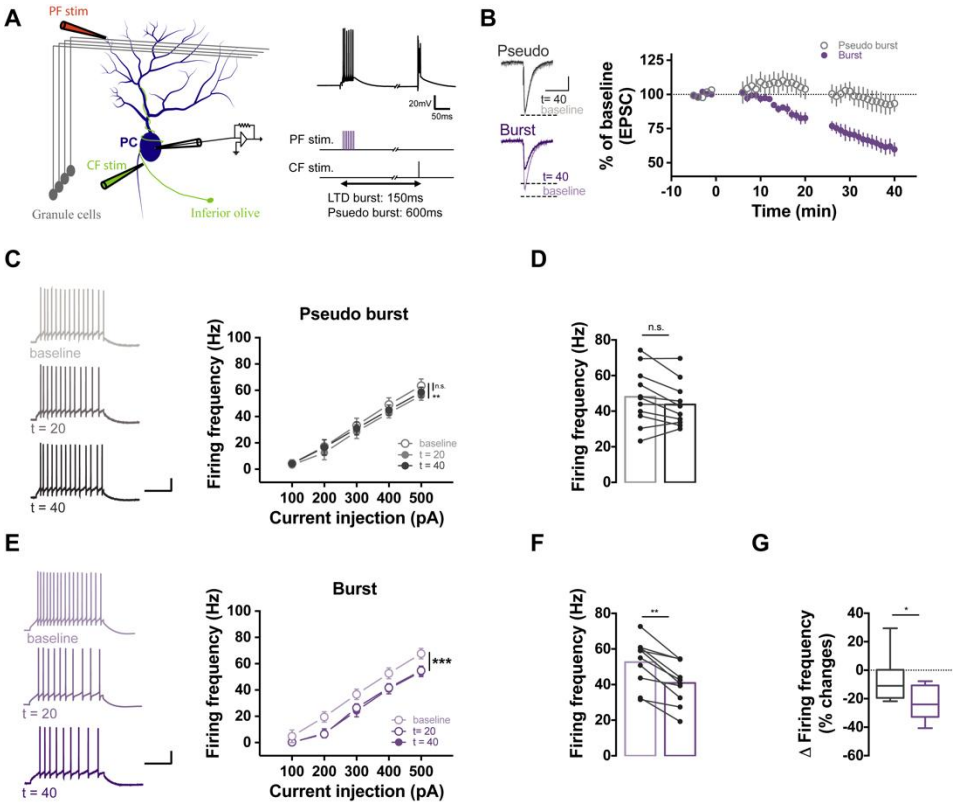

Figure 7. Synaptic LTD accompanied by LTD of intrinsic excitability. (A) Induction protocols for LTD-Burst and LTD-Pseudo. Thirty times of 7 PF and single CF stimulation with 150 ms interval could induce the PF–PC LTD but 600 ms interval could not. (B) Normalized EPSC of both groups. LTD was successfully induced in Burst group and there were no changes of EPSCs in Pseudo burst group. Pseudo burst, open, n = 11; LTD burst, filled purple, n = 10. Scale bars in raw traces, 100 pA (vertical) and 50 ms (horizontal). (C – D) Intrinsic excitability of Pseudo burst group. There was statistical significance between baseline and the 20 min after induction (n = 11, p = 0.002), but the significance disappeared at 40 min (p = 0.092). Scale bars in raw traces, 20 mV (vertical) and 200 ms (horizontal). (E – F) LTD-Burst group. Numbers of spikes were significantly reduced after LTD induction ($F = 21.1$, $p < 0.001$). Scale bars in raw traces are the same as in C. (G) Box and whisker plots showing the % value of change in firing frequency in Pseudo burst (grey) and Burst group (purple). For statistics, two-way RM ANOVA was used for C and E. Post hoc Tukey's test was used for different time group comparison. Error bar indicates SEM. **p < 0.01, ***p < 0.001.

3.2 LTD-IE has different developing kinetics from synaptic LTD

Since the excitability change was monitored at two-time points after LTD induction, the temporal kinetics of intrinsic plasticity was unclear. To clarify this, the depolarizing current eliciting 10-20 spikes (ranging from 100 to 300 pA of current injection) was injected and the spike count was continuously measured in the current clamp mode before and after delivery of induction protocols. The LTD-IE was found to be immediately elicited after LTD induction, and magnitude of intrinsic plasticity showed slight further development but it did not reach the statistical significance (fig. 8A and B). When I applied LTD-Pseudo protocol as a control, there were no significant changes in spike count (fig. 8A and B).

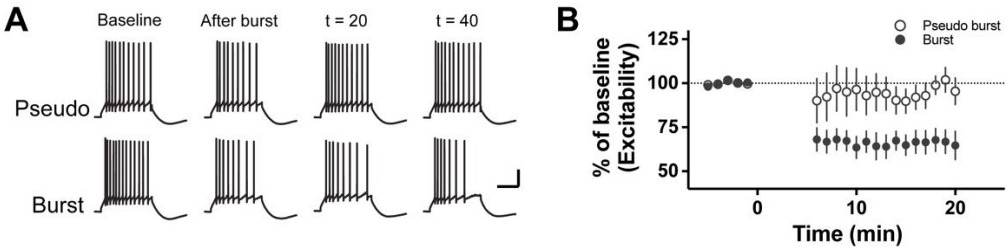

Figure 8. LTD-IE showed an immediate reduction after induction. (A) Raw traces in several time points. Scale bars, 20 mV (vertical) and 200 ms (horizontal). (B) Normalized spike count. LTD-Pseudo group showed a slight reduction after stimulation, but its spike count gradually rises and was fully recovered at 20 min (open, n = 7). Unlike the Pseudo burst group, the Burst group showed an immediate reduction after the induction protocol (filled, n = 10).

3.3 LTD-IE was not reversed by subsequent LTP-IE induction.

Synaptic LTP and LTD are in complementary. Indeed, reversible changes in synaptic efficacy at PF-PC synapses has been shown in *in-vitro* slice recording and behavior test (Boyden and Raymond, 2003; Coesmans et al., 2003) . These findings lead to a question whether intrinsic plasticity also shows the reversibility. To test this, I developed the LTP-IE protocol modifying from previous studies (Belmeguenai et al., 2010; Nataraj et al., 2010). Precisely timed pulse train (5 Hz / 3 s, pulse duration: 100 ms) was injected every 5 s for 5 min in current clamp mode (fig. 9A; upper panel). The amplitude of pulse train was 100 – 150 pA higher than injecting current eliciting 5 – 15 spikes. Application of this protocol exhibited the potentiation of spike count ($n = 9$, $F = 6.70$, $p < 0.001$, One- way RM ANOVA; fig. 9A).

After confirmation of the LTP-IE protocol, I delivered two types of serial-ordered protocol following: 1) LTP-IE – LTP-IE – LTD-burst – LTP-IE (PPDP serial); 2) LTD-burst – LTD-burst – LTP-IE – LTD-burst (DDPD serial). In the PPDP serial, the first application of LTP-IE significantly potentiated PC excitability (135.2 ± 3.3 % of baseline, $n = 10$, $p = 0.043$, post-hoc tukey test after One-way RM ANOVA compared to the value of prior period; fig. 9B), but there were no further changes after following the second induction of LTP-IE (144.5 ± 8.5 % of baseline, $p = 0.939$). Application of LTD-burst protocol and the third LTP protocol resulted in slight depotentiation (123.1 ± 14.9 % of baseline) and repotentiation of excitability (141.9 ± 18.1 % of baseline), respectively, but these level of change were not significantly different from that measured before induction ($p = 0.404$ and $p = 0.654$, respectively). Next, I applied DDPD serial to test if LTP-IE protocol reversed LTD-IE. LTD-IE was fully saturated at once after application of LTD-inducing protocol (42.5 ± 5.3 % of baseline, $n = 4$, $p < 0.001$, post-hoc tukey test after One-way RM ANOVA compared to the value of prior period; fig. 9C), further reduction of excitability, thereby, was not observed after the second induction of LTD (36.5 ± 6.1 % of baseline, $p = 0.847$). Application of

LTP-IE protocol could not result in a significant change of the excitability compared to that measured after the first and second induction of LTD (41.0 ± 10.6 % of baseline, $p = 0.940$). Finally, the third LTD-burst protocol was delivered, and there was no alteration of spike count (38.3 ± 8.8 % of baseline, $p = 0.991$). These data suggested that the intrinsic plasticity of PCs cannot be reversed by the opposite direction of plasticity induction.

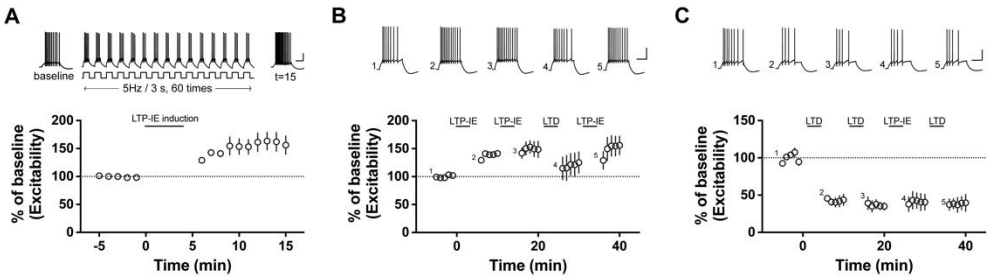

Figure 9. Reverse of intrinsic plasticity. (A) LTP-IE was induced by induction protocol. Raw traces in baseline, induction protocol, and 15 min after induction (top, left to right). Excitability was directly increased and maintained after induction (bottom, $n = 9$, $p < 0.001$). B, Normalized spike count under the PPDP serial. The first LTP-IE stably induced potentiation of excitability ($n = 10$, $p < 0.043$) and there was no further potentiation after the second LTP-IE induction ($p < 0.939$, cf. prior period). After LTD, the third LTP induction brought slight depotentiation and repotentiation, respectively, but this was not significant (LTD induction, $p = 0.404$; the third LTP induction, $p = 0.654$, cf. prior period). C, Normalized spike count under DDPD serial. Like the PPDP serial, the first LTD induced reduction of excitability ($n = 4$, $p < 0.001$) and no further changes after the second LTD induction ($p = 0.847$). LTP-IE induction and the third LTD had no effect on excitability (LTP-IE induction, $p = 940$; the third LTD induction, $p = 0.991$). For statistics, one-way RM ANOVA was used. Post hoc Tukey's test was used for different time group comparisons. Error bar indicates SEM.

3.4 The number of recruited synapses were not correlated to the magnitude of the neuronal plasticity.

LTD-IE is the concomitant of paired stimulation of PF with CF, and incomplete paired stimuli could not lead to persistent excitability change. This observation indicates that the coincidence of synaptic activation is a prerequisite for the intrinsic plasticity. I then inquired whether LTD-IE is dependent on the number of activated synapses by synaptic stimulation. Given that a previous study described the number of synapses on PC dendrite by its area through electron microscopy measurement (Napper and Harvey, 1988), confocal Ca^{2+} imaging was performed to quantify extent activated dendritic area in response to PF stimulation and estimated the number of synapses recruited by LTD induction. The stimulation intensity was adjusted to elicit from approximately 200 to 600 pA of the evoked EPSC. With this intensity, I delivered LTD-Burst protocol without CF stimulation and estimated the number of recruited synapses based on the previous report. In this recording, I confirmed that larger stimuli intensity caused activation of more synapses ($p < 0.001$, $r = 0.72$; fig. 10A and B). Based on this result, I analyzed the correlation between stimulation intensity and magnitude of the LTD-IE. The magnitude of the excitability change was not in stimulation intensity-dependent manner ($p = 0.37$, $r = 0.24$; fig. 10C), indicating that there was no correlation between the numbers of activated synapses and intrinsic plasticity in my observation. In addition, I found that synaptic LTD also did not show significant correlation with stimulation intensity ($p = 0.75$, $r = 0.11$; fig. 10D). Taken together, temporal coincidence of PF and CF activation is the more significant element for induction of the PC plasticity than the number of recruited active synapses.

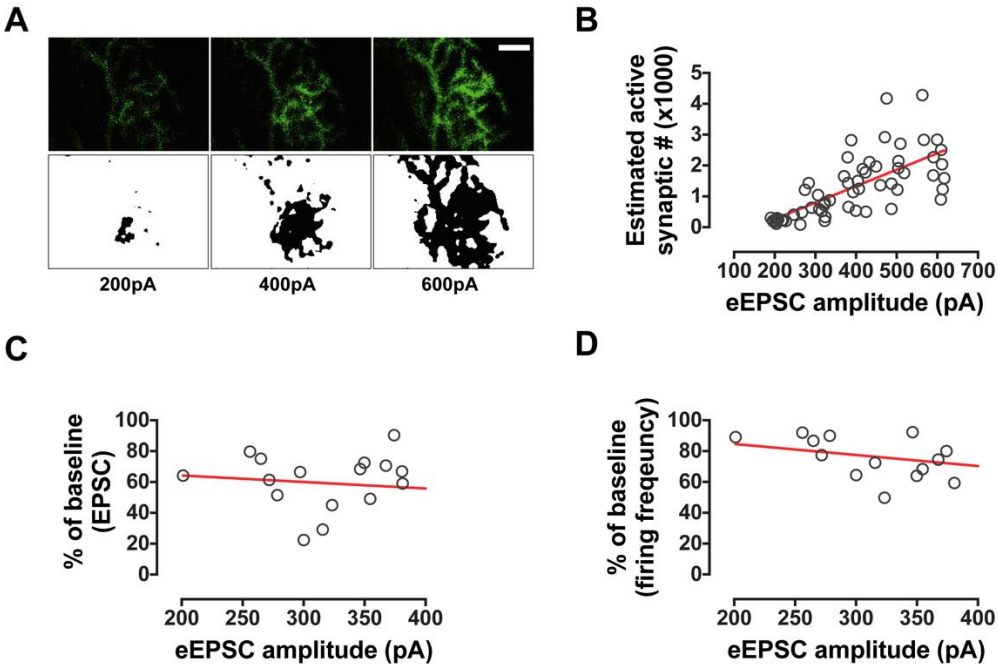

Figure 10. Correlation between recruited number of synapses and plasticity. (A) Confocal Ca^{2+} images (top) and their binary images (bottom) for analysis. The activated dendritic area was increased by an increment of stimulation intensity. Scale bars, 10 μm. (B) Linear regression between estimated the number of active synapses and stimulation intensity. There was a positive correlation between the number of active synapses and stimulation intensity (Pearson's $r = 0.723$, $p < 0.001$). (C) Correlation between reduced excitability in LTD-IE and stimulation intensity. There was no correlation between reduced excitability and stimulation intensity (Pearson's $r = 0.240$, $p = 0.370$). (D) Correlation between the magnitude of synaptic LTD and stimulation intensity. There was no correlation between magnitude of synaptic LTD and stimulation intensity (Pearson's $r = 0.115$, $p = 0.752$)

3.5 Information processing after LTD induction

Given that the cerebellar PCs integrate tremendous input from the sub-cortical region and generate the final output signal to its relay neurons, I questioned whether the strategy for the information processing would be changed during the alteration of intrinsic excitability following synaptic depression. To answer this, two types of information processing in PCs were focused: (1) temporally, distributed input signal is integrated within a dendrite (fig. 11A). (2) Spike frequency adaption (SFA) operates to filter the output signal by attenuating an unnecessary firing (Benda and Herz, 2003; Pozzorini et al., 2013) (fig. 11D). Temporal summation was evaluated by calculating the ratio of fifth excitatory postsynaptic potential (EPSP) to the first elicited by 5 PF stimuli with 10 Hz and 20 Hz. Reduction of EPSP was observed 40 min after the Burst but not the Pseudo-burst in comparison to the baseline (t = 40, Pseudo-burst, n = 11, 1.1 ± 1.0; Burst, n = 9, 0.7 ± 1.1; p = 0.019, post-hoc tukey test after Two-way RM ANOVA; fig. 11B). The EPSP5/EPSP1 ratio, nonetheless, was not changed (t = 40, 0.9 ± 0.06 (Pseudo-burst) vs. 0.9 ± 0.04 (Burst), p = 0. 804, independent *t*-test; fig. 11C - F), indicating that the PF-LTD resulted in the decrease of the absolute EPSP value without changes in the strategy for the temporal summation of the inputs.

To determine the SFA, all inter-spike-interval (ISI) of the evoked spike train elicited by injecting current of 500 pA was calculated and normalized to the first ISIs to determine the spike frequency adaptation (SFA; fig. 11E). Despite the reduction of the firing rates corresponding to the synaptic LTD, there was no significant change in calculated SFA compared to the baseline in all groups regardless of what protocol was used (Fig 11. F - I). Taken together, I concluded that synaptic LTD might not manifest the changes in the strategy of information process, but modify gain responses for generating the AP spike.

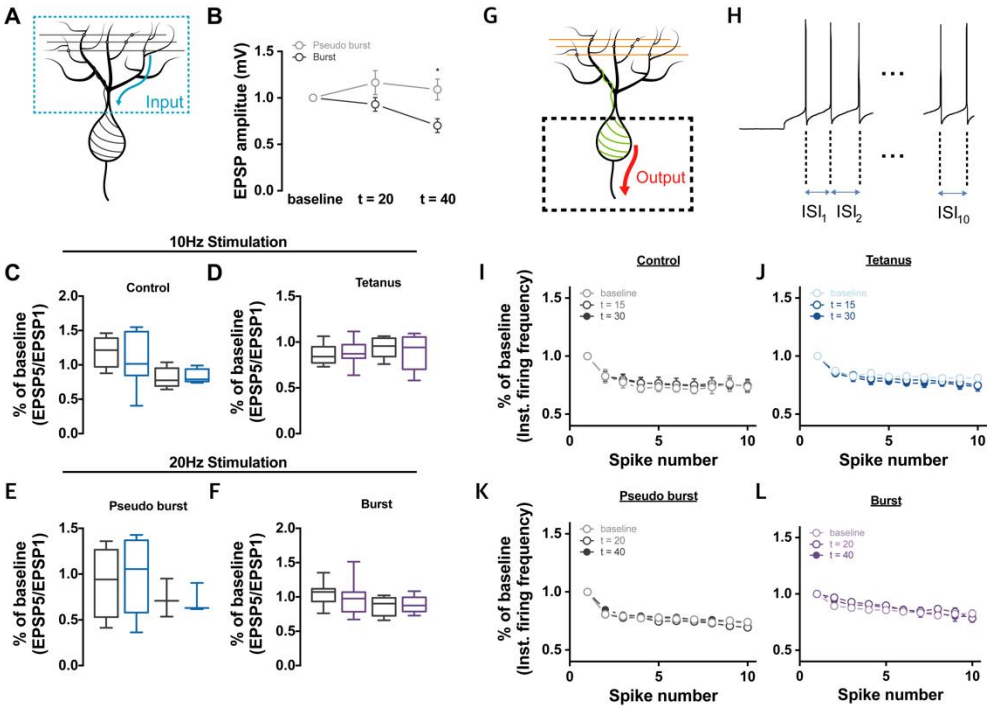

Figure 11. Information processing strategy was not changed after LTD-IE. (A) Schematic for input processing in PCs. (B) Normalized EPSP in Pseudo burst and Burst groups. PF-LTD caused reduction of EPSP compared with the Pseudo group (Pseudo, n = 11; Burst; n = 9, F = 4.6, p = 0.048). (C) Normalized EPSP summation in LTD-Pseudo and LTD-Burst groups. The normalized summation value was not influenced by LTD induction. (Pseudo, n = 11; Burst; n = 9; 20 min, p = 0.167; 40 min, p = 0.084). (D) Schematic for output processing in PCs. (E) Counting ISIs. Ten ISIs were measured to analyze SFA. (F – I). Normalized instantaneous frequency of all groups. Through time points, the power of frequency adaptation was not changed in the control (F), LTD-Tetanus (G), LTD-Burst (H), and LTD-Pseudo (I) groups. For statistics, two-way RM ANOVA was used for B and independent t test for C. Post hoc Tukey's test was used for different time group comparisons. Error bar indicates SEM. *p < 0.05.

3.6 LTD-IE required the Ca^{2+}-signal but depended on the Ca^{2+}-activated K^+ channels.

What is the intracellular signalling involved in the intrinsic plasticity? As I described above, precisely paired activation of PF and CF is a pivotal factor for induction of both synaptic and intrinsic plasticity. It suggests that the LTD-IE may share the signalling pathway for PF-LTD. Thus, I firstly asked if the LTD-IE is dependent on the Ca^{2+} signalling, which has been implicated in determining the PF-PC LTD (Konnerth et al., 1992). When the intracellular Ca^{2+} signalling was blocked by adding Ca^{2+} chelator BAPTA (10 mM) to the pipette solution, PF-PC LTD was completely abolished ($n = 10$; fig. 12A). In the same recording, prominent change of excitability after LTD induction was not exhibited in presence of BAPTA ($n = 5$, $F = 1.262$, $p = 0.334$; fig. 12B), suggesting that the Ca^{2+} is the necessary for the intrinsic plasticity.

It has widely been described that the intrinsic plasticity is derived from the changes in ion channel conductance and/or expression (Belmeguenai et al., 2010; Narayanan et al., 2010; Shim et al., 2016; van Welie and Lac, 2011). I observed that mAHP was significantly reduced while fAHP was unchanged by application of LTD-inducing protocols. It has been widely described that the SK channels determine the mAHP rather than fAHP. In addition, SK channels have been regarded as the major component for LTP-IE (Belmeguenai et al., 2010; Grasselli et al., 2016). Thus, I tested if this type of ion channels were required for the excitability change. Bath application of apamin (100 nM), selective antagonist of SK-channels, did not affect to the induction of synaptic and intrinsic plasticity (synaptic plasticity: $n = 7$; intrinsic plasticity: $n = 7$, $F = 11.317$, $p < 0.001$, One-way RM ANOVA; fig. 12E - G). Taken together, I conclude that activity-dependent downregulation of intrinsic excitability is not derived from Ca^{2+}-activated K^+ channel albeit the Ca^{2+}-dependency of LTD-IE.

The intracellular Ca^{2+} derived from synaptic activation governs a variety of Ca^{2+}-sensing molecules, such as PKC. To investigate whether LTD-IE requires

PKC activation as in synaptic plasticity, LTD-burst protocol was delivered with an internal solution including PKC inhibitor peptide, PKC (19-36). Interestingly, while both synaptic and intrinsic plasticity were normally induced and maintained in the presence of inactive control peptide, [Glu^{27}]-PKC (19-36) [synaptic plasticity: n = 7; intrinsic plasticity: n = 8, p = 0.005, F = 8.48, Two-way RM ANOVA; fig. 12C and D), changes of synaptic efficacy and excitability were not induced by PKC (19-36) (synaptic plasticity: n = 6; intrinsic plasticity: n = 13, p = 0.288, F = 1.41, Two-way RM ANOVA). Collectively, the LTD-IE might share a common intracellular pathway with PF-LTD, in that PKC activation underlies LTD-IE.

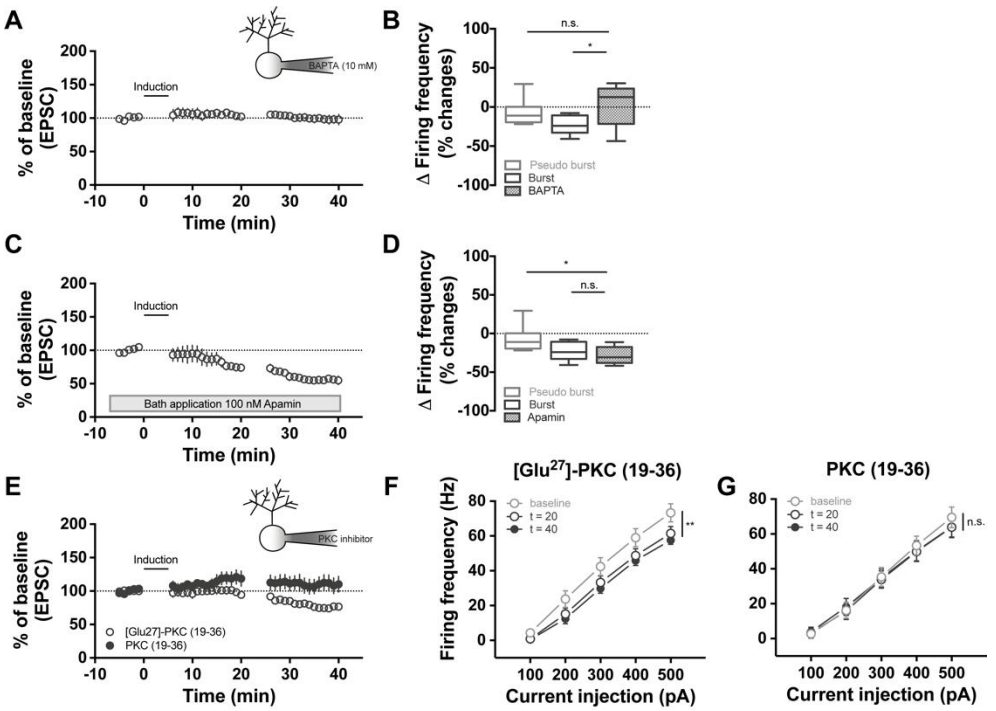

Figure 12. Synaptic LTD and LTD-IE share the intracellular Ca^{2+} and PKC pathway as an underlying mechanism but SK channels were not related. (A – B) LTD induction under BAPTA-containing internal solution. PF–PC LTD was completely blocked by 10 mM BAPTA (n = 10) (A), LTD-IE was also abolished under high concentration of BAPTA (n = 5, F = 1.703, p = 0.219) (B). (C – D) SK channel blocker treatment. (C) Apamin (100 nM) was not able to block LTD induction (n = 7). (D) LTD-IE was induced. Excitability of each time point was significantly reduced (after burst, n = 5; 20 min, n = 5; 40 min, n = 4; F = 16.255, p = 0.001). (E – F) PKC inhibitor and control peptide treatment. (E) PKC inhibitor peptide, PKC (19 –36) (10 μM), blocked LTD induction (filled, n = 6), but LTD was successfully induced in control peptide ([Glu ^{27}] PKC(19 –36), 10 μM; open, n = 7). D, Excitability of control peptide group showed LTD-IE from immediately after induction protocol to end of the recording (after burst, n = 8; 20 min, n = 8; 40 min, n = 6; F = 13.754, p < 0.001), but no significant reduction of excitability was observed in PKC inhibitor group (after burst, n = 13; 20 min, n = 8; 40 min, n = 6; (F = 1.618, p = 0.211). For statistics, one-way RM ANOVA was used for B, D, and F. Post hoc Tukey's test was used for different time group comparisons. Error bar indicates SEM. **p < 0.01, ***p < 0.001, n.s. = not significant.

Discussion

In this study, I show that conjunctive activation of PF and CF that induces of PF-PC LTD down-regulate the intrinsic excitability, resulting in the synergistic decrease of neuronal net output. This novel phenomenon shares intracellular Ca^{2+} signalling and PKC pathway with synaptic LTD but is not regulated by SK channels which were known as critical factors for LTP-IE. In the aspect of information processing, dendritic temporal summation and SFA power were not changed by the LTD-IE, indicating that the strategy for the handling information of PCs insensitively reflects the LTD induction.

The bidirectional modulation of the intrinsic excitability in PCs

Intrinsic plasticity complements the synaptic transmission and enables to fulfill optimal signal transduction within a local circuit in the region- and cell type-specific manners (Brager and Johnston, 2007; Mahon and Charpier, 2012; Nataraj et al., 2010). In the cerebellum, there are two possible expectations in terms of the direction of intrinsic plasticity associated with synaptic LTD: 1) PF-PC LTD may induce reduction of the intrinsic excitability of PCs leading to disinhibition on the next relay neurons such as neurons in the DCN or the VN. In this case, PC excitability is modulated with the same direction of PF-PC synaptic modification, resulting in enhanced activity of the DCN and the VN via disinhibition; 2) Alternatively, PF-PC LTD may induce LTP-IE of PCs, strengthening the inhibitory output of PC on the next relay neurons including the VN. This increased inhibition to the VN, however, is also possible to enhance the activity of neural circuit via boosting up the rebound activity followed by strong hyperpolarisation in the relay neurons (Sekirnjak et al., 2003). This work support the former expectation in which the down-regulation of intrinsic excitability occurred with the synaptic LTD in PCs. These results are parallel with the prediction of which cerebellum-dependent motor learning is associated with the reduced cortical activity (Lev-Ram et al., 2003).

Recently, (Yang and Santamaria, 2016) reported that synaptic LTD induction potentiates PC excitability showing the opposite to the observation I presented here. The authors paired PF stimulation and the somatic depolarisation, instead of CF stimulation, with 1 Hz to induce the LTD. This protocol may trigger synaptic and intrinsic plasticity via activation of the different intracellular signalling from this experimental condition. In contrast, I delivered PF and CF stimulation with two types of protocol to reflect more physiological circumstance and applied the Pseudo-burst induction protocol to exclude bias of long-term recording. Conjunctive activation of PF and CF successfully induces not only the synaptic LTD but also the LTD-IE. Considering the LTP-IE accompanied with LTP induction in PCs (Belmeguenai et al., 2010), this work provides insight into the bidirectional modulation of intrinsic excitability in a stimuli-pattern specific manner. The same polarity of plasticity between synaptic strength and intrinsic excitability may enable to emphasise the decreased or potentiated synaptic current by newly tuned membrane excitability, by which total net output of the neurons are generated through multiplication of the synaptic current and intrinsic excitability. Surprisingly, temporal EPSP summation and SFA are not altered by the induction of plasticity, indicating that PCs consistently maintain the strategy to process information and filter the output signal after LTD-IE occurs. Taken together, I suggest functional roles of the PC intrinsic plasticity as the amplifier within a motor learning circuitry.

Underlying mechanism of LTD-IE

Intrinsic plasticity including LTP- and LTD-IE can be triggered by the synaptic stimulation inducing LTP and LTD, respectively (Belmeguenai et al., 2010), indicating that the synaptic plasticity and intrinsic plasticity share the molecular cascades for plasticity induction. Coupled activation by PF and CF is the prerequisite for cerebellar LTD induction, which is established through the positive feedback loop of PKC-MAPK signalling. By using intracellular Ca^{2+} chelator and

inhibitor peptide of PKC, I confirmed that intracellular Ca^{2+} signalling plays a central role in the LTD-IE induction and synaptic and intrinsic plasticity has a common pathway. Besides, LTD is mediated by the more complex interaction between kinases and phosphatases. These interactions have also implicated in the intrinsic plasticity through the ion channel regulation (Belmeguenai et al., 2010; Brager and Johnston, 2007; Cudmore and Turrigiano, 2004; Shim et al., 2016). I observed the alteration of AP firing properties, such as reduction of input resistance and mAHP, reflecting the changes in the ion channel conductance and/or expression level. Since it has been described that the mAHP correlates to the SK channels, I tested the involvement of SK channels in LTD-IE though the bath application of apamin (Kato et al., 2006; Pedarzani et al., 2005). This expectation is neglected because 1) attenuation of mAHP is also shown without changes in excitability when unpaired synaptic stimuli are delivered (Pseudo-burst), and 2) application of apamin, SK channel inhibitor, is ineffective to the LTD-IE induction. LTD-IE induction also results in the reduction of input resistance. This change is derived from the activity-dependent modulation of ion channels, such as voltage-gated K^+ channels, and hyperpolarization-activated cyclic nucleotide gated (HCN) channels (Hyun et al., 2013; Shim et al., 2016), rather than the SK channels. Given the down-regulation of the intrinsic excitability, even though the voltage threshold is shifted to hyperpolarisation after LTD induction, changes of input resistance may have a larger impact on the intrinsic excitability via reducing voltage deflection in response to the given current. In this study, I observed the aspect of the intrinsic plasticity accompanied by synaptic LTD and concluded that synaptic and intrinsic plasticity are mediated by the similar signalling cascades. It remains to be elucidated what precise mechanism underlies in intrinsic plasticity.

Intrinsic plasticity in motor learning circuitry

What are the physiological consequences of the intrinsic plasticity of cerebellar PCs? The neural plasticity occurs in the cerebellar cortex and the VN are important

components for VOR learning (Boyden et al., 2004; Ito, 2013). Given the note that cerebellar PCs are the only neuron connecting to the VN from the cerebellar cortex, the activity-dependent modulation of the PC excitability would have physiological significance for motor learning. A mathematical model demonstrated the serial process for long-term memory consolidation of eye movement learning (Yamazaki et al., 2015). According to the study, depression of synaptic weight between PF-PC precedes the changes in synaptic strength between MF-VN in the learning phase. Interestingly, the synaptic weight of MF-VN synapses continuously strengthens in post-training phase for several hours even though PF-PC LTD is recovered after training. This theoretical expectation is parallel with previous studies reporting that post-training phase is important for consolidation (Kassardjian et al., 2005; Okamoto et al., 2011a; 2011b). The intrinsic plasticity, therefore, may precisely instruct the neural plasticity in the VN neurons to consolidate the memory. In addition, the data presented here suggests the bidirectional modulation of intrinsic excitability in response to synaptic plasticity. This bi-directionality of the intrinsic plasticity of PC may have an essential role in cerebellum-dependent motor learning circuitry since the polarity of synaptic plasticity are selectively engaged with learning paradigms, gain-up and –down (Boyden et al., 2006). Taken together, I hypothesise that the VN neurons receive the learning pattern via the bidirectional modulation of the intrinsic plasticity and synaptic plasticity in the cerebellar cortex. In other words, PCs might collect the information through synaptic plasticity and transfer the information by modifying their excitability.

This engaged behavioral evidence leads to the question whether LTD-IE can be reversed by application of LTP-inducing protocol because the neural activity is dynamically regulated in response to the behavioral modification. However, the data I presented here shows that LTD-IE cannot be reversed into LTP-IE, and vice versa. These results might be possibly explained by following reasons: 1) Lev-Ram et al., (2003) described that synaptic plasticity induced by a higher frequency of PF stimulation than 1 Hz cannot be reversed because the stronger stimuli result in

more saturation of plasticity (Lev-Ram et al., 2003); 2) Moreover, the total duration of recording and stimulation interval may be not enough to elicit the reversibility. The mathematical model suggested the change of cerebellar PC output is gradually developed for 2 to 4 hour after the learning phase (Yamazaki et al., 2015). In addition, the behavioral reversal test indicates that reversal change of excitability might build over a longer time than observed in slice recording (Boyden and Raymond, 2003). Since intrinsic plasticity may be involved in several behavioral consequences, unrevealed features of the intrinsic plasticity in behavior should be clarified in further study.

Chapter 4

Synergies between synaptic depression and intrinsic plasticity of the cerebellar Purkinje cells determining the Purkinje cell output

Introduction

Many theories have described that experience and use-dependent modifications of intrinsic excitability (intrinsic plasticity) could be the one other side of memory engram (Daoudal and Debanne, 2003; Debanne et al., 2018; Shim et al., 2018). Given that the sensory information is conveyed to the post-synaptic neurons via forms of action potential (AP) firing, the modulation of excitability may shape information flow and maximize the memory storage in the brain. The changes in synaptic weight is ultimately reflected by postsynaptic spike output in order to appropriately transduce the information in the network (Mittmann and Häusser, 2007). In fact, intrinsic excitability determines the patterns of integrating synaptic inputs and net output of the neuron (Hoffman et al., 1997; Lev-Ram et al., 2003; Shim et al., 2017; Watanabe et al., 2002). Thus, understanding how neurons coordinate neuronal input and output signal in an activity-dependent fashion could broaden understanding of how information is processed in the neural local circuits.

There has been accumulating evidence indicating the physiological significance of the activity-dependent cerebellar Purkinje cell (PC) intrinsic plasticity on the cerebellar function beyond long-term depression at parallel fiber – PC synapses (PF-PC LTD) theory, the classical view of cellular basis for cerebellar-dependent motor learning (Shim et al., 2017). Together with the study describing that repetitive PF activation triggers PF-PC LTP as well as LTP-IE, the intrinsic plasticity is bidirectionally modulated corresponding to the polarity of synaptic plasticity (Belmeguenai et al., 2010). These results suggest that intrinsic plasticity may amplify the changes in synaptic efficacy to determine the PC output. The multiple lines of evidence has described that alteration of PF synaptic weight influences on the spiking activity such as pause duration of spiking activity (Grasselli et al., 2016; Mittmann and Häusser, 2007; Steuber et al., 2007). Those literatures propose that the changes in modality of spiking activity would affect to the relay neurons of PCs such as deep cerebellar nuclei (DCN) and vestibular nuclei (VN) neurons through disinhibitory effects. However, how the cerebellar

PCs coordinate the synaptic plasticity and PC output signals to appropriately tune the postsynaptic spiking activity is still less understood.

In the present study, I investigated the synergies between synaptic and intrinsic plasticity in the floccular PCs. Indeed, the LTD-IE in the floccular PCs followed timing rules governing the associative PF-PC LTD matched to behavioral learning rule (Suvrathan and Raymond, 2018). As the PF-PC LTD, the LTD-IE also required mGluR1-PKC pathway and CaMKII signaling, indicating that the intrinsic plasticity shares intracellular signaling for synaptic plasticity. The depression of synaptic efficacy in the PCs is reflected by postsynaptic spiking activity when both PF-PC LTD and LTD-IE occurred. Furthermore, I compared the PF-evoked spiking activity by delivering the PF stimulation in the two different dendritic branches of the same neuron. Strikingly, synaptically evoked spiking activity was found to be decreased when conditioned PF was activated, indicating that the synergistic plasticity may be formed in an activated branch-specific manner. Thus, synaptic plasticity at the PF-PC synapses may affect to PC spiking output in a supralinear manner.

Material and Methods

1. Animals and Slice preparation

All animal use was in accordance with protocols approved by the Institution's Animal Care and Use Committee of Seoul National University College of Medicine. Cerebellar coronal slices were dissected into 250 μm by vibratome (Leica, VT1200) from anaesthetized 4- 6 weeks old male C57BL/6 mice in ice-cold standard artificial cerebrospinal fluid (aCSF) contained with the following (in mM): 125 NaCl, 2.5 KCl, 1 $MgCl_2$, 2 $CaCl_2$, 1.25 NaH_2PO_4, 26 $NaHCO_3$, 10 glucose bubbled with 95% O2 and 5% CO2. For recovery, slices were incubated at 32 ˚C for 30 minutes and further 1 hour at room temperature.

2. Electrophysiology

Slices were put onto a submerged recording chamber on the stage of Olympus microscope (BX50WI, Japan) and perfused with aCSF, and kept in place with a nylon-strung platinum anchor. All recordings were performed using multiclamp 700B patch-clamp amplifier (Axon Instruments) with a sampling frequency of 20 kHz and signals were filtered at 2 kHz. In all recordings, inhibitory synaptic inputs were totally blocked by 100 μM picrotoxin to monitor only the excitatory synaptic transmission. Patch pipettes (3-4 MΩ) were borosilicate glass and filled with internal solution. Composition of the internal solution is described in the Material and Method of Part 1. The membrane potential was held on -70 mV in voltage-clamp (VC) and current-clamp mode (CC). Recordings were discarded if the series resistance (R_s) varied by > 15% and the injection current for the holding potential exceeded 600 pA. PFs in the molecular layer and CF in the granule cell layer were stimulated by an ACSF-filled electrode (fig. 13A). I used three different protocols to induce the PF-PC LTD in CC mode for 5 min: 1) tetanizing of PF and CF simultaneously (1 Hz, 300 times for 5 min) tetanizing of PF followed by single CF stimulation with the stimulus interval of 120 ms (1Hz, 300 times for 5 min), 3) 7 times of burst stimulation of PF with 100 Hz followed by single CF stimulation with the stimulus interval of 150 ms (30 times and sweep interval 10 s for 5 min).

To evaluate the PCs excitability, a series of current steps of 500 ms duration ranging from +100 pA to +500 pA with increments of 100 pA with a step interval of 4.5 s from a membrane potential of -70 mV was injected in CC mode.

3. Data acquisition and analysis

All data were acquired by Clampex software (Molecular Devices) and analyzed by IgorPro 8.1 (Wavemetrics). I evaluated the LTD by normalizing to the average of baseline PF-EPSC, and recording was excluded if the baseline current or the number of evoked spikes varied by > 20 %. R_S was calculated by fitting a single exponentials to the voltage responses of the test pulse (-5 mV).

Data were presented as mean ± SEM and statistical evaluations were performed using normality test, equal variant test, independent *t*-test, One-way repetitive measured (RM) ANOVA and Two-way RM ANOVA with post *hoc* tukey test by Origin 8.5 and SigmaPlot 12.0 software. Sample size was approved by power analysis using the G*power 3.1.9.2.

Results

4.1 Timing rules of intrinsic plasticity of floccular PCs

Since the PF-PC LTD of the flocculus, sub-region of the cerebellum taking part in motor learning, has been found to be matched to behavioral function (Suvrathan et al., 2016), I firstly verified whether intrinsic plasticity would also follow the distinctive timing rule for plasticity induction by using whole-cell patch clamp recordings in the acute floccular slices from young adult mice (4 – 6 weeks old). All recordings were performed in the presence of inhibitor for inhibitory synaptic transmission (100μM picrotoxin) (fig. 13A). To confirm this, three different protocols for LTD induction were tested in the floccular slices: 1) tetanizing of PF and CF simultaneously (PF-$LTD_{ISI=0}$, 1 Hz, 300 times for 5 min; fig. 13B left), 2) tetanizing of PF followed by single CF stimulation with the stimulus interval of 120 ms (PF-$LTD_{ISI=120}$, 1Hz, 300 times for 5 min; fig. 13B middle), 3) 7 times of burst stimulation of PF with 100 Hz followed by single CF stimulation with the stimulus interval of 150 ms (30 times and sweep interval 10 s for 5 min; PF-$LTD_{ISI=150Burst}$; fig. 13B right) (Shim et al., 2017; Suvrathan et al., 2016). Consistent with the previous study, the associative PF-PC LTD was exerted by the delayed pairing of PF and CF stimulation but not by simultaneous stimulation [fig. 13C; % of baseline: PF-$LTD_{ISI=0}$ = 120.00 ± 17.33%, n = 7; PF-$LTD_{ISI=120}$ = 59.23 ± 6.46%, n = 7; PF-$LTD_{ISI=150bust}$ = 65.13 ± 6.61% of baseline, n = 7; F = 6.99, p = 0.005, One-way ANOVA]. During the recordings, the access resistance, paired-pulse ratio (PPR) and input resistance were monitored, and the data was discared if the changes in access resistance exceed 20% compared to baseline (fig. 13D – F). The PF-$LTD_{ISI=0}$ protocol did not alter the PPR, implying postsynaptic formation of synaptic plasticity (fig. 13E). Interestingly, the LTD-IE was exhibited by only the LTD-inducing protocols (PF-$LTD_{ISI=120}$ and PF-$LTD_{ISI=150bust}$) whereas simultaneous stimulation of PF and CF failed to induce LTD-IE as well as PF-PC LTD (fig. 14A

– C; Δfiring frequency: PF-LTD$_{ISI=0}$ = -12.06 ± 6.95 Hz, n = 5; ISI$_{120}$ = -43.87 ± 9.98 Hz, n = 5, p = 0.028, Mann-whitney). The temporal summation of the EPSP was comparable between the protocols, indicating that the induction of LTD may give rise to reduction of input and output signals without integration patterns of synaptic inputs (fig. 14D). Reduced intrinsic excitability of PCs after LTD induction may lead to attenuation of PF impact on the postsynaptic spiking output. Thus, I furthermore investigated whether the spike output of the PCs would reflect the PF-PC LTD. The readout of the spiking output of the PCs after LTD induction was the number of spikes evoked by 20 of PF stimulation with 20Hz (fig. 14E and F). The PF-evoked spiking output was robustly decreased after LTD induction (spike count: baseline = 25.83 ± 2.96; t=40 = 9.50 ± 1.36, n = 6, p = 0.0312, Wilcoxon test), on the other hand, the simultaneous stimulation of PF and CF failed to affect to PC spiking activity (fig. 14E and F; Δspike count: ISI$_0$ = 0.30 ± 12.02%, n = 6; ISI$_{120}$ = -60.52 ± 6.65%, n = 6, p = 0.002, Mann-Whitney test). Altogether, I concluded that the activity-dependent modulation of the PC excitability in the flocculus matches to behavioral learning rules in align with the timing rule governing synaptic LTD. In addition, the PF-PC LTD influences on the postsynaptic spiking output, supporting the assumption that the cerebellar LTD would decrease the cerebellar cortical output on to the downstream neurons of the cerebellar PCs.

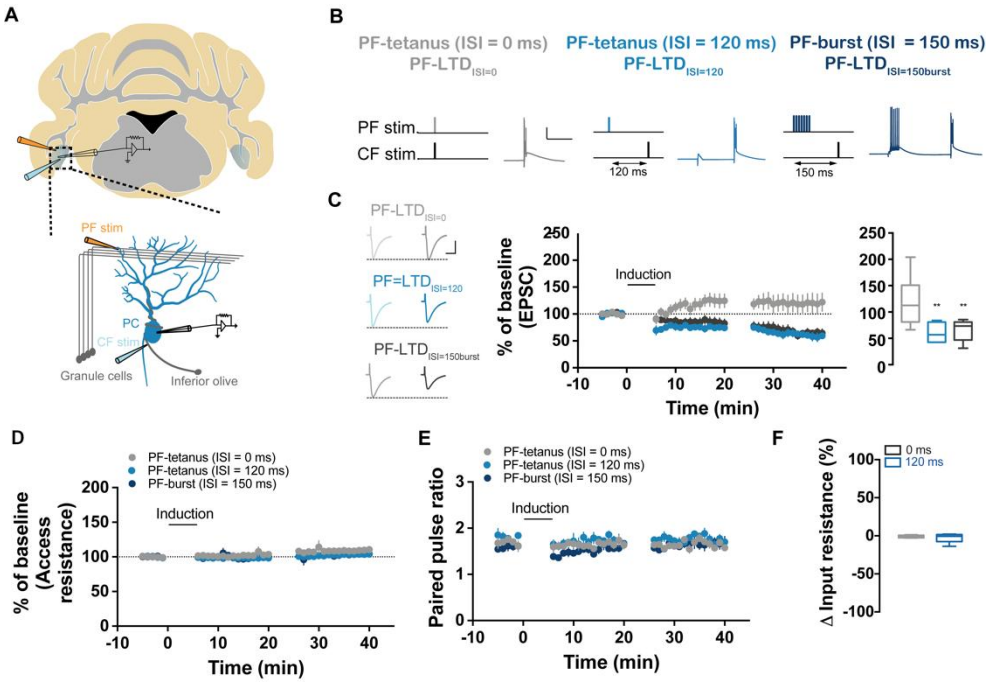

Figure 13. Timing rules for induction of PF-PC LTD. (A) Illustration of the cerebellar flocculus (upper) and the recording site for synaptic plasticity (bottom). (B) Three protocols were used for induction of LTD and LTD-IE. Tetanizing of PF with 1 Hz for 5 min was delivered and single CF was stimulated simultaneously or following tetanizing with interval of 120 ms [PF-$LTD_{ISI=0}$, top (grey) vs. PF-$LTD_{ISI=120}$, middle (blue)], or the PF-burst protocol consisted of 7 times of burst stimulation into PF with 100 Hz followed by CF activation with interval of 150 ms in every 10 s for 5 min [PF-$LTD_{ISI=150burst}$ ms), bottom (dark blue)]. (C) Plots and summarizing box and whisker plots (right) of changes in eEPSC from PF-$LTD_{ISI=0}$ (grey, n = 7), PF-$LTD_{ISI=120}$ (blue, n = 7) and PF-$LTD_{ISI=150burst}$ (dark blue, n = 9). Consistent to previous observation, delayed activation of CF with 120 ms and 150 ms of delay from PF activation induced PF-PTD LTD ($F = 9.256$, $p = 0.001$, One-way ANOVA). Insets (left) show the representative trace of eEPSC before and after induction. Scale bar: 25 ms (horizontal) and 50 ms (vertical). (D) Plots showing the changes in access resistance before and after induction. The data showing the changes in access resistance was over 20% compared to baseline was discarded. (E) Plots showing the changes in paired-pulse ratio before and after induction. All protocols did not significantly affect to PPR. (F) Box and whisker plots showing the changes in input resistance before and after induction. There were no significant changes in input resistance after induction compared to baseline.

For statistics, one-way ANOVA was used for C and post *hoc* Tukey's test was used for different group comparison. Asterisks in the panel C (right) denote statistical significances by post *hoc* Tukey's test after One-way ANOVA.

Error bar indicates SEM. **$p < 0.01$.

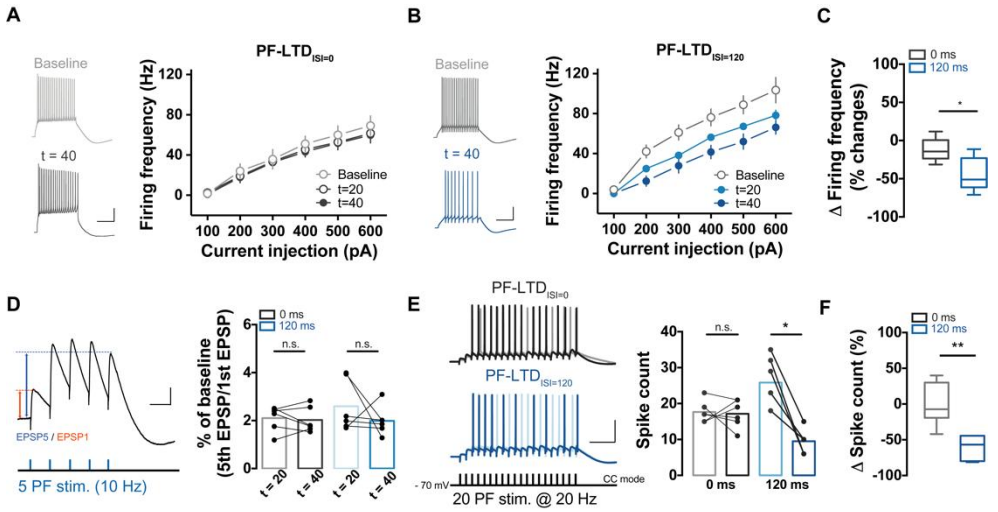

Figure 14. Timing rules for induction of LTD-IE. (A – B) Plots showing frequency – current (F/I) curve of PF-LTD$_{ISI=0}$ (A: grey; n = 5) and PF-LTD$_{ISI=120}$ (B: blue; n = 5). Insets show representative traces of depolarization-induced AP train. Intrinsic excitability was significantly decreased after LTD induction with PF-LTD$_{ISI=120}$. Scale: 200 ms (horizontal) and 20 mV (vertical). (C) Summarizing box and whisker plots showing comparison of Δ firing frequency between groups (Δfiring frequency: PF-LTD$_{ISI=0}$ = -12.06±6.95%, n = 5; PF-LTD$_{ISI=120}$ = -43.87 ± 9.98%, n = 5, p = 0.03, Mann-whitney). (D) Bar graph showing the changes in temporal summation of the EPSP from two protocols (black: PF-LTD$_{ISI=0}$; blue: PF-LTD$_{ISI=120}$). Summation was determined by calculating the ratio of 5th EPSP amplitude to 1st EPSP amplitude (PF-LTD$_{ISI=0}$: p = 0.71, n = 6; PF-LTD$_{ISI=120}$: p = 0.36, n = 6). Insets (right) show a representative trace and protocol. EPSP summation was not changed after LTD induction. Scale: 100 ms (horizontal) and 5 mV (vertical). (E) Bar graphs showing the changes in PF-evoked spike count between before and after induction from the groups (grey: PF-LTD$_{ISI=0}$ before induction; black: PF-LTD$_{ISI=0}$ after induction, n = 6; light blue: PF-LTD$_{ISI=120}$ before induction; blue: PF-LTD$_{ISI=120}$ after induction, n = 7). Only in PF-LTD$_{ISI=120}$ showed the significant reduction of the PF-evoked spike count (PF-evoked spike count: baseline = 25.83 ± 2.96 vs. t = 40 = 9.50 ± 1.36, p = 0.03, Wilcoxon test) compared to PF-LTD$_{ISI=0}$ (PF-evoked spike count: baseline = 17.67 ± 1.23 vs. t = 40 = 17.17 ± 1.60, p = 0.81, Wilcoxon test). Insets show representative traces of PF-evoked spikes, elicited by stimulating 20 times of PF with 20 Hz. Scale: 250 ms (horizontal) and 20 mV (vertical). (F) Box and whisker plots showing the PF-evoked spike count from PF-LTD$_{ISI=0}$ (grey) and PF-LTD$_{ISI=120}$ (blue). LTD-inducing protocol robustly decreased the PF-evoked spiking activity (Δspike count: PF-LTD$_{ISI=0}$ = 0.30 ± 12.02% vs. PF-LTD$_{ISI=120}$ = -60.52 ± 6.65%, p = 0.002, Mann-whitney test).
For statistics, one-way RM ANOVA was used for A and B and post hoc Tukey's test was used for different time group comparison. Mann-Whitney test was used for C and F and Wilcoxon test was used for comparison of paired data set in D and E (middle). Error bar indicates SEM. n.s. denotes 'not significant'; *P < 0.05, **p < 0.01, ***p < 0.001.

4.2 Intrinsic plasticity shares intracellular signaling for PF-PC LTD

I previously reported that synaptic LTD and LTD-IE were dependent on the intracellular Ca^{2+} elevation and PKC signaling (Shim et al., 2017). Also, the intrinsic plasticity of the floccular PCs was found to be exerted when PF-PC LTD occurred (fig. 14B), indicating that the LTD-IE in PCs may share signaling pathway for PF-PC LTD. Thus, I investigated whether the LTD-IE would share underlying mechanisms governing synaptic LTD. To address this, the competitive antagonist of mGluR1, (S)-(+)-α-Amino-4-carboxy-2-methylbenzeneaceticacid (LY 367385, 100μM) was applied in the recording chamber in order to inhibit mGluR1 activation during the induction of PF-PC LTD. In the light of the previous studies, inhibition of mGluR1 prevented the forming PF-PC LTD in the floccular PCs (Fiala et al., 1996). In addition to the synaptic plasticity, the LTD-IE was not shown in the presence of LY 367385 [fig. 15A and B; % of baseline (A): LY367385-treated = 96.04 ± 7.41%, n = 5, p = 0.02, compared to the value shown in fig. 14B; Firing frequency: $F(2, 8) = 3.12$, $p = 0.10$, Two-way RM ANOVA]. Interestingly, the excitability of PCs was decreased 20 min after induction, however, the changes in excitability was totally abolished 40 min after induction, indicating that the intrinsic plasticity accompanied by synaptic depression required mGluR1-PKC signaling pathway (firing frequency at 500 pA injection : baseline = 68.37 ± 2.37 Hz; t=20 = 49.64 ± 4.59 Hz; t=40 = 62.75 ± 6.89 Hz, n = 5, baseline vs. t=20: $p = 0.0001$; baseline vs. t=40: $p = 0.18$, post-*hoc* tukey test). PF-evoked spike output also showed no significant changes after LTD-induction with mGluR1 antagonist compared to the baseline (fig. 15C and D; Δspike count: -4.06 ±5.81%, n = 5, p = 0.002, Mann-Whitney test, compared to the value shown in fig. 14H after LTD induction).

Given that mGluR-PKC signaling-dependent cerebellar LTD has been found to be supported by Ca2+-dependent kinase activity such as Ca^{2+}/calmodulin-dependent protein kinase II (CaMKII) (Kawaguchi and Hirano, 2013), I tested if

CaMKII signaling would be also involved in LTD and LTD-IE in the floccular PCs. To inhibit the CaMKII signaling during the LTD induction, 4-[(2S)-2-[(5-isoquinolinylsulfonyl)methylamino]-3-oxo-3-(4-phenyl-1-piperazinyl)propyl] phenyl isoquinolinesulfonic acid ester (KN-62, 3 μM) was applied into the slices throughout recordings (n = 7). In presence of CaMKII inhibitor, KN-62, neither PF-PC LTD, LTD-IE nor PF-evoked spike count was not elicited (fig. 15E – H), indicating that the mGluR1 signaling may play a critical role in synaptic and intrinsic plasticity of the cerebellar PCs.

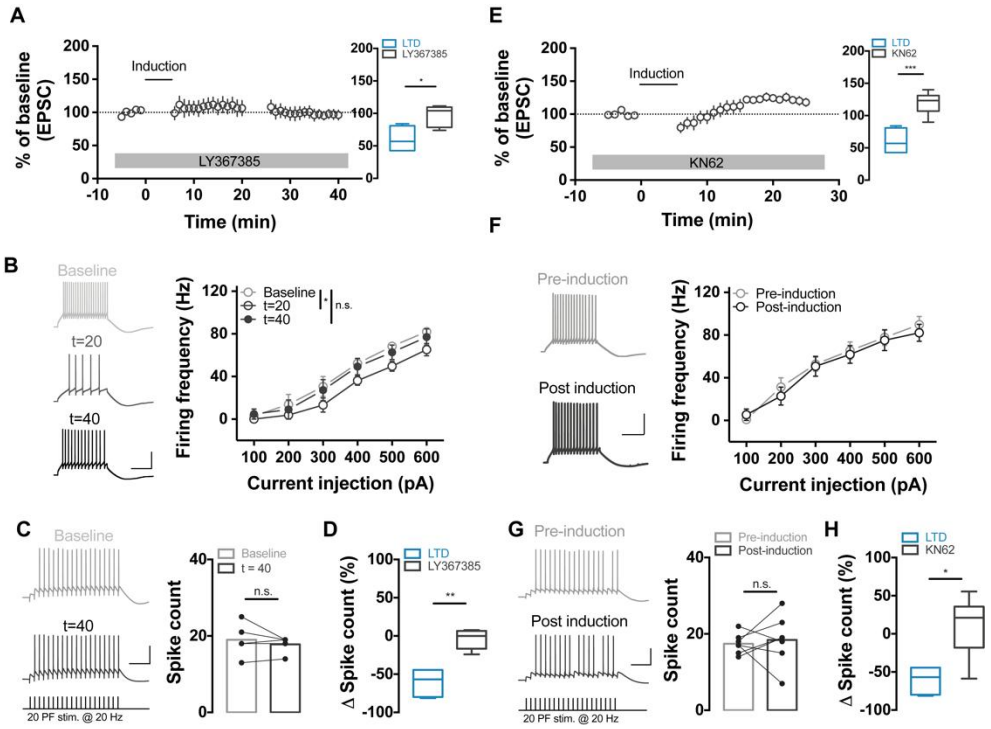

Figure 15. The LTD-IE is dependent of mGluR1 signaling. (A) Plots (left) showing the normalized eEPSC before and after LTD induction in a presence of mGluR1 inhibitor, LY367385 (100 μM) and summarizing box and whisker plots (right) of changes in eEPSC corresponding to ISI_{120} (blue, value shown in fig. 14B, n = 7) and LY36738-treated group (black, n = 5). Compared to ISI_{120}, LY367385 prevented induction of PF-LTD (p = 0.02, Mann-whitney test). (B) Plots showing frequency – current (F/I) curve of LY367385-treated group corresponding to time after induction (grey: baseline; black open: t = 20; black closed: t = 40, n = 4, p = 0.10, Two-way RM ANOVA). The statistical difference was shown only at t = 20 compared to baseline and there was no significance between baseline and t = 40 (baseline vs. t = 20: p = 0.001; baseline vs. t = 40: p = 0.18, post-*hoc* tukey test). Insets show representative traces of depolarization-induced AP train. Scale: 200 ms (horizontal) and 20 mV (vertical). (C) Bar graphs showing the changes in PF-evoked spike count between before and after induction in a presence of LY367385 (grey: baseline; black: t = 40). There was no significant changes in PF-evoked spike count before and after LTD induction (PF-evoked spike count: baseline = 19 ± 1.98 vs. t = 40 = 17.8 ± 0.97, p = 0.63, Wilcoxon test). Insets show representative traces of PF-evoked spikes, elicited by stimulating 20 times of PF with 20 Hz. Scale: 250 ms (horizontal) and 20 mV (vertical). (D) Box and whisker plots showing the PF-evoked spike count from ISI_{120} (blue) and LY367385-treated group (grey). Inhibition of mGluR1 prevented the changes in PF-evoked spike output (Δspike count in LY367385- treated group = -4.06 ±5.81%, comparison with the value of ISI_{120}, p = 0.01, Mann-whitney test). (E) Plots (left) showing the normalized eEPSC before and after LTD induction in a presence of CaMKII inhibitor, KN62 (3 μM) and summarizing box and whisker plots (right) of changes in eEPSC corresponding to ISI_{120} (blue, value shown in fig. 14B, n = 7) and KN62-treated group (black, n = 7). Compared to ISI_{120}, KN62 prevented induction of PF-LTD (p = 0.0003, Mann-whitney test). (F) Plots showing frequency – current (F/I) curve of LY367385-treated group corresponding to time after induction (grey: pre-induction; black: post-induction, n = 5). Insets show representative traces of depolarization-induced AP train. Scale: 200 ms (horizontal) and 20 mV (vertical). (G) Bar graphs showing the changes in PF-evoked spike count between before and after induction in a presence of KN62 (grey: pre-induction; black: post-induction). There was no significant changes in PF-evoked spike count before and after LTD induction (PF-evoked spike count: pre-induction = 17.43 ± 0.10 vs. post-induction = 18.43 ± 2.47, p = 0.63, Wilcoxon test). Insets show representative traces of PF-evoked spikes, elicited by stimulating 20 times of PF with 20 Hz. Scale: 250 ms (horizontal) and 20 mV (vertical). (H) Box and whisker plots showing the PF-evoked spike count from ISI_{120} (blue) and KN62-treated group (grey). Inhibition of CaMKII prevented the changes in PF-evoked spike output (Δspike count in KN62-treated group = 7.17 ± 17.71%, comparison with the value of ISI_{120}, p = 0.02, Mann-whitney test).

For statistics, Mann-whitney test was used for A (right), D, E (right) and H and Wilcoxon test was used for comparison of paired data set in C and G. Two-way RM ANOVA was used for B and post hoc Tukey's test was used for different time group comparison. Error bar indicates SEM. n.s. denotes 'not significant'; *P < 0.05, **p < 0.01, ***p < 0.001. * in panel B indicated statistical difference between each time point and significances was tested by post-*hoc* tukey test of Two-way RM ANOVA.

4.3 Conditioned PF branches contributing to robust reduction of spike output of the PCs.

Synaptic plasticity is thought to be highly localized whereas intrinsic plasticity could lead to global changes in neuronal activity. This assumption seems as if the intrinsic plasticity distorts the input specificity from the localized alteration of synaptic gain. Several lines of evidence have described that each individual dendritic branches of a neuron could be an information processing unit, (Govindarajan et al., 2006; Ohtsuki et al., 2012; Wilms and Häusser, 2015; Zang et al., 2018). I asked if the cerebellar PCs would associate the PF-PC LTD with the LTD-IE reflecting postsynaptic spiking output in an activated-branch specific manner. To answer this, electrical stimuli were delivered into the two different branches of PFs beams (fig. 16A and B). During the induction period, PF-PC LTD protocol was delivered at the conditioning site (conditioned PF) whereas the PF tetanizing was omitted at the other site of the branch (unconditioned PF). PF-PC LTD and LTD-IE were exhibited as shown in fig. 14B and D [% of baseline (C): conditioned PF = 67.16 ± 3.51% vs. unconditioned PF = 110.10 ± 5.05%, n = 8, p = 0.0002; Firing frequency (D): pre-induction = 71.41 ± 5.83 Hz vs. post-induction = 47.41 ± 4.75, F (1, 7) = 35.09, p = 0.0006, Two-way RM ANOVA, p < 0.0001, post-*hoc* tukey test]. However, there was no change in synaptic weight at the non-conditioned branch (% of baseline: conditioned PF = 67.16 ± 3.51% vs. unconditioned PF = 110.10 ± 5.051%, p = 0.0002, Mann-whitney test). Notably, the PF-evoked spike count was robustly decreased when conditioned PF was stimulated whereas unconditioned PF-evoked spike count showed slight but not significant reduction compared to baseline (fig. 16E and F; Δspike count: conditioned PF = -52.28 ± 4.35%; unconditioned PF = -11.71 ± 5.97%, n = 8, p = 0.0006, Mann-whitney test). Thus, synaptic LTD and LTD-IE may synergistically coordinate input-output signals. Moreover, these results implicate the highly localized occurrence of synaptic and intrinsic plasticity, supporting the idea that synergistic cooperation of spiking output during the learning.

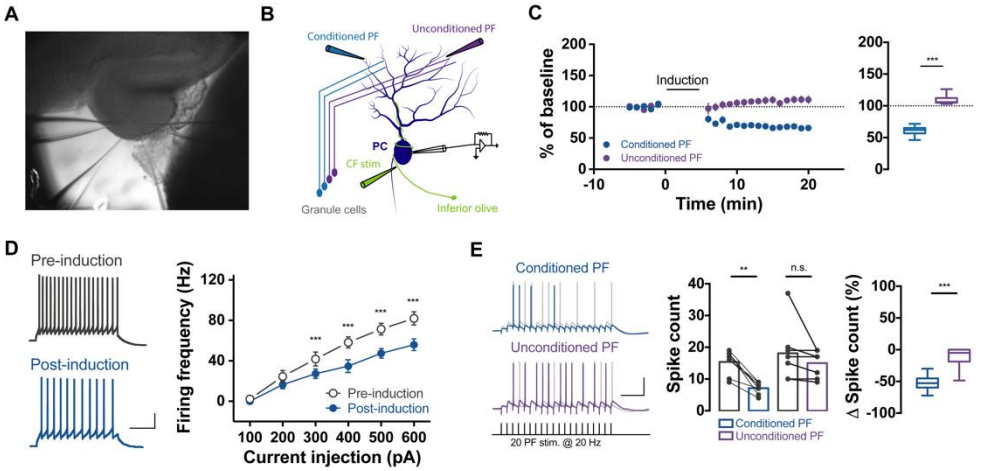

Figure 16. Synergistic plasticity of the PC spike output. (A – B) DIC image and illustration of experimental strategy. Two sites of PF branches of the one neuron were stimulated. (B) LTD-inducing protocol was delivered into the one site of PF branch (conditioned PF, blue) and tetanizing was omitted in the other side of PF branch (unconditioned PF, purple). (C) Plots (left) showing the normalized eEPSC before and after LTD induction in the two different branches and summarizing box and whisker plots (right) of changes in eEPSC of conditioned PF (blue, n = 8) and unconditioned PF (purple, n = 8). PF-PC LTD occurred only in the conditioned PF (% of baseline: conditioned PF = 67.16 ± 3.51% vs. unconditioned PF = 110.10 ± 5.05%, Mann-whitney test). (D) Plots showing frequency – current (F/I) curve pre and post induction of LTD (black open: pre-induction; blue closed: post-induction; n = 8, p = 0.0006, Two-way RM ANOVA). Insets show representative traces of depolarization-induced AP train. Scale: 200 ms (horizontal) and 20 mV (vertical). (E) Bar graphs showing the changes in PF-evoked spike count between conditioned PF and unconditioned PF (grey upper: pre-induction at conditioned PF; blue: post-induction at conditioned PF; grey lower: pre-induction at unconditioned PF; purple: post-induction at unconditioned PF). There was significant changes in PF-evoked spike count when conditioned PF was stimulated (spike count: pre-induction = 15.38 ± 1.34; post-induction = 7.13 ± 0.64, n = 8, p = 0.008) while spike count was not changed when unconditioned PF was stimulated (spike count: pre-induction = 18.13 ± 3.00; post-induction = 15 ± 1.43, n = 8, p = 0.13). Insets show representative traces of PF-evoked spikes, elicited by stimulating 20 times of PF with 20 Hz. Scale: 250 ms (horizontal) and 20 mV (vertical). (F) Box and whisker plots showing the PF-evoked spike count from conditioned PF (blue) and unconditioned PF (black). Changes in PF-evoked spike output was prominent at the conditioned PF compared to unconditioned PF (Δspike count in conditioned PF = -52.28 ± 4.35% vs. unconditioned PF = -11.71 ± 5.97, p = 0.0006, Mann-whitney test).

For statistics, Mann-whitney test was used for C (right) and F and Wilcoxon test was used for comparison of paired data set in E. Two-way RM ANOVA was used for D and post hoc Tukey's test was used for different time group comparison. Error bar indicates SEM. n.s. denotes 'not significant', **p < 0.01, ***p < 0.001. * in panel D indicated statistical difference between each time point and significances was tested by post-*hoc* tukey test of Two-way RM ANOVA.

4.4 Sufficient changes in spiking output requires both of plasticity, synaptic and intrinsic plasticity .

Would the spiking output of PCs reflect either PF-PC LTD or LTD-IE? To clarify this, I pharmacologically inhibited PF-PC LTD without excitability changes by applying the first small-molecule inhibitor (FSC231, 50 μM) which prevents internalization of α-amino-3-hydroxy-5-methyl-4-isoxazolepropionic acid (AMPA) receptors (Ho et al., 2009; Schonewille et al., 2011; Thorsen et al., 2010). As a control, DMSO was applied to recording chamber, instead of FSC231. The FSC231 effectively inhibited PF-PC LTD compared to the data shown in fig 14B (PF-tetanus ISI_0) and DMSO control (fig. 17A; % of baseline: DMSO = 63.33 ± 3.33%, n = 5; FSC231 = 93.60 ± 4.61%, n = 5, p = 0.0014, One-way ANOVA post-hoc tuckey test, comparing to data of ISI_0). In contrary to effect on the synaptic plasticity, FSC231 did not affect to the LTD-IE [fig. 17B - D; (B) Firing frequency: DMSO: $F(5, 20) = 4.64$, $p = 0.0057$, Two-way RM ANOVA; FSC231 = $F(1, 4) = 8.88$, $p = 0.04$]. The PF-evoked spiking activity was found to be decreased in both DMSO-treated control and FSC231-treated slices after induction of PF-PC LTD (fig. 17E). However, the extent of changes in PF-evoked spike count was indeed more robust in the FSC231-treated group compared to DMSO-control (fig. 17F; Δspike count: DMSO = -65.15 ± 5.70%, FSC231 = -31.76 ± 11.85%, p = 0.039, t-test).

Next, I further tested if excitability changes *per se* would enable to be reflected in spiking output. To prove this, I used a transgenic mice model, the PC-specific stromal interaction molecule 1 knockout mice ($STIM1^{PKO}$), previously confirmed the impairment of intrinsic plasticity without deficit of synaptic plasticity (Ryu et al., 2017). Consistent with the previous study, the synaptic plasticity was comparable between genotypes, however, the $STIM1^{PKO}$ exhibited deficit of the LTD-IE compared to wildtype littermates ($STIM1^{WT}$) (fig. 18A – D; synaptic plasticity: $STIM1^{WT}$ n = 6, $STIM1^{PKO}$ n = 6, synaptic plasticity: p = 0.81, Mann-

whitney test; intrinsic plasticity: $STIM1^{WT}$: F (5, 25) = 78, $p < 0.001$; $STIM1^{PKO}$: F(1, 5) = 1.42, p = 0.29, Two-way RM ANOVA). Notably, the PF-spike output was significantly decreased in $STIM1^{WT}$ compared to $STIM1^{PKO}$, however, % of changes in the spike count was found to be obvious in $STIM1^{WT}$, as the results from inhibition of PICK1 (fig. 18E and F; Δspike count: $STIM1^{WT}$ = -64.17 ± 6.48, n = 6; $STIM1^{KO}$ = -26.17 ± 4.18, n = 6, p = 0.004, Mann-whitney test). Altogether, the activity-dependent modulation of neuronal output requires synergistic coordination of synaptic input and neuronal excitability change.

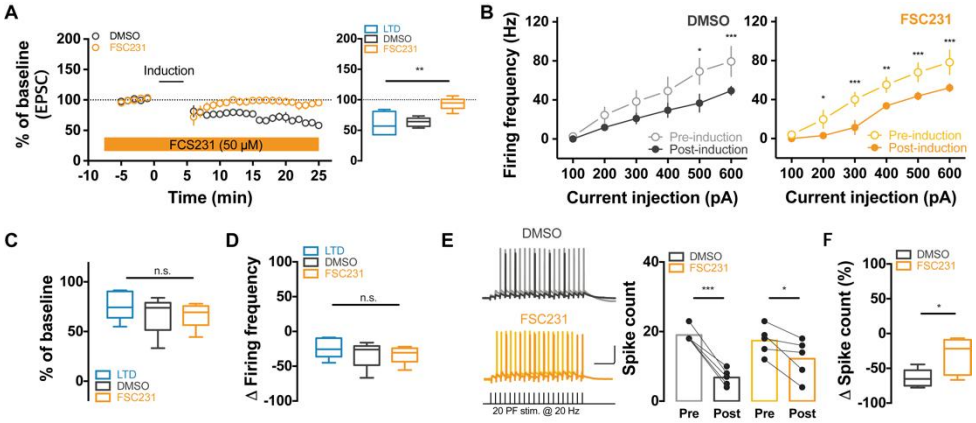

Figure 17. Activity-dependent modulation of PC spike output required synergies between synaptic and intrinsic plasticity: effect of synaptic plasticity on the spiking output. (A) Plots (left) showing the normalized eEPSC before and after LTD induction in a presence of PICK1 inhibitor, FSC231 (50 μM, orange, n = 5) and DMSO control (1:1000, black, n = 5) and summarizing box and whisker plots (right) of changes in eEPSC. Compared to ISI_{120}, FSC231 prevented induction of PF-LTD (% of baseline: DMSO control = 63.33 ± 3.33%, p = 0.86; FSC231 = 93.60 ± 4.61%, p = 0.001, One-way ANOVA post-*hoc* tukey test compared to ISI_{120}). (B) Plots showing frequency – current (F/I) curve of DMSO control and FSC231-treated group corresponding to time after induction (grey open: DMSO pre-induction; black closed: DMSO post-induction, n =5, F(5, 20) = 4.64, p = 0.006; orange open: FSC231 pre-induction; orange: FSC231 post-inuction, n = 5, F(1, 4) = 8.88, p = 0.04, Two-way RM ANOVA). LTD-IE was exhibited in both DMSO- and FSC231-treated groups. Insets show representative traces of depolarization-induced AP train. Scale: 200 ms (horizontal) and 20 mV (vertical). (C – D) Box and whisker plots showing the changes in excitability after LTD induction throughout the groups including ISI_{120} (blue), DMSO- (black) and FSC231-treated groups (orange). There were no significant differences of excitability change between groups [(C): F(2, 12) = 0.61, p = 0.56; (D): F(2, 12) = 0.61, p = 0.56, One-way ANOVA]. (E) Bar graphs showing the changes in PF-evoked spike count between before and after induction in a presence of FSC231 (light orange: pre-induction; orange: post-induction) and DMSO (grey: pre-induction; black: post-induction). The PF-evoked spike count before and after LTD induction was significantly reduced in both groups (spike count: DMSO pre-induction = 19.00 ± 1.00; post-induction = 6.80 ± 1.07, n = 5, p = 0.0006, FSC231 pre-induction = 17.4 ± 1.86; post-induction = 12.2 ± 2.538, n = 5, p = 0.039, paired t-test). Insets show representative traces of PF-evoked spikes, elicited by stimulating 20 times of PF with 20 Hz. Scale: 250 ms (horizontal) and 20 mV (vertical). (F) Box and whisker plots showing the PF-evoked spike count from DMSO (black) and FSC231-treated group (orange). The PF-evoked spike count shored less decrease in the FSC231 treated group compared to DMSO control (Δspike count: DMSO = -65.15 ± 5.70% vs. FSC231 = -31.76 ± 11.85%, p = 0.04, t-test).

For statistics, One-way ANOVA test was used for A, C and D and post-hoc tukey test was used for different individual group comparison. And Two-way RM ANOVA was used for B and post hoc Tukey's test was used for different time group comparison and paired t-test was used for E and t-test was used for F. Error bar indicates SEM. n.s. denotes 'not significant'; *P < 0.05, **p < 0.01, ***p < 0.001. * in panel A indicated statistical difference between subgroups and significances was tested by post-*hoc* tukey test of Owo-way RM ANOVA. * in panel B indicated statistical difference between each time point and significances was tested by post-*hoc* tukey test of Two-way RM ANOVA and

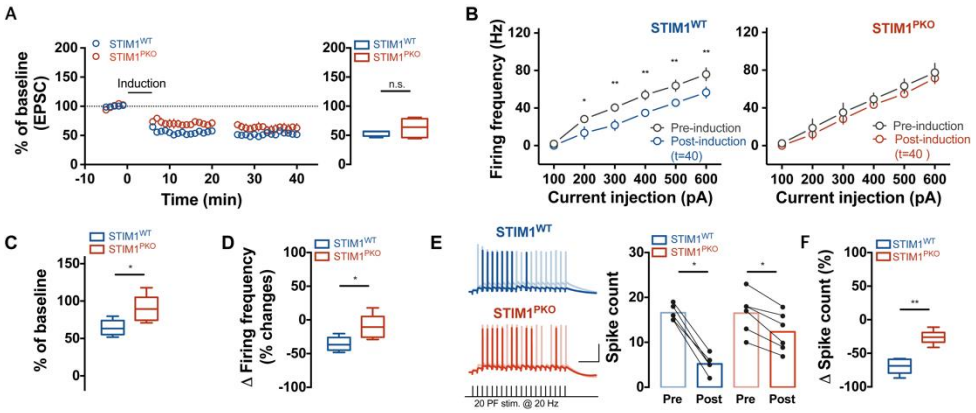

Figure 18. Activity-dependent modulation of PC spike output required synergies between synaptic and intrinsic plasticity: effect of intrinsic plasticity on the spiking output. (A) Plots (left) showing the normalized eEPSC before and after LTD induction from STIM1^{WT} (blue, n = 6) and STIM1^{PKO} (red, n = 6) and summarizing box and whisker plots (right) of changes in eEPSC. The changes in eEPSC was comparable between genotypes (% of baseline: STIM1^{WT} = 56.71 ± 3.68% vs. STIM1^{PKO} = 62.92 ± 6.47%, p = 0.82, Mann-whitney test). (B) Plots showing frequency – current (F/I) curve of STIM1^{WT} (left) and STIM1^{PKO} (right) corresponding to time after induction. LTD-IE was impaired in STIM1^{PKO} while LTD-IE was intact in wildtype littermates [STIM1^{WT} : black = pre-induction; blue = post-induction, n = 6, F (5, 25) = 78, p < 0.001; STIM1^{PKO}: black = pre-induction; red = post-induction, n = 6, F(1, 5) = 1.42, p = 0.29, Two-way RM ANOVA]. Insets show representative traces of depolarization-induced AP train. Scale: 200 ms (horizontal) and 20 mV (vertical). (C – D) Box and whisker plots showing the changes in excitability after LTD induction throughout the groups between genotypes. There were significant differences of excitability change between genotypes [(C): p = 0.03; (D): p = 0.03]. (E) Bar graphs showing the changes in PF-evoked spike count between before and after induction from STIM1^{WT} (light blue: pre-induction; blue: post-induction) and STIM1^{PKO} (light red: pre-induction; red: post-induction). The PF-evoked spike count before and after LTD induction was significantly reduced in both groups (spike count: STIM1^{WT} pre-induction = 17.00 ± 0.77; post-induction = 6.25 ± 1.13, n = 6, p = 0.03, STIM1^{PKO} pre-induction = 16.5 ± 1.84; post-induction = 12.33 ± 1.76, n = 6, p = 0.03, Wilcoxon test). Insets show representative traces of PF-evoked spikes, elicited by stimulating 20 times of PF with 20 Hz. Scale: 250 ms (horizontal) and 20 mV (vertical). (F) Box and whisker plots showing the PF-evoked spike count from STIM1^{WT} (blue) and STIM1^{PKO} (red). The PF-evoked spike count shored less decrease in the STIM1^{PKO} compared to STIM1^{WT} (Δspike count: STIM1^{WT} = -64.17 ± 6.477% vs. STIM1^{PKO} = -26.17 ± 4.18%, p = 0.004, Mann-whitney test).

For statistics, Mann-whitney test was used for A, C, D and F and Wilcoxon test was used for paired data set of E. And Two-way RM ANOVA was used for B and post hoc Tukey's test was used for different time group comparison. Error bar indicates SEM. n.s. denotes 'not significant'; *P < 0.05, **p < 0.01, ***p < 0.001. * in panel B indicated statistical difference between each time point and significances was tested by post-*hoc* tukey test of Two-way RM ANOVA.

4.5 Supralinearity of spiking output coordination after induction of PC plasticity

The significant changes in spike output after the synaptic plasticity was shown when the intrinsic plasticity was accompanied in the conditioned dendritic branch-specific manner. Thus, the relationship of synaptic plasticity or intrinsic plasticity with the spiking output would not be assumed to be correlated. However, the whole data of changes in synaptic weight or intrinsic excitability was found to be correlated with postsynaptic spike output (fig. 19A and B; spike output – synaptic plasticity: $R^2 = 0.47$, $p < 0.0001$, $n = 65$; spike output – intrinsic plasticity: $R^2 = 0.18$, $p = 0.001$, $n = 59$). These data might result from the bias because the whole data set includes various outcomes corresponding to the experimental condition. Activity-dependent alteration of synaptic weight, excitability and PF-evoke spike count were indeed divergent depending on the experimental condition such as pharmacology or induction protocol I used (fig. 20A – C). Based on the experimental group, the whole data set was categorized by following four groups: 1) PF-$LTD_{ISI=0}$, LY367385 and KN62-treated group showed changes in neither synaptic weight nor excitability (group-A), 2) FSC231-treated, unconditioned PF and $STIM1^{PKO}$ groups showed either changes in synaptic weight (Group-B) or 3) intrinsic excitability (Group-C) and 4) PF-$LTD_{ISI=120}$, DMSO, conditioned PF and $STIM1^{WT}$ group displayed cooccurrence of both plasticity (group-D). Interestingly, the changes in spike output were distinct between groups and there was no correlative relationship between spike output and changes in neuronal activity (fig. 19D and E). Rather, the spiking output of the cerebellar PCs after LTD induction was shown to be supralinear manner. Notably, the cumulative fraction revealed that modulation of spike output was robustly classified and moreover, the synaptic plasticity sufficiently was reflected by postsynaptic spiking output when the intrinsic plasticity is accompanied (fig. 19F and G).

Furthermore, to avoid the bias of classification, I re-categorized the whole data

set with unsupervised way based on the data. Criteria for classification was 20 % of changes compared to their baseline. In parallel with supervised categorization, spike output was also modulated by a supralinear manner (fig. 19H and I). Although the changes in spiking output in the Group-C and Group-D groups were comparable, the impact of the synaptic plasticity on the PC output signals was more prominent in the Group-D group (fig. 19J and K). In conclusion, the synergies between synaptic and intrinsic plasticity of the cerebellar PCs may control the PC output in order to sufficiently convey an information to cerebellar-targeted neurons. Moreover, the input-output signal coordination is modulated in a supralinear fashion.

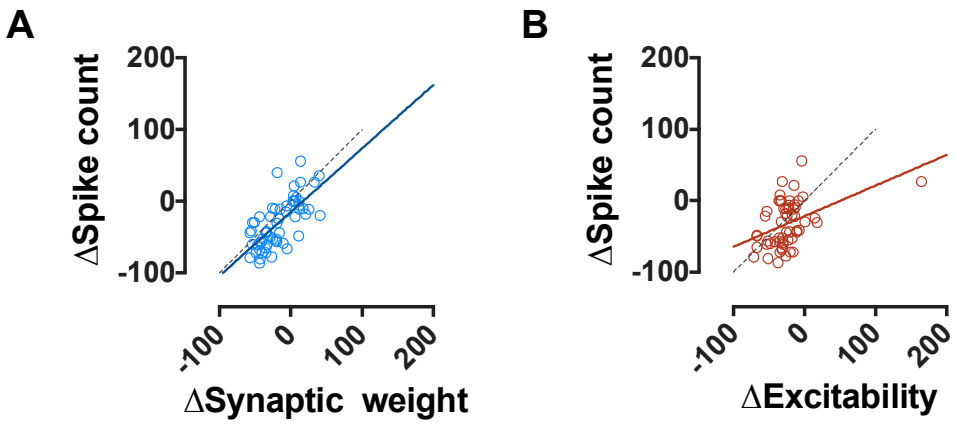

Figure 19. Linearity of spiking output between changes in synaptic weight and excitability. Extent of alteration of synaptic weight and excitability were found to be correlated with spike output of the PCs when whether neuronal activity changed was not regarded.

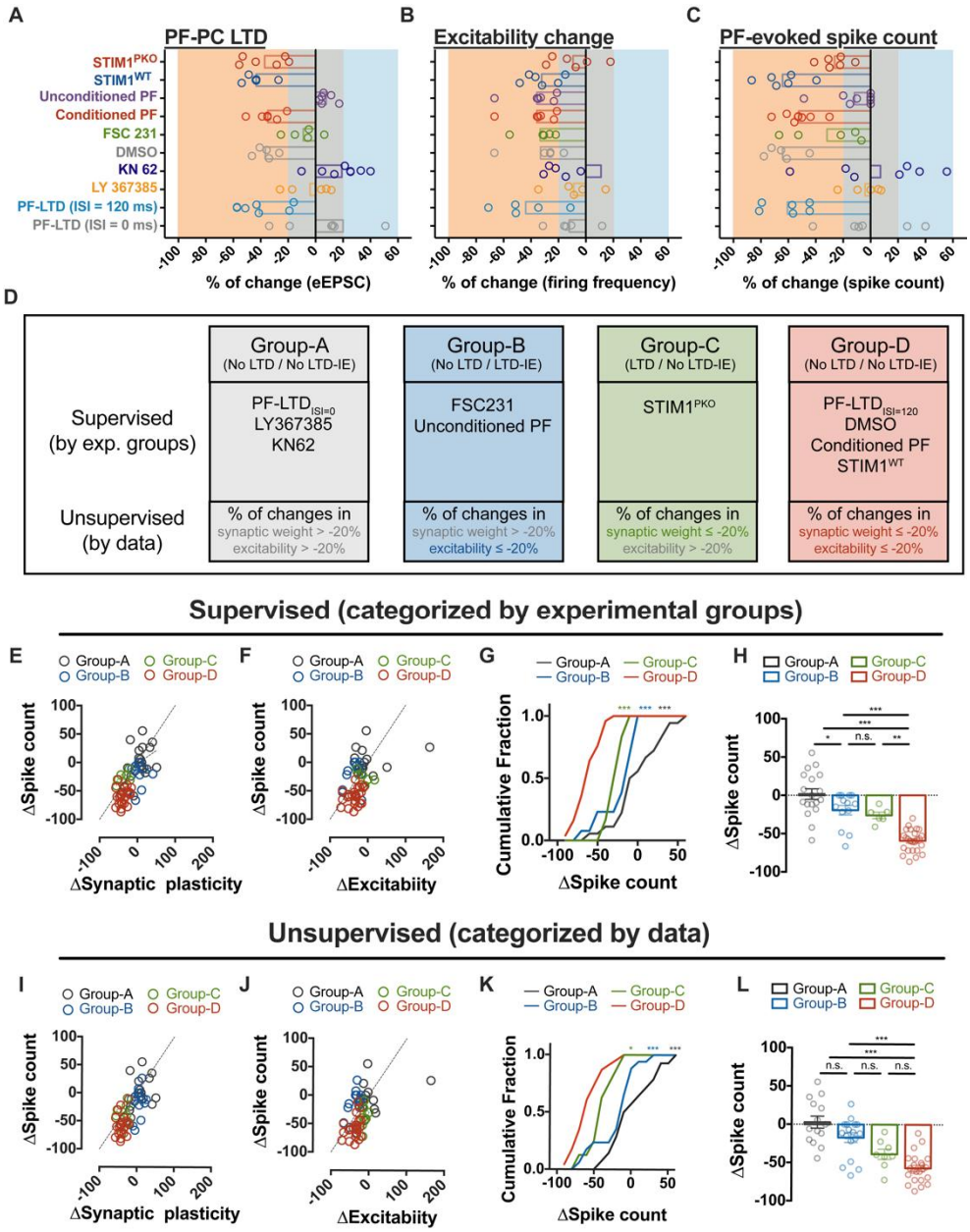

Figure 20. Supralinearity of spiking output coordination after induction of PC plasticity. (A – C) Bar graph and scatter plots showing changes in synaptic weight (A), excitability (B) and PF-evoked spike output (C). Changes in neuronal activity over -20 % was criterion for depression which colored in orange; Changes in neuronal activity exceeding 20% was criterion potentiation which colored in blue; Otherwise was 'not changed' which colored in grey. (D) Categorization standard following four sub-groups based on experimental condition (Supervised) or data (Unsupervised): 1) without changes in synaptic weight and intrinsic excitability (No LTD / No LTD-IE; Group-A, black), 2) occurrence of LTD-IE without changes in synaptic weight (No LTD / LTD-IE; Group B, blue), 3) Occurrence of PF-PC LTD without LTD-IE (LTD / No LTD-IE; Group-C, green), 4) cooccurrence of PF-PC LTD

and LTD-IE; LTD / LTD-IE, red). (E – F) Scatter plots showing relationship between spike output and synaptic plasticity (E), spike output and intrinsic plasticity (F). Each sub-groups were categorized by experimental condition (supervised). Distribution of data was distinguishable between subgroups. (G) Cumulative fractions showing distribution of spike output corresponding sub-groups. Group-D was shown to be distinctive outcomes of plasticity induction from other sub-groups (Each colors of asterisks indicated statistical differences compared to Group-D with other subgroups: green = difference between Group-C ($p = 0.0001$) and D; blue = between Group-B and D ($p = 0.0001$); black = between Group-A and D ($p = 0.0003$, Kolmogorov-Smirnov test). (H) Summarizing bar graphs showing differences of spike output between sub-groups. Compared to Group-A (Δspike output = 1.57 ± 6.88%, n = 18), Group-D showed prominent reduction of spike output (Δspike output = -59.48 ± 2.88%, n = 25, $p < 0.0001$, One-way ANOVA post-*hoc* tukey test). Spike output was Sub-groups showing changes in either synaptic weight or excitability were relatively less than the data shown in Group-D (Δspike output: Group-B = -19.42 ±6.22%, n = 13; Group-C = -26.17 ± 4.18%, n = 6, between Group-B and D: $p < 0.0001$; between Group-C and D: $p = 0.021$, One-way ANOVA post-*hoc* tukey test). (I – J) Scatter plots showing relationship between spike output and synaptic plasticity (I), spike output and intrinsic plasticity (J). Each sub-groups were categorized by data (unsupervised). Depression of synaptic weight or excitability was determined by changed value below -20% compared to baseline of each data. Similar to scatter plots shown in panel E and F, distribution of data was also distinguishable between subgroups. (K) Cumulative fractions showing distribution of spike output corresponding sub-groups. Group-D was shown to be distinctive outcomes of plasticity induction from other sub-groups (Each colors of asterisks indicated statistical differences compared to Group-D with other subgroups: blue = difference between Group-B and D ($p < 0.0003$); black = between Group-A and D ($p < 0.0001$, Kolmogorov-Smirnov test). There was also significant difference between Group-C and D ($p = 0.02$). (L) Summarizing bar graphs showing differences of spike output between sub-groups. Compared to Group-A (Δspike output = 3.67 ± 8.41%, n = 14), Group-D also showed prominent reduction of spike output (Δspike output = -56.82 ± 3.92%, n = 23, $p < 0.0001$, One-way ANOVA post-*hoc* tukey test). Spike output was Sub-groups showing changes in either synaptic weight or excitability were relatively less than the data shown in Group-D (Δspike output: Group-B = -17.10 ± 6.27%, n = 17; Group-C = -38.71 ± 6.74, n = 8, between Group-B and D: $p < 0.0001$; between Group-C and D: $p = 0.25$; between group-B and C: $p = 0.15$, One-way ANOVA post-*hoc* tukey test). The aspects of spike output changes after LTD induction of the Supervised categorization were similar to the Unsupervised categorization of sub-groups of whole data. Altogether, the activity-dependent modulation of spike output may require the synergies between synaptic and intrinsic plasticity, implying supralinearity of input-output coordination.

Discussion

Modern theories of neuroscience have assumed that synaptic plasticity may control neuronal output in an activity-dependent manner. Colleagues and I previously suggested that the intrinsic plasticity of the cerebellar PCs accompanying the synaptic plasticity may play a role in shaping the neuronal net output during learning (Shim et al., 2017; 2018). This work broadens the previous understanding of the role of intrinsic plasticity in the information processing. Dendritic branch-specific formation of LTD-IE as well as PF-PC LTD may control the neuronal net output in an activity-dependent manner.

In the present study, elucidate several features of intrinsic plasticity of the cerebellar PCs in the flocculus. First of all, formation of LTD-IE in PCs is dependent on the precise timing rules and intracellular signaling cascade for governing the PF-PC LTD. In addition, the intrinsic plasticity may be formed at the conditioned dendritic branches where the synaptic plasticity is induced. This branch-specificity of synaptic and intrinsic plasticity in PCs enables the synaptic inputs to robustly affect to neuronal net output. Notably, the synaptic input-driven spiking activity of PCs is shown to be significantly decreased when the conditioned dendritic branch is stimulated whereas the synaptic inputs from the unconditioned branches may be neglected. Altogether, the neuronal output is determined by synergistic coordination of input-output signals in the dendrosomatic axis.

Synaptic plasticity is thought to be formed at the specific synaptic area. On the other hand, intrinsic plasticity may seem to be a global change of the neurons, hence the intrinsic plasticity would distort the synapse-specificity of the synaptic plasticity. If the intrinsic plasticity controls the neuronal output signals *per se*, the neurons unable to distinguish the spatiotemporal patterns of synaptic inputs from insignificant inputs. Given the morphological features of the cerebellar PC dendrite, this scenario would not be efficient to process the sensory information. There is

accumulating evidence showing that information processing in the dendrites is compartmentalized (Fu et al., 2012; Legenstein and Maass, 2011; Ohtsuki et al., 2012; Zang et al., 2018). Interestingly, the membrane potential and responsiveness to synaptic inputs are found to be heterogeneity in individual dendritic branches of the cerebellar PCs, implicating that the not only the synaptic plasticity but also the intrinsic plasticity in PCs could be formed in a spatially restricted area of the dendritic branches. In fact, the branch specificity has been also implicated in clustered plasticity model, describing that the neighboring synaptic sites form functional clustering along dendritic branches in that the similar information is preferentially processed in the clustered synapses (Fu et al., 2012; Govindarajan et al., 2011). Notably, the clustered dendritic activation has been found to process the spatiotemporal patterns of synaptic inputs encoding a similar sensory information (Wilms and Häusser, 2015), suggesting that the computational units for information processing may be individual dendritic branches. In this scenario, the learned pattern of the PC output in response to the familiar sensory stimuli would be elicited by functional clusters of dendrosomatic occurrence of synaptic and intrinsic plasticity of PCs. Consequently, the branch-specificity of the synaptic and intrinsic plasticity may enable the PCs to separate the learned pattern from novel information. Taken together, the way to process the information in the cerebellar cortex is highly structured and clustered, therefore, localized induction of synaptic and intrinsic plasticity may play a significant role in information storage and furthermore modifying the behavioral outcomes. Furthermore, the branch-specific formation of synaptic and intrinsic plasticity may not only contribute to synergistic modulation of spike output in an activity-dependent manner but also expand the dendritic capacity for effective information processing in the cerebellar PCs.

Linking synaptic plasticity and spike output, several observations have revealed that synaptic plasticity alters spike pause duration, delay to fire the AP spike after PF or CF activation (Grassi and Pettorossi, 2001; Steuber et al., 2007). The altered duration of spike pause of PCs is assumed to relieve tonic inhibition onto their

relay neurons, such as DCN thereby depression of the PC-DCN synaptic strength. Consequently, the altered responsiveness against the synaptic gain would affect to postsynaptic spiking activity. Given that the pattern of the spiking activity in the cerebellar PCs indeed plays a pivotal role in information storage of the cerebellar learning (De Zeeuw et al., 2011; Wulff et al., 2009), the functional role of the spike pause might contribute to information processing in the cerebellum. Alternatively, I demonstrated the unrevealed feature of the intrinsic plasticity contributing to the integration of synaptic inputs thereby prominent depression of the PC output. Taken together, synaptic plasticity at the PF-PC synapses may modify the way to process the information quantitatively (the PF-evoked spike generation) as well as qualitatively (duration of spike pause).

What would be consequences of supralinearity of the PC output modulation? Given the anatomical feature of the cerebellar PCs, understanding of how the PC output is coordinated in an activity-dependent manner is essential. In the cerebellar motor learning circuits, several implications have assumed that the memory should be transferred from the cerebellar cortex to sub-cortical area such as VN (Anzai et al., 2010; Boyden et al., 2004; 2006; Johansson et al., 2014; Nagao et al., 2013; Okamoto et al., 2011a; Shutoh et al., 2006). Inactivation of the cerebellar cortex within a few hours after motor learning causes the impairment of memory storage whereas blockade of cerebellar activity over a day after learning exhibits no significant effects on the memory formation. Those results suggests that the plasticity in the cerebellar cortex may contribute to the memory acquisition and the plasticity in the VN may be involved in the long-term memory storage. Given the note that the plasticity in the VN neurons is dependent on the PC activity, the activity-dependent changes in the cerebellar output would provide the instructive signals for plasticity induction in the VN. Interestingly, (Ryu et al., 2017) have recently demonstrated that the memory consolidation deficit mice model ($STIM1^{PKO}$) shows impairment of intrinsic plasticity while synaptic plasticity is intact. The authors suggest that the improper modulation of cerebellar output might

underlie the memory consolidation deficit. Notably, I found that the PC spike output after LTD induction in the mice line ($STIM1^{PKO}$) showed no prominent changes in the PF-evoked spike count compared to wildtype littermate (fig. 18). Therefore, the appropriate input-output coordination requires synergies between PF-PC synaptic plasticity and intrinsic plasticity. In conclusion, supralinearity of the input-output coordination after induction of PC plasticity may contribute to memory transfer to the sub-cortical area through tuning the cerebellar output signals.

Bibliography

Afshari, F.S., Ptak, K., Khaliq, Z.M., Grieco, T.M., Slater, N.T., McCrimmon, D.R., and Raman, I.M. (2004). Resurgent Na currents in four classes of neurons of the cerebellum. J. Neurophysiol. *92*, 2831–2843.

Ango, F., Prézeau, L., Muller, T., Tu, J.C., Xiao, B., Worley, P.F., Pin, J.P., Bockaert, J., and Fagni, L. (2001). Agonist-independent activation of metabotropic glutamate receptors by the intracellular protein Homer. Nature *411*, 962–965.

Anzai, M., Kitazawa, H., and Nagao, S. (2010). Effects of reversible pharmacological shutdown of cerebellar flocculus on the memory of long-term horizontal vestibulo-ocular reflex adaptation in monkeys. Neurosci. Res. *68*, 191–198.

Aramori, I., and Nakanishi, S. (1992). Signal transduction and pharmacological characteristics of a metabotropic glutamate receptor, mGluR1, in transfected CHO cells. Neuron *8*, 757–765.

Atluri, P.P., and Regehr, W.G. (1996). Determinants of the Time Course of Facilitation at the Granule Cell to Purkinje Cell Synapse. J. Neurosci. *16*, 5661–5671.

Belmeguenai, A., Hosy, E., Bengtsson, F., Pedroarena, C.M., Piochon, C., Teuling, E., He, Q., Ohtsuki, G., De Jeu, M.T.G., Elgersma, Y., et al. (2010). Intrinsic plasticity complements long-term potentiation in parallel fiber input gain control in cerebellar Purkinje cells. J. Neurosci. *30*, 13630–13643.

Benda, J., and Herz, A.V.M. (2003). A universal model for spike-frequency adaptation. Neural Comput *15*, 2523–2564.

Beraneck, M., and Idoux, E. (2012). Reconsidering the role of neuronal intrinsic properties and neuromodulation in vestibular homeostasis. Front Neurol *3*, 25.

Bliss, T.V., and Lomo, T. (1973). Long-lasting potentiation of synaptic transmission in the dentate area of the anaesthetized rabbit following stimulation of the perforant path. J Physiol *232*, 331–356.

Bloedel, J.R., and Bracha, V. (1995). On the cerebellum, cutaneomuscular reflexes, movement control and the elusive engrams of memory. Behav Brain Res *68*, 1–44.

Bosch, M.K., Carrasquillo, Y., Ransdell, J.L., Kanakamedala, A., Ornitz, D.M., and Nerbonne, J.M. (2015). Intracellular FGF14 (iFGF14) Is Required for Spontaneous and Evoked Firing in Cerebellar Purkinje Neurons and for Motor Coordination and Balance. J. Neurosci. *35*, 6752–6769.

Boyden, E.S., and Raymond, J.L. (2003). Active reversal of motor memories reveals rules governing memory encoding. Neuron *39*, 1031–1042.

Boyden, E.S., Katoh, A., and Raymond, J.L. (2004). Cerebellum-dependent learning: the role of multiple plasticity mechanisms. Annu. Rev. Neurosci. *27*, 581–609.

Boyden, E.S., Katoh, A., Pyle, J.L., Chatila, T.A., Tsien, R.W., and Raymond, J.L. (2006). Selective engagement of plasticity mechanisms for motor memory storage. Neuron *51*, 823–834.

Brager, D.H., and Johnston, D. (2007). Plasticity of intrinsic excitability during long-term depression is mediated through mGluR-dependent changes in I(h) in hippocampal CA1 pyramidal neurons. J. Neurosci. *27*, 13926–13937.

Brakeman, P.R., Lanahan, A.A., O'Brien, R., Roche, K., Barnes, C.A., Huganir, R.L., and Worley, P.F. (1997). Homer: a protein that selectively binds metabotropic glutamate receptors. Nature *386*, 284–288.

Brysch, W., Creutzfeldt, O.D., Lüno, K., Schlingensiepen, R., and Schlingensiepen, K.H. (1991). Regional and temporal expression of sodium channel messenger RNAs in the rat brain during development. Exp Brain Res *86*, 562–567.

BuzsÁk, G. (1998). Memory consolidation during sleep: a neurophysiological

perspective. Journal of Sleep Research *7*, 17–23.

Caldwell, J.H., Schaller, K.L., Lasher, R.S., Peles, E., and Levinson, S.R. (2000). Sodium channel Na(v)1.6 is localized at nodes of ranvier, dendrites, and synapses. Proc. Natl. Acad. Sci. U.S.a. *97*, 5616–5620.

Callaway, J.C., and Ross, W.N. (1997). Spatial distribution of synaptically activated sodium concentration changes in cerebellar Purkinje neurons. J. Neurophysiol. *77*, 145–152.

Carr, M.F., Jadhav, S.P., and Frank, L.M. (2011). Hippocampal replay in the awake state: a potential substrate for memory consolidation and retrieval. Nat. Neurosci. *14*, 147–153.

Chang, M.C., Park, J.M., Pelkey, K.A., Grabenstatter, H.L., Xu, D., Linden, D.J., Sutula, T.P., McBain, C.J., and Worley, P.F. (2010). Narp regulates homeostatic scaling of excitatory synapses on parvalbumin-expressing interneurons. Nat. Neurosci. *13*, 1090–1097.

Chang, W., Park, J.M., Kim, J., and Kim, S.J. (2012). TRPC-Mediated Current Is Not Involved in Endocannabinoid-Induced Short-Term Depression in Cerebellum. Korean J. Physiol. Pharmacol. *16*, 139–144.

Chidiac, P., Hebert, T.E., Valiquette, M., Dennis, M., and Bouvier, M. (1994). Inverse agonist activity of beta-adrenergic antagonists. Mol. Pharmacol. *45*, 490–499.

Clark, B.A., Monsivais, P., Branco, T., London, M., and Häusser, M. (2005). The site of action potential initiation in cerebellar Purkinje neurons. Nat. Neurosci. *8*, 137–139.

Clopath, C., Badura, A., De Zeeuw, C.I., and Brunel, N. (2014). A cerebellar learning model of vestibulo-ocular reflex adaptation in wild-type and mutant mice. J. Neurosci. *34*, 7203–7215.

Coesmans, M., Smitt, P.A.S., Linden, D.J., Shigemoto, R., Hirano, T., Yamakawa,

Y., van Alphen, A.M., Luo, C., van der Geest, J.N., Kros, J.M., et al. (2003). Mechanisms underlying cerebellar motor deficits due to mGluR1-autoantibodies. Ann. Neurol. *53*, 325–336.

Coetzee, W.A., Amarillo, Y., Chiu, J., Chow, A., Lau, D., McCormack, T., Moreno, H., Nadal, M.S., Ozaita, A., Pountney, D., et al. (1999). Molecular diversity of K+ channels. Ann. N. Y. Acad. Sci. *868*, 233–285.

Crestani, A.P., Krueger, J.N., Barragan, E.V., Nakazawa, Y., Nemes, S.E., Quillfeldt, J.A., Gray, J.A., and Wiltgen, B.J. (2018). Metaplasticity contributes to memory formation in the hippocampus. Neuropsychopharmacol *114*, 1–7.

Cudmore, R.H., and Turrigiano, G.G. (2004). Long-Term Potentiation of Intrinsic Excitability in LV Visual Cortical Neurons. J. Neurophysiol. *92*, 341–348.

Cudmore, R.H., Fronzaroli-Molinieres, L., Giraud, P., and Debanne, D. (2010). Spike-Time Precision and Network Synchrony Are Controlled by the Homeostatic Regulation of the D-Type Potassium Current. J. Neurosci. *30*, 12885–12895.

Daoudal, G., and Debanne, D. (2003). Long-term plasticity of intrinsic excitability: learning rules and mechanisms. Learn. Mem. *10*, 456–465.

de Ruiter, M.M., De Zeeuw, C.I., and Hansel, C. (2006). Voltage-gated sodium channels in cerebellar Purkinje cells of mormyrid fish. J. Neurophysiol. *96*, 378–390.

De Zeeuw, C.I., Hoebeek, F.E., Bosman, L.W.J., Schonewille, M., Witter, L., and Koekkoek, S.K. (2011). Spatiotemporal firing patterns in the cerebellum. Nat. Rev. Neurosci. *12*, 327–344.

Debanne, D., Inglebert, Y., and Russier, M. (2018). Plasticity of intrinsic neuronal excitability. Curr. Opin. Neurobiol. *54*, 73–82.

Dell'Orco, J.M., Wasserman, A.H., Chopra, R., Ingram, M.A.C., Hu, Y.-S., Singh, V., Wulff, H., Opal, P., Orr, H.T., and Shakkottai, V.G. (2015). Neuronal Atrophy Early in Degenerative Ataxia Is a Compensatory Mechanism to Regulate

Membrane Excitability. J. Neurosci. *35*, 11292–11307.

Desai, N.S., Rutherford, L.C., and Turrigiano, G.G. (1999). Plasticity in the intrinsic excitability of cortical pyramidal neurons. Nat. Neurosci. *2*, 515–520.

Dodson, P.D., and Forsythe, I.D. (2004). Presynaptic K+ channels: electrifying regulators of synaptic terminal excitability. Trends Neurosci. *27*, 210–217.

Edgerton, J.R., and Reinhart, P.H. (2003). Distinct contributions of small and large conductance Ca2+-activated K+ channels to rat Purkinje neuron function. J Physiol *548*, 53–69.

Egorova, P.A., Zakharova, O.A., Vlasova, O.L., and Bezprozvanny, I.B. (2016). In vivo analysis of cerebellar Purkinje cell activity in SCA2 transgenic mouse model. J. Neurophysiol. *115*, 2840–2851.

Ehlers, M.D. (2003). Activity level controls postsynaptic composition and signaling via the ubiquitin-proteasome system. Nat. Neurosci. *6*, 231–242.

Etzion, Y., and Grossman, Y. (1998). Potassium currents modulation of calcium spike firing in dendrites of cerebellar Purkinje cells. Exp Brain Res *122*, 283–294.

Etzion, Y., and Grossman, Y. (2001). Highly 4-aminopyridine sensitive delayed rectifier current modulates the excitability of guinea pig cerebellar Purkinje cells. Exp Brain Res *139*, 419–425.

Fan, Y., Fricker, D., Brager, D.H., Chen, X., Lu, H.-C., Chitwood, R.A., and Johnston, D. (2005). Activity-dependent decrease of excitability in rat hippocampal neurons through increases in I(h). Nat. Neurosci. *8*, 1542–1551.

Fiala, J.C., Grossberg, S., and Bullock, D. (1996). Metabotropic glutamate receptor activation in cerebellar Purkinje cells as substrate for adaptive timing of the classically conditioned eye-blink response. J. Neurosci. *16*, 3760–3774.

Francesconi, A., and Duvoisin, R.M. (2000). Opposing effects of protein kinase C and protein kinase A on metabotropic glutamate receptor signaling: selective

desensitization of the inositol trisphosphate/Ca2+ pathway by phosphorylation of the receptor-G protein-coupling domain. Proc. Natl. Acad. Sci. U.S.a. *97*, 6185–6190.

Frankland, P.W., and Bontempi, B. (2005). The organization of recent and remote memories. Nat. Rev. Neurosci. *6*, 119–130.

Friedman, A.K., Walsh, J.J., Juarez, B., Ku, S.M., Chaudhury, D., Wang, J., Li, X., Dietz, D.M., Pan, N., Vialou, V.F., et al. (2014). Enhancing depression mechanisms in midbrain dopamine neurons achieves homeostatic resilience. Science *344*, 313–319.

Fu, M., Yu, X., Lu, J., and Zuo, Y. (2012). Repetitive motor learning induces coordinated formation of clustered dendritic spines in vivo. Nature *483*, 92–95.

Fukushima, K., Buharin, E.V., and Fukushima, J. (1993). Responses of floccular Purkinje cells to sinusoidal vertical rotation and effects of muscimol infusion into the flocculus in alert cats. Neurosci. Res. *17*, 297–305.

Fukushima, K., Chin, S., Fukushima, J., and Tanaka, M. (1996). Simple-spike activity of floccular Purkinje cells responding to sinusoidal vertical rotation and optokinetic stimuli in alert cats. Neurosci. Res. *24*, 275–289.

Galante, M., Nistri, A., and Ballerini, L. (2000). Opposite changes in synaptic activity of organotypic rat spinal cord cultures after chronic block of AMPA/kainate or glycine and GABAA receptors. J Physiol *523 Pt 3*, 639–651.

Galliano, E., Gao, Z., Schonewille, M., Todorov, B., Simons, E., Pop, A.S., D'Angelo, E., van den Maagdenberg, A.M.J.M., Hoebeek, F.E., and De Zeeuw, C.I. (2013). Silencing the Majority of Cerebellar Granule Cells Uncovers Their Essential Role in Motor Learning and Consolidation. Cell Rep *3*, 1239–1251.

Gao, Z., Proietti-Onori, M., Lin, Z., Brinke, Ten, M.M., Boele, H.-J., Potters, J.-W., Ruigrok, T.J.H., Hoebeek, F.E., and De Zeeuw, C.I. (2016). Excitatory Cerebellar Nucleocortical Circuit Provides Internal Amplification during Associative Conditioning. Neuron *89*, 645–657.

Gao, Z., van Beugen, B.J., and De Zeeuw, C.I. (2012). Distributed synergistic plasticity and cerebellar learning. Nat. Rev. Neurosci. *13*, 619–635.

Gähwiler, B.H., and Llano, I. (1989). Sodium and potassium conductances in somatic membranes of rat Purkinje cells from organotypic cerebellar cultures. J Physiol *417*, 105–122.

Giovannucci, A., Badura, A., Ben Deverett, Najafi, F., Pereira, T.D., Gao, Z., Ozden, I., Kloth, A.D., Pnevmatikakis, E., Paninski, L., et al. (2017). Cerebellar granule cells acquire a widespread predictive feedback signal during motor learning. Nat. Neurosci. *20*, 727–734.

Govindarajan, A., Israely, I., Huang, S.-Y., and Tonegawa, S. (2011). The dendritic branch is the preferred integrative unit for protein synthesis-dependent LTP. Neuron *69*, 132–146.

Govindarajan, A., Kelleher, R.J., and Tonegawa, S. (2006). A clustered plasticity model of long-term memory engrams. Nat. Rev. Neurosci. *7*, 575–583.

Grasselli, G., He, Q., Wan, V., Adelman, J.P., Ohtsuki, G., and Hansel, C. (2016). Activity-Dependent Plasticity of Spike Pauses in Cerebellar Purkinje Cells. Cell Rep *14*, 2546–2553.

Grassi, S., and Pettorossi, V.E. (2001). Synaptic plasticity in the medial vestibular nuclei: role of glutamate receptors and retrograde messengers in rat brainstem slices. Prog. Neurobiol. *64*, 527–553.

Gruol, D.L., Dionne, V.E., and Yool, A.J. (1989). Multiple voltage-sensitive K+ channels regulate dendritic excitability in cerebellar Purkinje neurons. Neurosci. Lett. *97*, 97–102.

Gruol, D.L., Jacquin, T., and Yool, A.J. (1991). Single-channel K+ currents recorded from the somatic and dendritic regions of cerebellar Purkinje neurons in culture. J. Neurosci. *11*, 1002–1015.

Guo, C.C., Ke, M.C., and Raymond, J.L. (2014). Cerebellar encoding of multiple

candidate error cues in the service of motor learning. J. Neurosci. *34*, 9880–9890.

Haghdoust, H., Janahmadi, M., and Behzadi, G. (2007). Physiological role of dendrotoxin-sensitive K+ channels in the rat cerebellar Purkinje neurons. Physiol Res *56*, 807–813.

Halverson, H.E., Khilkevich, A., and Mauk, M.D. (2015). Relating cerebellar purkinje cell activity to the timing and amplitude of conditioned eyelid responses. J. Neurosci. *35*, 7813–7832.

Harvey, A.L. (2001). Twenty years of dendrotoxins. Toxicon *39*, 15–26.

Hauge, S.A., Tracy, J.A., Baudry, M., and Thompson, R.F. (1998). Selective changes in AMPA receptors in rabbit cerebellum following classical conditioning of the eyelid-nictitating membrane response. Brain Res. *803*, 9–18.

Hebb, D.O. (1949). The organization of behavior : a neuropsychological theory (New York: Wiley).

Hengen, K.B., Lambo, M.E., Van Hooser, S.D., Katz, D.B., and Turrigiano, G.G. (2013). Firing rate homeostasis in visual cortex of freely behaving rodents. Neuron *80*, 335–342.

Ho, M.T., Ho, T.M., Pelkey, K.A., Pelletier, J.G., Huganir, R.L., Lacaille, J.-C., and McBain, C.J. (2009). Burst firing induces postsynaptic LTD at developing mossy fibre-CA3 pyramid synapses. J Physiol *587*, 4441–4454.

Hodgkin, A.L., and Huxley, A.F. (1945). Resting and action potentials in single nerve fibres. J Physiol *104*, 176–195.

Hodgkin, A.L., and Huxley, A.F. (1952a). A quantitative description of membrane current and its application to conduction and excitation in nerve. J Physiol *117*, 500–544.

Hodgkin, A.L., and Huxley, A.F. (1952b). Currents carried by sodium and potassium ions through the membrane of the giant axon of Loligo. J Physiol *116*,

449–472.

Hodgkin, A.L., Huxley, A.F., and Katz, B. (1952). Measurement of current-voltage relations in the membrane of the giant axon of Loligo. J Physiol *116*, 424–448.

Hoffman, D.A., Magee, J.C., Colbert, C.M., and Johnston, D. (1997). K+ channel regulation of signal propagation in dendrites of hippocampal pyramidal neurons. Nature *387*, 869–875.

Hounsgaard, J., and Midtgaard, J. (1988). Intrinsic determinants of firing pattern in Purkinje cells of the turtle cerebellum in vitro. J Physiol *402*, 731–749.

Hourez, R., Servais, L., Orduz, D., Gall, D., Millard, I., de Kerchove d'Exaerde, A., Cheron, G., Orr, H.T., Pandolfo, M., and Schiffmann, S.N. (2011). Aminopyridines correct early dysfunction and delay neurodegeneration in a mouse model of spinocerebellar ataxia type 1. J. Neurosci. *31*, 11795–11807.

Hu, J.-H., Park, J.M., Park, S., Xiao, B., Dehoff, M.H., Kim, S., Hayashi, T., Schwarz, M.K., Huganir, R.L., Seeburg, P.H., et al. (2010). Homeostatic Scaling Requires Group I mGluR Activation Mediated by Homer1a. Neuron *68*, 1128–1142.

Hyun, J.H., Eom, K., Lee, K.-H., Bae, J.Y., Bae, Y.C., Kim, M.-H., Kim, S., Ho, W.-K., and Lee, S.-H. (2015). Kv1.2 mediates heterosynaptic modulation of direct cortical synaptic inputs in CA3 pyramidal cells. J Physiol *593*, 3617–3643.

Hyun, J.H., Eom, K., Lee, K.-H., Ho, W.-K., and Lee, S.-H. (2013). Activity-dependent downregulation of D-type K+ channel subunit Kv1.2 in rat hippocampal CA3 pyramidal neurons. J Physiol *591*, 5525–5540.

Inoshita, T., and Hirano, T. (2018). Occurrence of long-term depression in the cerebellar flocculus during adaptation of optokinetic response. Elife *7*, 113.

Irie, T., and Trussell, L.O. (2017). Double-Nanodomain Coupling of Calcium Channels, Ryanodine Receptors, and BK Channels Controls the Generation of Burst Firing. Neuron *96*, 856–870.e4.

Ito, M. (1982). Cerebellar control of the vestibulo-ocular reflex--around the flocculus hypothesis. Annu. Rev. Neurosci. *5*, 275–296.

Ito, M. (2013). Error detection and representation in the olivo-cerebellar system. Front Neural Circuits *7*, 1.

Jahnsen, H., and Llinás, R. (1984). Electrophysiological properties of guinea-pig thalamic neurones: an in vitro study. J Physiol *349*, 205–226.

Jin, X.-H., Wang, H.-W., Zhang, X.-Y., Chu, C.-P., Jin, Y.-Z., Cui, S.-B., and Qiu, D.-L. (2017). Mechanisms of Spontaneous Climbing Fiber Discharge-Evoked Pauses and Output Modulation of Cerebellar Purkinje Cell in Mice. Front Cell Neurosci *11*, 247.

Jirenhed, D.-A., Rasmussen, A., Johansson, F., and Hesslow, G. (2017). Learned response sequences in cerebellar Purkinje cells. Proc. Natl. Acad. Sci. U.S.a. *114*, 6127–6132.

Johansson, F., Jirenhed, D.-A., Rasmussen, A., Zucca, R., and Hesslow, G. (2014). Memory trace and timing mechanism localized to cerebellar Purkinje cells. Proc. Natl. Acad. Sci. U.S.a. *111*, 14930–14934.

Johnston, D., Hoffman, D.A., and Poolos, N.P. (2000). Potassium Channels and Dendritic Function in Hippocampal Pyramidal Neurons. Epilepsia *41*, 1072–1073.

Jörntell, H., and Hansel, C. (2006). Synaptic Memories Upside Down: Bidirectional Plasticity at Cerebellar Parallel Fiber-Purkinje Cell Synapses. Neuron *52*, 227–238.

Kammermeier, P.J., Xiao, B., Tu, J.C., Worley, P.F., and Ikeda, S.R. (2000). Homer Proteins Regulate Coupling of Group I Metabotropic Glutamate Receptors to N-Type Calcium and M-Type Potassium Channels. J. Neurosci. *20*, 7238–7245.

Kandel, E.R., Dudai, Y., and Mayford, M.R. (2014). The molecular and systems biology of memory. Cell *157*, 163–186.

Kassardjian, C.D., Tan, Y.-F., Chung, J.-Y.J., Heskin, R., Peterson, M.J., and Broussard, D.M. (2005). The site of a motor memory shifts with consolidation. J. Neurosci. *25*, 7979–7985.

Kato, M., Tanaka, N., Usui, S., and Sakuma, Y. (2006). The SK channel blocker apamin inhibits slow afterhyperpolarization currents in rat gonadotropin-releasing hormone neurones. J Physiol *574*, 431–442.

Kawaguchi, S.-Y., and Hirano, T. (2013). Gating of long-term depression by Ca2+/calmodulin-dependent protein kinase II through enhanced cGMP signalling in cerebellar Purkinje cells. J Physiol *591*, 1707–1730.

Kay, A.R., Sugimori, M., and Llinás, R. (1998). Kinetic and stochastic properties of a persistent sodium current in mature guinea pig cerebellar Purkinje cells. J. Neurophysiol. *80*, 1167–1179.

Ke, M.C., Guo, C.C., and Raymond, J.L. (2009). Elimination of climbing fiber instructive signals during motor learning. Nat. Neurosci. *12*, 1171–1179.

Keck, T., Keller, G.B., Jacobsen, R.I., Eysel, U.T., Bonhoeffer, T., and Hübener, M. (2013). Synaptic scaling and homeostatic plasticity in the mouse visual cortex in vivo. Neuron *80*, 327–334.

Khaliq, Z.M., Gouwens, N.W., and Raman, I.M. (2003). The contribution of resurgent sodium current to high-frequency firing in Purkinje neurons: an experimental and modeling study. J. Neurosci. *23*, 4899–4912.

Khavandgar, S., Walter, J.T., Sageser, K., and Khodakhah, K. (2005). Kv1 channels selectively prevent dendritic hyperexcitability in rat Purkinje cells. J Physiol *569*, 545–557.

Kim, S.J., and Linden, D.J. (2007). Ubiquitous Plasticity and Memory Storage. Neuron *56*, 582–592.

Kimpo, R.R., Rinaldi, J.M., Kim, C.K., Payne, H.L., and Raymond, J.L. (2014). Gating of neural error signals during motor learning. Elife *3*, e02076.

Konnerth, A., Dreessen, J., and Augustine, G.J. (1992). Brief dendritic calcium signals initiate long-lasting synaptic depression in cerebellar Purkinje cells. Proc. Natl. Acad. Sci. U.S.a. *89*, 7051–7055.

Kreitzer, A.C., and Regehr, W.G. (2001). Cerebellar depolarization-induced suppression of inhibition is mediated by endogenous cannabinoids. J. Neurosci. *21*, RC174.

Lambo, M.E., and Turrigiano, G.G. (2013). Synaptic and intrinsic homeostatic mechanisms cooperate to increase L2/3 pyramidal neuron excitability during a late phase of critical period plasticity. J. Neurosci. *33*, 8810–8819.

Lee, K.Y., Royston, S.E., Vest, M.O., Ley, D.J., Lee, S., Bolton, E.C., and Chung, H.J. (2015). N-methyl-D-aspartate receptors mediate activity-dependent down-regulation of potassium channel genes during the expression of homeostatic intrinsic plasticity. Mol Brain *8*, 4.

Legenstein, R., and Maass, W. (2011). Branch-specific plasticity enables self-organization of nonlinear computation in single neurons. J. Neurosci. *31*, 10787–10802.

Lev-Ram, V., Mehta, S.B., Kleinfeld, D., and Tsien, R.Y. (2003). Reversing cerebellar long-term depression. Proc. Natl. Acad. Sci. U.S.a. *100*, 15989–15993.

Lien, C.-C., and Jonas, P. (2003). Kv3 potassium conductance is necessary and kinetically optimized for high-frequency action potential generation in hippocampal interneurons. J. Neurosci. *23*, 2058–2068.

Lisman, J., Cooper, K., Sehgal, M., and Silva, A.J. (2018). Memory formation depends on both synapse-specific modifications of synaptic strength and cell-specific increases in excitability. Nat. Neurosci. *21*, 309–314.

Litschig, S., Gasparini, F., Rueegg, D., Stoehr, N., Flor, P.J., Vranesic, I., Prézeau, L., Pin, J.P., Thomsen, C., and Kuhn, R. (1999). CPCCOEt, a noncompetitive metabotropic glutamate receptor 1 antagonist, inhibits receptor signaling without affecting glutamate binding. Mol. Pharmacol. *55*, 453–461.

Llinás, R., and Jahnsen, H. (1982). Electrophysiology of mammalian thalamic neurones in vitro. Nature *297*, 406–408.

Llinás, R., and Sugimori, M. (1980). Electrophysiological properties of in vitro Purkinje cell dendrites in mammalian cerebellar slices. J Physiol *305*, 197–213.

Mahon, S., and Charpier, S. (2012). Bidirectional plasticity of intrinsic excitability controls sensory inputs efficiency in layer 5 barrel cortex neurons in vivo. J. Neurosci. *32*, 11377–11389.

Martina, M., Yao, G.L., and Bean, B.P. (2003). Properties and functional role of voltage-dependent potassium channels in dendrites of rat cerebellar Purkinje neurons. J. Neurosci. *23*, 5698–5707.

Matsukawa, H., Wolf, A.M., Matsushita, S., Joho, R.H., and Knöpfel, T. (2003). Motor dysfunction and altered synaptic transmission at the parallel fiber-Purkinje cell synapse in mice lacking potassium channels Kv3.1 and Kv3.3. J. Neurosci. *23*, 7677–7684.

McCormick, D.A., and Pape, H.C. (1990). Noradrenergic and serotonergic modulation of a hyperpolarization-activated cation current in thalamic relay neurones. J Physiol *431*, 319–342.

McElvain, L.E., Bagnall, M.W., Sakatos, A., and Lac, du, S. (2010). Bidirectional plasticity gated by hyperpolarization controls the gain of postsynaptic firing responses at central vestibular nerve synapses. Neuron *68*, 763–775.

McKay, B.E., and Turner, R.W. (2004). Kv3 K+ channels enable burst output in rat cerebellar Purkinje cells. Eur. J. Neurosci. *20*, 729–739.

Midtgaard, J., Lasser-Ross, N., and Ross, W.N. (1993). Spatial distribution of Ca2+ influx in turtle Purkinje cell dendrites in vitro: role of a transient outward current. J. Neurophysiol. *70*, 2455–2469.

Miles, F.A., and Lisberger, S.G. (1981a). The “error” signals subserving adaptive gain control in the primate vestibulo-ocular reflex. Ann. N. Y. Acad. Sci. *374*,

513–525.

Miles, F.A., and Lisberger, S.G. (1981b). Plasticity in the vestibulo-ocular reflex: a new hypothesis. Annu. Rev. Neurosci. *4*, 273–299.

Minami, I., Kengaku, M., Smitt, P.S., Shigemoto, R., and Hirano, T. (2003). Long-term potentiation of mGluR1 activity by depolarization-induced Homer1a in mouse cerebellar Purkinje neurons. Eur. J. Neurosci. *17*, 1023–1032.

Mittmann, W., and Häusser, M. (2007). Linking synaptic plasticity and spike output at excitatory and inhibitory synapses onto cerebellar Purkinje cells. J. Neurosci. *27*, 5559–5570.

Mizukoshi, K., Kobayashi, H., Ohashi, N., and Watanabe, Y. (1983). Quantitative analysis of the human visual vestibulo-ocular reflex in sinusoidal rotation. Acta Otolaryngol Suppl *393*, 58–64.

Nagao, S., Honda, T., and Yamazaki, T. (2013). Transfer of memory trace of cerebellum-dependent motor learning in human prism adaptation: a model study. Neural Netw *47*, 72–80.

Nakashima, A., Takeuchi, H., Imai, T., Saito, H., Kiyonari, H., Abe, T., Chen, M., Weinstein, L.S., Yu, C.R., Storm, D.R., et al. (2013). Agonist-independent GPCR activity regulates anterior-posterior targeting of olfactory sensory neurons. Cell *154*, 1314–1325.

Napper, R.M., and Harvey, R.J. (1988). Quantitative study of the Purkinje cell dendritic spines in the rat cerebellum. J. Comp. Neurol. *274*, 158–167.

Narayanan, R., Dougherty, K.J., and Johnston, D. (2010). Calcium store depletion induces persistent perisomatic increases in the functional density of h channels in hippocampal pyramidal neurons. Neuron *68*, 921–935.

Nataraj, K., Le Roux, N., Nahmani, M., Lefort, S., and Turrigiano, G. (2010). Visual Deprivation Suppresses L5 Pyramidal Neuron Excitability by Preventing the Induction of Intrinsic Plasticity. Neuron *68*, 750–762.

Naudé, J., Cessac, B., Berry, H., and Delord, B. (2013). Effects of cellular homeostatic intrinsic plasticity on dynamical and computational properties of biological recurrent neural networks. J. Neurosci. *33*, 15032–15043.

Nelson, A.B., Gittis, A.H., and Lac, du, S. (2005). Decreases in CaMKII activity trigger persistent potentiation of intrinsic excitability in spontaneously firing vestibular nucleus neurons. Neuron *46*, 623–631.

Nolan, M.F., Dudman, J.T., Dodson, P.D., and Santoro, B. (2007). HCN1 channels control resting and active integrative properties of stellate cells from layer II of the entorhinal cortex. J. Neurosci. *27*, 12440–12451.

Nolan, M.F., Malleret, G., Lee, K.H., Gibbs, E., Dudman, J.T., Santoro, B., Yin, D., Thompson, R.F., Siegelbaum, S.A., Kandel, E.R., et al. (2003). The hyperpolarization-activated HCN1 channel is important for motor learning and neuronal integration by cerebellar Purkinje cells. Cell *115*, 551–564.

Notomi, T., and Shigemoto, R. (2004). Immunohistochemical localization of Ih channel subunits, HCN1-4, in the rat brain. J. Comp. Neurol. *471*, 241–276.

O'Leary, T., Williams, A.H., Franci, A., and Marder, E. (2014). Cell types, network homeostasis, and pathological compensation from a biologically plausible ion channel expression model. Neuron *82*, 809–821.

Ohtsuki, G., Piochon, C., Adelman, J.P., and Hansel, C. (2012). SK2 channel modulation contributes to compartment-specific dendritic plasticity in cerebellar Purkinje cells. Neuron *75*, 108–120.

Okamoto, T., Endo, S., Shirao, T., and Nagao, S. (2011a). Role of cerebellar cortical protein synthesis in transfer of memory trace of cerebellum-dependent motor learning. J. Neurosci. *31*, 8958–8966.

Okamoto, T., Shirao, T., Shutoh, F., Suzuki, T., and Nagao, S. (2011b). Post-training cerebellar cortical activity plays an important role for consolidation of memory of cerebellum-dependent motor learning. Neurosci. Lett. *504*, 53–56.

Ovsepian, S.V., Steuber, V., Le Berre, M., O'Hara, L., O'Leary, V.B., and Dolly, J.O. (2013). A defined heteromeric KV1 channel stabilizes the intrinsic pacemaking and regulates the output of deep cerebellar nuclear neurons to thalamic targets. J Physiol *591*, 1771–1791.

Park, S., Kramer, E.E., Mercaldo, V., Rashid, A.J., Insel, N., Frankland, P.W., and Josselyn, S.A. (2016). Neuronal Allocation to a Hippocampal Engram. Neuropsychopharmacol *41*, 2987–2993.

Pedarzani, P., McCutcheon, J.E., Rogge, G., Jensen, B.S., Christophersen, P., Hougaard, C., Strøbaek, D., and Stocker, M. (2005). Specific enhancement of SK channel activity selectively potentiates the afterhyperpolarizing current I(AHP) and modulates the firing properties of hippocampal pyramidal neurons. J. Biol. Chem. *280*, 41404–41411.

Poo, M.-M., Pignatelli, M., Ryan, T.J., Tonegawa, S., Bonhoeffer, T., Martin, K.C., Rudenko, A., Tsai, L.-H., Tsien, R.W., Fishell, G., et al. (2016). What is memory? The present state of the engram. BMC Biol. *14*, 40.

Pozzorini, C., Naud, R., Mensi, S., and Gerstner, W. (2013). Temporal whitening by power-law adaptation in neocortical neurons. Nat. Neurosci. *16*, 942–948.

Preston, A.R., and Eichenbaum, H. (2013). Interplay of hippocampus and prefrontal cortex in memory. Curr. Biol. *23*, R764–R773.

Ramakers, G.M.J., and Storm, J.F. (2002). A postsynaptic transient K+ current modulated by arachidonic acid regulates synaptic integration and threshold for LTP induction in hippocampal pyramidal cells. Proc. Natl. Acad. Sci. U.S.a. *99*, 10144–10149.

Raman, I.M., and Bean, B.P. (1997). Resurgent sodium current and action potential formation in dissociated cerebellar Purkinje neurons. J. Neurosci. *17*, 4517–4526.

Raman, I.M., and Bean, B.P. (1999). Ionic currents underlying spontaneous action potentials in isolated cerebellar Purkinje neurons. J. Neurosci. *19*, 1663–1674.

Raman, I.M., and Bean, B.P. (2001). Inactivation and recovery of sodium currents in cerebellar Purkinje neurons: evidence for two mechanisms. Biophys. J. *80*, 729–737.

Raman, I.M., Sprunger, L.K., Meisler, M.H., and Bean, B.P. (1997). Altered Subthreshold Sodium Currents and Disrupted Firing Patterns in Purkinje Neurons of Scn8a Mutant Mice. Neuron *19*, 881–891.

Rancz, E.A., and Häusser, M. (2010). Dendritic spikes mediate negative synaptic gain control in cerebellar Purkinje cells. Proc. Natl. Acad. Sci. U.S.a. *107*, 22284–22289.

Restivo, L., Vetere, G., Bontempi, B., and Ammassari-Teule, M. (2009). The formation of recent and remote memory is associated with time-dependent formation of dendritic spines in the hippocampus and anterior cingulate cortex. J. Neurosci. *29*, 8206–8214.

Rinaldi, A., Defterali, C., Mialot, A., Garden, D.L.F., Beraneck, M., and Nolan, M.F. (2013). HCN1 channels in cerebellar Purkinje cells promote late stages of learning and constrain synaptic inhibition. J Physiol *591*, 5691–5709.

Roosterman, D. (2014). Agonist-dependent and -independent dopamine-1-like receptor signalling differentially regulates downstream effectors. Febs J. *281*, 4792–4804.

Rudy, B., and McBain, C.J. (2001). Kv3 channels: voltage-gated K+ channels designed for high-frequency repetitive firing. Trends Neurosci. *24*, 517–526.

Rutherford, L.C., DeWan, A., Lauer, H.M., and Turrigiano, G.G. (1997). Brain-Derived Neurotrophic Factor Mediates the Activity-Dependent Regulation of Inhibition in Neocortical Cultures. J. Neurosci. *17*, 4527–4535.

Ryu, C., Jang, D.C., Jung, D., Kim, Y.G., Shim, H.G., Ryu, H.-H., Lee, Y.-S., Linden, D.J., Worley, P.F., and Kim, S.J. (2017). STIM1 Regulates Somatic Ca2+Signals and Intrinsic Firing Properties of Cerebellar Purkinje Neurons. J. Neurosci. *37*, 8876–8894.

Sacco, T., and Tempia, F. (2002). A-type potassium currents active at subthreshold potentials in mouse cerebellar Purkinje cells. J Physiol *543*, 505–520.

Safo, P., and Regehr, W.G. (2008). Timing dependence of the induction of cerebellar LTD. Neuropharmacology *54*, 213–218.

Santoro, B., Wainger, B.J., and Siegelbaum, S.A. (2004). Regulation of HCN channel surface expression by a novel C-terminal protein-protein interaction. J. Neurosci. *24*, 10750–10762.

Satoh, H., Qu, L., Suzuki, H., and Saitow, F. (2013). Depolarization-induced depression of inhibitory transmission in cerebellar Purkinje cells. Physiol Rep *1*, e00061.

Sausbier, M., Hu, H., Arntz, C., Feil, S., Kamm, S., Adelsberger, H., Sausbier, U., Sailer, C.A., Feil, R., Hofmann, F., et al. (2004). Cerebellar ataxia and Purkinje cell dysfunction caused by Ca2+-activated K+ channel deficiency. Proc. Natl. Acad. Sci. U.S.a. *101*, 9474–9478.

Schaller, K.L., and Caldwell, J.H. (2003). Expression and distribution of voltage-gated sodium channels in the cerebellum. Cerebellum *2*, 2–9.

Scheer, A., Fanelli, F., Costa, T., De Benedetti, P.G., and Cotecchia, S. (1996). Constitutively active mutants of the alpha 1B-adrenergic receptor: role of highly conserved polar amino acids in receptor activation. Embo J. *15*, 3566–3578.

Schonewille, M., Belmeguenai, A., Koekkoek, S.K., Houtman, S.H., Boele, H.J., Van Beugen, B.J., Gao, Z., Badura, A., Ohtsuki, G., Amerika, W.E., et al. (2010). Purkinje Cell-Specific Knockout of the Protein Phosphatase PP2B Impairs Potentiation and Cerebellar Motor Learning. Neuron *67*, 618–628.

Schonewille, M., Gao, Z., Boele, H.-J., Veloz, M.F.V., Amerika, W.E., Simek, A.A.M., De Jeu, M.T., Steinberg, J.P., Takamiya, K., Hoebeek, F.E., et al. (2011). Reevaluating the role of LTD in cerebellar motor learning. Neuron *70*, 43–50.

Schreurs, B.G., Gusev, P.A., Tomsic, D., Alkon, D.L., and Shi, T. (1998).

Intracellular correlates of acquisition and long-term memory of classical conditioning in Purkinje cell dendrites in slices of rabbit cerebellar lobule HVI. J. Neurosci. *18*, 5498–5507.

Schreurs, B.G., Tomsic, D., Gusev, P.A., and Alkon, D.L. (1997). Dendritic excitability microzones and occluded long-term depression after classical conditioning of the rabbit's nictitating membrane response. J. Neurophysiol. *77*, 86–92.

Sekirnjak, C., Martone, M.E., Weiser, M., Deerinck, T., Bueno, E., Rudy, B., and Ellisman, M. (1997). Subcellular localization of the K+ channel subunit Kv3.1b in selected rat CNS neurons. Brain Res. *766*, 173–187.

Sekirnjak, C., Vissel, B., Bollinger, J., Faulstich, M., and Lac, du, S. (2003). Purkinje cell synapses target physiologically unique brainstem neurons. J. Neurosci. *23*, 6392–6398.

Shepherd, J.D., Rumbaugh, G., Wu, J., Chowdhury, S., Plath, N., Kuhl, D., Huganir, R.L., and Worley, P.F. (2006). Arc/Arg3.1 mediates homeostatic synaptic scaling of AMPA receptors. Neuron *52*, 475–484.

Shim, H.G., Jang, D.C., Lee, J., Chung, G., Lee, S., Kim, Y.G., Jeon, D.E., and Kim, S.J. (2017). Long-Term Depression of Intrinsic Excitability Accompanied by Synaptic Depression in Cerebellar Purkinje Cells. J. Neurosci. *37*, 5659–5669.

Shim, H.G., Jang, S.-S., Jang, D.C., Jin, Y., Chang, W., Park, J.M., and Kim, S.J. (2016). mGlu1 receptor mediates homeostatic control of intrinsic excitability through Ih in cerebellar Purkinje cells. J. Neurophysiol. *115*, 2446–2455.

Shim, H.G., Lee, Y.-S., and Kim, S.J. (2018). The Emerging Concept of Intrinsic Plasticity: Activity-dependent Modulation of Intrinsic Excitability in Cerebellar Purkinje Cells and Motor Learning. Exp Neurobiol *27*, 139–154.

Shutoh, F., Ohki, M., Kitazawa, H., Itohara, S., and Nagao, S. (2006). Memory trace of motor learning shifts transsynaptically from cerebellar cortex to nuclei for consolidation. Neuroscience *139*, 767–777.

Smit, M.J., Leurs, R., Alewijnse, A.E., Blauw, J., Van Nieuw Amerongen, G.P., Van De Vrede, Y., Roovers, E., and Timmerman, H. (1996). Inverse agonism of histamine H2 antagonist accounts for upregulation of spontaneously active histamine H2 receptors. Proc. Natl. Acad. Sci. U.S.a. *93*, 6802–6807.

Smith, M.R., Nelson, A.B., and Lac, du, S. (2002). Regulation of firing response gain by calcium-dependent mechanisms in vestibular nucleus neurons. J. Neurophysiol. *87*, 2031–2042.

Smith, S.L., and Otis, T.S. (2003). Persistent Changes in Spontaneous Firing of Purkinje Neurons Triggered by the Nitric Oxide Signaling Cascade. J. Neurosci. *23*, 367–372.

Southan, A.P., and Robertson, B. (2000). Electrophysiological characterization of voltage-gated K(+) currents in cerebellar basket and purkinje cells: Kv1 and Kv3 channel subfamilies are present in basket cell nerve terminals. J. Neurosci. *20*, 114–122.

Squire, L.R., and Wixted, J.T. (2011). The cognitive neuroscience of human memory since H.M. Annu. Rev. Neurosci. *34*, 259–288.

Stemmler, M., and Koch, C. (1999). How voltage-dependent conductances can adapt to maximize the information encoded by neuronal firing rate. Nat. Neurosci. *2*, 521–527.

Steuber, V., Mittmann, W., Hoebeek, F.E., Silver, R.A., De Zeeuw, C.I., Häusser, M., and De Schutter, E. (2007). Cerebellar LTD and pattern recognition by Purkinje cells. Neuron *54*, 121–136.

Storm, J.F. (1988). Temporal integration by a slowly inactivating K+ current in hippocampal neurons. Nature *336*, 379–381.

Straka, H., Vibert, N., Vidal, P.P., Moore, L.E., and Dutia, M.B. (2005). Intrinsic membrane properties of vertebrate vestibular neurons: function, development and plasticity. Prog. Neurobiol. *76*, 349–392.

Streng, M.L., Popa, L.S., and Ebner, T.J. (2017). Climbing fibers predict movement kinematics and performance errors. J. Neurophysiol. *118*, 1888–1902.

Stuart, G., and Häusser, M. (1994). Initiation and spread of sodium action potentials in cerebellar Purkinje cells. Neuron *13*, 703–712.

Sugiyama, Y., Kawaguchi, S.-Y., and Hirano, T. (2008). mGluR1-mediated facilitation of long-term potentiation at inhibitory synapses on a cerebellar Purkinje neuron. Eur. J. Neurosci. *27*, 884–896.

Sun, Q.-Q. (2009). Experience-dependent intrinsic plasticity in interneurons of barrel cortex layer IV. J. Neurophysiol. *102*, 2955–2973.

Sutton, M.A., Taylor, A.M., Ito, H.T., Pham, A., and Schuman, E.M. (2007). Postsynaptic decoding of neural activity: eEF2 as a biochemical sensor coupling miniature synaptic transmission to local protein synthesis. Neuron *55*, 648–661.

Suvrathan, A., and Raymond, J.L. (2018). Depressed by Learning-Heterogeneity of the Plasticity Rules at Parallel Fiber Synapses onto Purkinje Cells. Cerebellum *202*, 437–439.

Suvrathan, A., Payne, H.L., and Raymond, J.L. (2016). Timing Rules for Synaptic Plasticity Matched to Behavioral Function. Neuron *92*, 959–967.

Tang, W., and Jadhav, S.P. (2018). Sharp-wave ripples as a signature of hippocampal-prefrontal reactivation for memory during sleep and waking states. Neurobiol Learn Mem.

Tateyama, M., and Kubo, Y. (2006). Dual signaling is differentially activated by different active states of the metabotropic glutamate receptor 1alpha. Proc. Natl. Acad. Sci. U.S.a. *103*, 1124–1128.

Thorsen, T.S., Madsen, K.L., Rebola, N., Rathje, M., Anggono, V., Bach, A., Moreira, I.S., Stuhr-Hansen, N., Dyhring, T., Peters, D., et al. (2010). Identification of a small-molecule inhibitor of the PICK1 PDZ domain that inhibits hippocampal LTP and LTD. Proc. Natl. Acad. Sci. U.S.a. *107*, 413–418.

Titley, H.K., Heskin-Sweezie, R., and Broussard, D.M. (2010). The Bidirectionality of Motor Learning in the Vestibulo-ocular Reflex Is a Function of Cerebellar mGluR1 Receptors. J. Neurophysiol. *104*, 3657–3666.

Titley, H.K., Watkins, G.V., Lin, C., Weiss, C., McCarthy, M., Disterhoft, J.F., and Hansel, C. (2018). Intrinsic Excitability Increase in Cerebellar Purkinje Cells Following Delay Eyeblink Conditioning in Mice. bioRxiv 306639.

Tu, J.C., Xiao, B., Naisbitt, S., Yuan, J.P., Petralia, R.S., Brakeman, P., Doan, A., Aakalu, V.K., Lanahan, A.A., Sheng, M., et al. (1999). Coupling of mGluR/Homer and PSD-95 complexes by the Shank family of postsynaptic density proteins. Neuron *23*, 583–592.

Turecek, J., Jackman, S.L., and Regehr, W.G. (2016). Synaptic Specializations Support Frequency-Independent Purkinje Cell Output from the Cerebellar Cortex. Cell Rep *17*, 3256–3268.

Turrigiano, G., Abbott, L.F., and Marder, E. (1994). Activity-dependent changes in the intrinsic properties of cultured neurons. Science *264*, 974–977.

Valkova, C., Liebmann, L., Krämer, A., Hübner, C.A., and Kaether, C. (2017). The sorting receptor Rer1 controls Purkinje cell function via voltage gated sodium channels. Sci Rep *7*, 41248.

van Welie, I., and Lac, du, S. (2011). Bidirectional control of BK channel open probability by CAMKII and PKC in medial vestibular nucleus neurons. J. Neurophysiol. *105*, 1651–1659.

Vega-Saenz de Miera, E.C., Rudy, B., Sugimori, M., and Llinás, R. (1997). Molecular characterization of the sodium channel subunits expressed in mammalian cerebellar Purkinje cells. Proc. Natl. Acad. Sci. U.S.a. *94*, 7059–7064.

Wagner, M.J., Kim, T.H., Savall, J., Schnitzer, M.J., and Luo, L. (2017). Cerebellar granule cells encode the expectation of reward. Nature *544*, 96–100.

Walter, J.T., Alviña, K., Womack, M.D., Chevez, C., and Khodakhah, K. (2006).

Decreases in the precision of Purkinje cell pacemaking cause cerebellar dysfunction and ataxia. Nat. Neurosci. *9*, 389–397.

Wang, D.-J., Yang, D., Su, L.-D., Xie, Y.-J., Zhou, L., Sun, C.-L., Wang, Y., Wang, X.-X., Zhou, L., and Shen, Y. (2012). Cytosolic phospholipase A2 alpha/arachidonic acid signaling mediates depolarization-induced suppression of excitation in the cerebellum. PLoS ONE *7*, e41499.

Wang, W., Nakadate, K., Masugi-Tokita, M., Shutoh, F., Aziz, W., Tarusawa, E., Lorincz, A., Molnár, E., Kesaf, S., Li, Y.-Q., et al. (2014). Distinct cerebellar engrams in short-term and long-term motor learning. Proc. Natl. Acad. Sci. U.S.a. *111*, E188–E193.

Watanabe, S., Hoffman, D.A., Migliore, M., and Johnston, D. (2002). Dendritic K+ channels contribute to spike-timing dependent long-term potentiation in hippocampal pyramidal neurons. Proc. Natl. Acad. Sci. U.S.a. *99*, 8366–8371.

Williams, S.R., Christensen, S.R., Stuart, G.J., and Häusser, M. (2002). Membrane potential bistability is controlled by the hyperpolarization-activated current I(H) in rat cerebellar Purkinje neurons in vitro. J Physiol *539*, 469–483.

Wilms, C.D., and Häusser, M. (2015). Reading out a spatiotemporal population code by imaging neighbouring parallel fibre axons in vivo. Nat Commun *6*, 6464.

Womack, M.D., and Khodakhah, K. (2003). Somatic and dendritic small-conductance calcium-activated potassium channels regulate the output of cerebellar Purkinje neurons. J. Neurosci. *23*, 2600–2607.

Womack, M.D., Chevez, C., and Khodakhah, K. (2004). Calcium-activated potassium channels are selectively coupled to P/Q-type calcium channels in cerebellar Purkinje neurons. J. Neurosci. *24*, 8818–8822.

Woodruff-Pak, D.S., Green, J.T., Levin, S.I., and Meisler, M.H. (2006). Inactivation of sodium channel Scn8A (Na-sub(v)1.6) in Purkinje neurons impairs learning in Morris water maze and delay but not trace eyeblink classical conditioning. Behav. Neurosci. *120*, 229–240.

Wulff, P., Schonewille, M., Renzi, M., Viltono, L., Sassoè-Pognetto, M., Badura, A., Gao, Z., Hoebeek, F.E., van Dorp, S., Wisden, W., et al. (2009). Synaptic inhibition of Purkinje cells mediates consolidation of vestibulo-cerebellar motor learning. Nat. Neurosci. *12*, 1042–1049.

Yamazaki, T., and Nagao, S. (2012). A computational mechanism for unified gain and timing control in the cerebellum. PLoS ONE *7*, e33319.

Yamazaki, T., Nagao, S., Lennon, W., and Tanaka, S. (2015). Modeling memory consolidation during posttraining periods in cerebellovestibular learning. Proc. Natl. Acad. Sci. U.S.a. *112*, 3541–3546.

Yan, H., Pablo, J.L., Wang, C., and Pitt, G.S. (2014). FGF14 modulates resurgent sodium current in mouse cerebellar Purkinje neurons. Elife *3*, e04193.

Yang, Z., and Santamaria, F. (2016). Purkinje cell intrinsic excitability increases after synaptic long term depression. J. Neurophysiol. *116*, 1208–1217.

Zang, Y., Dieudonné, S., and De Schutter, E. (2018). Voltage- and Branch-Specific Climbing Fiber Responses in Purkinje Cells. Cell Rep *24*, 1536–1549.

Zhang, W., and Linden, D.J. (2003). The other side of the engram: experience-driven changes in neuronal intrinsic excitability. Nat. Rev. Neurosci. *4*, 885–900.

Zhou, Y., Won, J., Karlsson, M.G., Zhou, M., Rogerson, T., Balaji, J., Neve, R., Poirazi, P., and Silva, A.J. (2009). CREB regulates excitability and the allocation of memory to subsets of neurons in the amygdala. Nat. Neurosci. *12*, 1438–1443.

국문초록

소뇌 퍼킨지 세포 내재적 흥분성의 활동-의존적 조절

심 현 근
서울대학교 대학원
의과대학 의과학과 (생리학전공)

생명체는 끊임없이 주변환경에 반응하여 행동을 수정하며 이러한 적응은 변화하는 환경에서 생존에 필수적이다. 소뇌-운동 학습은 대표적인 적응 행동의 예이다. 다양한 감각 신호들이 소뇌로 전달되어 처리된 후 소뇌 출력을 통해 운동 협응이 이루어진다. 이러한 소뇌-운동 학습 및 소뇌 기능 조절의 세포 생리학적 기전으로 소뇌 퍼킨지 세포의 시냅스 장기저하가 오랫동안 주목받았다. 퍼킨지 세포의 시냅스 장기저하가 나타나지 않는 유전자 변형 동물 모델들에서 소뇌-운동 학습이 정상적으로 일어나지 않는 현상이 관찰되었기 때문에 시냅스 장기저하 이론은 오랜 시간 소뇌-운동 학습의 기전으로 지지 받았다. 하지만 최근 10 년 동안의 연구결과는 시냅스 장기저하만으로 소뇌-운동 학습 및 기능 조절을 설명할 수 없다고 반박한다. 특히 소뇌 퍼킨지 세포는 소뇌 피질로 전달된 감각신호를 처리하여 출력을 담당하는 유일한 신경세포이므로 운동 학습 상황에서 소뇌의 출력이 어떻게 조절되는지를 이해하는 것이 중요하게 인식되었다. 감각 신호가 신경 회로 내에서 전달될 때 활동 전압의 형태로 전달되기 때문에 활동

전압의 발생 빈도 및 패턴 조절 양상에 대한 이해는 소뇌 운동 학습의 기전을 밝히는 데에 중요하다. 본 박사학위 논문에서는 먼저 소뇌 퍼킨지 세포의 내재적 흥분성을 조절하는 여러가지 이온 통로들의 특성에 대해 정리하고 더 나아가 내재적 흥분성 가소성의 기전 및 생리학적 의의를 제시하였다. 소뇌 퍼킨지 세포의 흥분성은 활동-의존적 가소성을 보이는데, 시냅스의 활동이 아닌 소뇌 회로 활동성의 장기적인 변화에 대응하여 나타날 수 있다. 소뇌 회로의 활동을 2 일 간의 tetrodotoxin (TTX, 1μM) 처리를 통해 저해하였을 때 과분극에 의해 발생하는 내향전류 (I_h) 증가를 통한 소뇌 퍼킨지 세포의 흥분성이 감소되는 것을 전기생리학적 기록을 통해 관찰하였다. 이러한 장기적인 소뇌 회로의 활동성 변화에 의한 퍼킨지 세포의 내재적 흥분성 감소의 세포생리학적 기전으로서 대사성 글루타메이트 수용체의 길항제-비의존적인 활동성 증가 및 그로 인한 PKA 의 증가에 의해 발생함을 생화학 및 전기생리학적 방법을 통해 규명하였다. 이처럼 소뇌 퍼킨지 세포의 내재적 흥분성은 소뇌 회로 내에서 역동적으로 조절되어 소뇌 기능을 조절한다. 더 나아가 퍼킨지 세포의 흥분성 조절과 소뇌-기억형성과의 관계성을 검증하기 위해 소뇌-학습의 세포생리학적 기전으로 알려져있는 퍼킨지 세포 시냅스 장기저하 유도 후 흥분성의 변화를 관찰하였다. 흥미롭게도 퍼킨지 세포의 내재적 흥분성 역시 시냅스 가소성과 마찬가지로 평행섬유와 등반섬유의 활성을 통해 가소성을 보이는데 이 흥분성의 가소성은 대사성 글루타메이트 수용체, PKC 그리고 CaMKII 와 같은 시냅스 장기 저하를 야기하는 세포 내 신호전달기전을 필요로 한다. 이러한 실험결과를 통해 시냅스 장기저하가 발생할 때 소뇌 퍼킨지 세포의 내재적 흥분성 역시 같이 감소하여 소뇌 운동 시 소뇌 피질의 출력이 크게 감소함을 예상할 수 있다. 실제로 소뇌 퍼킨지 세포의 신경가소성을 유도한 후 평행섬유를

자극하여 나타나는 퍼킨지 세포의 활동 전압 발생 빈도를 측정해 본 결과, 시냅스 장기저하와 흥분성의 장기저하가 함께 발생했을 때에만 소뇌 퍼킨지 세포의 출력이 유의미하게 감소하는 것을 관찰하였다. 특히 퍼킨지 세포의 활동-의존적 흥분성의 가소성은 시냅스 가소성과 마찬가지로 특정 수상돌기 가지 특이적으로 발생함을 관찰하였다. 이를 통해 퍼킨지 세포의 시냅스 가소성과 흥분성 가소성의 유기적인 연합을 통해 소뇌 퍼킨지 세포의 출력신호가 조절되어 소뇌-운동학습을 조절함을 알 수 있다. 결론적으로 본 박사학위 논문의 연구결과들은 소뇌 퍼킨지 세포의 출력은 퍼킨지 세포의 시냅스 가소성 혹은 흥분성의 조절과 비선형관계를 보이며 이러한 시냅스 가소성과 내재적 가소성의 시너지는 소뇌 정보 저장 능력을 극대화하여 소뇌 기능 조절 및 정보저장에 중요한 역할을 담당하고 있음을 제시한다.

핵심어: 시냅스 가소성, 시냅스 장기저하, 내재적 흥분성, 소뇌 운동 학습

학번: 2012-23669

감사의 글

이 학위 논문을 작성하며 학위 기간 동안 오롯이 나만의 힘으로 이 순간이 온 것이 아님을 다시 한번 깨닫게 됩니다. 먼저 늘 한결같이 지지해주시고 기도해주신 부모님과 장인어른, 장모님께 감사의 말씀을 드립니다. 아울러 동생 연진과 처제 미경에게도 감사를 표합니다.

2012년 9월부터 시작된 결코 짧지 않은 학위 기간 동안 학문적으로 지지해주시고 기회를 주신 서울의대 생리학교실 김상정 교수님께 감사의 말씀을 드립니다. 교수님의 지도 및 논의를 통해 과학적으로 사고하는 법을 알게 되었습니다. 또한 함께 지도해주시고 늘 좋은 코멘트를 주신 김전 교수님과 이용석 교수님께도 감사의 말씀을 드립니다.

이 학위 논문이 보다 더 발전할 수 있도록 바쁘신 시간 중에 이 논문을 심사해주시고 조언해 주신 서울의대 생리학교실 서인석, 김성준 교수님, 을지의대 생리학교실 장원석 교수님께 감사의 말씀을 드립니다.

학위 기간 동안 함께 고생해 준 신경생리학 실험실 일원에게도 감사를 전합니다. 특히 실험실 사수였던 장성수 선생님, 바쁘신 중에도 늘 좋은 코멘트를 준 정지훈 박사님, 과학자로서 생각하는 법을 알려주신 이석찬 박사님, 전기생리학의 기초를 알려준 유창현 박사님, 공동 저자로 고생해준 장동철 박사님에게 다시 한번 감사의 말씀을 전합니다. 아울러 제 연구에 도움을 주었던 김용규 선생님, 김수용 선생님, 김승하 선생님, 이재건 선생님께도 감사의 인사를 드립니다.

학부 때부터 힘이 되어주시고 과학자로서의 길을 포기하지 않도록 아낌없이 지지해주시고 필요한 조언을 주셨던 중앙대학교 심리학과 정태연 교수님, 신맹식 교수님, 그리고 태성고등학교 조영준 선생님께 감사의 말씀을 드립니다. 세 분의 선생님이 아니었다면 저는 아마 지금 이 자리에 있지 못했을 것입니다.

마지막으로 그리고 무엇보다도, 사랑하는 아내 미선에게 큰 감사를 표합니다. 아내의 헌신적인 도움 덕분에 고된 학위 과정 기간이 고되지 않았고 언제나 즐겁게 생활할 수 있었습니다. 성공보다 실패가 많은 연구실 생활에서 아내의 응원은 언제나 저에게 큰 힘이 되었습니다. 좋은 동료로, 좋은 친구로, 좋은 아내로 늘 옆에 있어준 아내에게 다시 한번 큰 감사와 사랑을 전합니다.